



Fluid lipid membranes: From differential geometry to curvature stresses



Markus Deserno*

Department of Physics, Carnegie Mellon University, 5000 Forbes Avenue, Pittsburgh, PA 15213, USA

ARTICLE INFO

Article history:

Available online 13 May 2014

Keywords:

Lipid membranes
Helfrich theory
Differential geometry
Shape equation
Surface stresses
Surface torques

ABSTRACT

A fluid lipid membrane transmits stresses and torques that are fully determined by its geometry. They can be described by a stress- and torque-tensor, respectively, which yield the force or torque per length through any curve drawn on the membrane's surface. In the absence of external forces or torques the surface divergence of these tensors vanishes, revealing them as conserved quantities of the underlying Euler–Lagrange equation for the membrane's shape. This review provides a comprehensive introduction into these concepts without assuming the reader's familiarity with differential geometry, which instead will be developed as needed, relying on little more than vector calculus. The Helfrich Hamiltonian is then introduced and discussed in some depth. By expressing the quest for the energy-minimizing shape as a functional variation problem subject to geometric constraints, as proposed by Guven (2004), stress- and torque-tensors naturally emerge, and their connection to the shape equation becomes evident. How to reason with both tensors is then illustrated with a number of simple examples, after which this review concludes with four more sophisticated applications: boundary conditions for adhering membranes, corrections to the classical micropipette aspiration equation, membrane buckling, and membrane mediated interactions.

© 2014 Elsevier Ireland Ltd. All rights reserved.

1. Introduction

Lipid membranes are amazing soft matter structures. Self-assembled from single molecules into fluid films just a few nanometers thick, they can stably span macroscopic lateral scales. Many of their characteristic energies (such as the aggregation energy per lipid or the bending rigidity) are about an order of magnitude bigger than thermal energy, hence membranes are stable against thermal fluctuations but soft enough to be easily deformed, for instance by proteins and the energies available biochemically from ATP hydrolysis. For the same reason undulations of lipid bilayers are readily noticeable in a microscope as “flickering,” and they give rise to physically observable effects, for instance a long-range entropic repulsion between two fluctuating membranes. The strong drop in dielectric constant across just a few nanometers suffices to make membranes essentially perfect insulators for bare ionic charges, and they also constitute barriers over a range of permeabilities for a great many other solutes. Membranes hence compartmentalize space, but they can also change topology through fission and fusion events, which in turn can be exquisitely

controlled by several classes of protein machineries. Mixed membranes show a variety of different phases and phase coexistence regions, and these can couple back to their morphology. All of these facets of membrane chemistry and physics have been widely studied over the past decades, and they are the topics of numerous contributions in this special issue. The present review focuses on the large scale: how to describe membranes in a way that is both mathematically elegant and efficient as well as physically intuitive.

One curious aspect of the way lipids assemble into bilayers is that the emergent area per lipid is a remarkably stiff degree of freedom: membranes are hard to stretch but easy to bend. Of course, stretching and bending are not dimensionally equivalent, so the meaning of “lower in energy” will have a length scale hidden in it. A better way to phrase the statement is therefore as follows: Take a flat membrane patch and stretch it by some dimensionless strain s , thus increasing its energy. Alternatively, curve it into a closed but tensionless spherical vesicle of radius R . If the two energies happen to be equal, what is the value of R ? A simple calculation (see Section 3.2) gives the answer

$$R_s = \frac{1}{s} \sqrt{\frac{2(2\kappa + \bar{\kappa})}{K_A}}, \quad (1)$$

* Tel.: +1 4122684401.

E-mail address: deserno@andrew.cmu.edu

where κ and $\bar{\kappa}$ are the bending and Gaussian curvature modulus, respectively, and K_A is the area expansion modulus. Inserting typical values for these material parameters and choosing a strain of $s = 1\%$ leads to $R \approx 80$ nm. Quite small strains correspond to fairly large curvatures (in the sense that this radius is only about 20 times bigger than the bilayer thickness, while a membrane's lateral size can easily exceed its thickness by three to four orders of magnitude).

For the purpose of the present review, the probably most remarkable aspect of fluid lipid membranes that follows from this observation is that on length scales not much bigger than their own thickness, their physical behavior can be described with astonishing accuracy by a purely geometric Hamiltonian—one that penalizes curvature. In the early 1970s this insight dawned on Canham (1970), Helfrich (1973) and Evans (1974), and the theoretical (and often closely linked experimental) work that followed from this idea ushered in a golden era for membrane science.

Unfortunately, curvature elastic surfaces come along with some challenging math. For instance, more than a decade passed between the discovery of the energy functional (Canham, 1970; Helfrich, 1973; Evans, 1974) and the appearance of its associated Euler–Lagrange equation in the physics literature (Ou–Yang and Helfrich, 1987, 1989).^{1,2} This so-called “shape equation,” in turn, is a formidable fourth order partial nonlinear differential equation, and finding a general analytic solution for this behemoth seems a forlorn hope. In the 1990s substantial efforts were devoted to numerically solving this (or a closely related) equation—mostly for the special case of axisymmetry (Svetina and Žekš, 1989; Seifert and Lipowsky, 1990; Lipowsky, 1991; Seifert et al., 1991; Jülicher and Lipowsky, 1993, 1996; Jülicher and Seifert, 1994; Miao et al., 1994), but occasionally also for the general case (Heinrich et al., 1993; Kralj–Iglić et al., 1993). The reader will find more details on this in existing reviews (Seifert and Lipowsky, 1995; Seifert, 1997).

As important as the extensive numerical results have been, they might also have contributed to a feeling that outside heavy numerics or perturbation theory little can be said about the general case. The shape equation expressed in some parametrization does not readily reveal its structure, and even though a first integral for the axisymmetric case had been found (Zheng and Liu, 1993), its physical meaning remained elusive. And yet, there exists a link between the symmetry of variational problems and the solutions of their associated Euler–Lagrange equations: Noether's theorem (Goldstein et al., 2002). Continuous symmetries, such as translations and rotations, go along with conservation laws and, in field theory, conserved currents that permit one to discuss exact properties of these solutions even if one cannot actually find them. The consequence for membranes is that there exist objects—the stress and the torque tensor—which are divergence free as evaluated on the surface of the membrane (Capovilla and Guven, 2002a,b, 2004; Capovilla et al., 2002). The resulting conservation laws hold even if the specific membrane shape has no discernible translation or rotation symmetry, for they are a consequence of the symmetry of the Hamiltonian, not of a specific solution.

¹ The work by Ou–Yang and Helfrich (1987, 1989) introduced the shape equation to physicists, but in other communities it had been well known. The special case $K_0 = 0$ was worked out a decade earlier by Jenkins (a mechanical engineer) (Jenkins, 1977a,b), and mathematicians knew it long before then (Thomsen, 1924; Blaschke, 1929; Willmore, 1965, 1982; White, 1973; Pinkall and Sterling, 1987). Since including K_0 does not incur any additional complications, these earlier publications deserve more credit than is usually given to them in the physics community.

² Even afterwards, a widely used axisymmetric specialization of the shape equations was claimed to be incorrect (Hu and Ou–Yang, 1993; Naito et al., 1993; Zheng and Liu, 1993), a criticism that was refuted on the basis that more attention needs to be given to the boundaries during functional variation (Jülicher and Seifert, 1994).

The existence of stress- and torque-tensors, which are explicit functions of a membrane's geometry, affords profound insights not only into the nature of solutions, but also into questions of immediate practical relevance, such as: what force does a membrane respond with upon deformation? How does it adapt its shape when it adheres to a substrate or another membrane, and how does it remodel the other membrane in the latter case? And what types of forces does it transmit between multiple objects binding to it? Despite the stress tensor's intuitive physical meaning, physicists seem to be somewhat shy to use it, whereas for instance mechanical engineers have developed highly sophisticated frameworks largely unheard-of in the physics community (Jenkins, 1977a,b; Steigmann, 1999; Agrawal and Steigmann, 2008; Napoli and Vergori, 2010). I suspect the reasons are twofold: First, once physicists learn about Lagrangian or Hamiltonian Mechanics, the concepts of stress and force might appear a quaint remnant of the olden Newtonian days, best to be avoided. This of course is a luxury one can only afford in a world consisting of point particles, but not one that is populated with elastic continua.³ And second, in order to express the stress tensor in a geometric language free of the idiosyncrasies of arbitrary surface parametrizations, one needs some differential geometry (of course, so do the engineers). And even though the amount necessary to understand virtually the entire framework from scratch is remarkably modest, it might still prove too much of an activation barrier.

It is the purpose of this review to provide a helping hand over this barrier. While there are excellent textbooks on differential geometry aplenty (Kreyszig, 1991; do Carmo, 1976, 1992; Willmore, 2012; Spivak, 1970, 1975a,b; Lovelock and Rund, 1989; Frankel, 2004; Schutz, 1980; Darling, 1994; Flanders, 1989), the bare minimum necessary to follow most of the reasoning and all of the subsequent applications can be condensed into a couple of pages. This review is aimed towards researchers who wish to learn more about these concepts, but who have no working experience with differential geometry and do not wish to invest several months to study the mathematical prerequisites before they can decide whether it is even worthwhile to adopt this framework. What follows will therefore be akin to a teaser trailer, focusing on the highlights in an abbreviated fashion, hoping to convince the reader that it's worthwhile to watch the whole movie (or, even better, read the book).

This review is organized as follows. Section 2 starts by summarizing the essential differential geometry of two-dimensional surfaces embedded in three-dimensional space. Beginning with a general purpose parametrization, metric and curvature tensor are introduced, and their connecting integrability conditions are developed. Along the way the issues of co- and contravariant components are clarified and the notion of a covariant derivative is introduced. In Section 3 these tools are used to derive the Helfrich Hamiltonian as the essentially unique large-wavelength limit of what physics and symmetry permit, and its phenomenological parameters are discussed in some detail, after a quick glance at thin plate theory. The relation between bilayer and monolayer physics is discussed within the framework of parallel surfaces, and a few comments on higher order corrections are made. Section 4 derives the stress tensor from first principles, beginning with a motivation for why membrane stresses differ from those in soap films or simple fluid surfaces. After revisiting the concept of a surface variation, and arriving at the classical shape equation by varying the geometry and ultimately the Helfrich Hamiltonian piece-by-piece,

³ The Landau/Lifshitz volume on elasticity (Landau and Lifshitz, 1999) pithily disabuses the reader of this misconception by introducing the strain tensor in Chapter 1 paragraph 1, and the stress tensor in paragraph 2; however, elasticity is no longer part of the standard physics curriculum.

an alternative route is taken that immediately unveils a conserved quantity, which is subsequently identified as the stress tensor, and whose divergence is identical to the Euler–Lagrange derivative. This tensor measures the force per length transmitted through any curve drawn onto the membrane’s surface, and by expressing it in the Darboux frame of that surface curve, the stress tensor is stripped of its last tie to an arbitrary parametrization. The section closes with a number of simple examples that illustrate the stress tensor in frequently encountered situations. While stresses owe their conservation to translation invariance, torques are linked to rotation invariance, and Section 5 shows how this connection comes about. Specifically, the new concept of an intrinsic torque is discovered, which does not exist for surfaces merely characterized by a surface tension. Finally, Section 6 illustrates how to handle the stress- and torque-framework through a number of more advanced examples, namely: boundary conditions for adhering membranes, corrections to the classical micropipette aspiration equations, membrane buckling, and exact results for membrane mediated interactions.

While this review will make generous use of numerous mathematical tools, it seems nevertheless important to warn purists that a lot of mathematical subtleties will be swept under the physicist’s rug. Questions about existence or uniqueness, how many times differentiable a mapping has to be, how precisely many quantities are defined, what the exact conditions for several results are, etc., all these issues will be intentionally ignored. They have answers, of course, and these occasionally matter, but physicists tend to approach any new formalism with a mercenary cost–benefit analysis, first wanting to know whether it actually helps to solve new problems more swiftly than the tools they already know, and so they are in the habit of first requesting some hands-on working knowledge based on which they can judge whether learning the math more thoroughly is worth their time. In the spirit of this time-honored pragmatism (and good precedent (Kamien, 2002)), this review will focus on how to operate the machinery, delegating its inner workings to numerous excellent discussions in the mathematically impeccable literature (Kreyszig, 1991; do Carmo, 1976, 1992; Willmore, 2012; Spivak, 1970, 1975a,b; Lovelock and Rund, 1989; Frankel, 2004; Schutz, 1980; Darling, 1994; Flanders, 1989).

2. Differential geometry—a minimalist toolkit

Given that the lateral dimensions of lipid membranes tend to greatly exceed their thickness, we have every right to expect that the local lipid physics will only enter the large-scale membrane properties inasmuch as it sets the values of a small number of coupling constants in an effective larger-scale Hamiltonian. This is no wildly optimistic hope; this is how physics works when scales separate. The natural limit of this scale separation is to envision membranes as curved two-dimensional surfaces embedded in three-dimensional space, whose energy depends in some yet to be specified way on the geometry, especially the extent of curvature deformation. Linguistics alone therefore suggests that large-scale membrane physics is far from a linear problem, and these concerns turn out to be on the mark. However, it is important to understand the origin of the nonlinearities one is bound to encounter, since they arise for two very different reasons: On the one hand, the link between geometry and energetics—the Hamiltonian, if you will—could be arbitrarily complicated. On the other hand, the description of a curved surface itself is prone to involve nonlinear mathematics. The first point is ultimately an expression of the key underlying physics, and hence there is not much we can do if we dislike its form (other than approximating it until we feel comfortable dealing with it). The second one, however, will greatly reflect our choice in describing the surface and its geometry, for there are clever and not-so-clever ways of doing this. It thus behooves us to

first revisit some of the ingenious mathematical tools for dealing with curved surfaces, which permits us to circumnavigate some of the more tedious limitations that arise if we cling too closely to specific parametrizations.

2.1. How to describe a surface

Imagine that we wish to describe the surface of a sphere of radius R . Let us consider three possibilities for doing this. In the first one, take

$$z = \pm h(x, y) = \pm \sqrt{R^2 - x^2 - y^2}, \quad (2a)$$

where $\{x, y, z\}$ are Cartesian coordinates and both x and y are suitably restricted so that the square root remains real. The \pm -sign accounts for the “upper” and the “lower” half of the sphere.

As a second possibility, consider

$$\mathbf{r} = \mathbf{X}(\vartheta, \varphi) = R \begin{pmatrix} \sin \vartheta \cos \varphi \\ \sin \vartheta \sin \varphi \\ \cos \vartheta \end{pmatrix}, \quad \begin{matrix} \vartheta \in [0, \pi] \\ \varphi \in [0, 2\pi] \end{matrix}, \quad (2b)$$

where now $\{\vartheta, \varphi\}$ are spherical polar coordinates, and we evidently must be a bit careful at the poles, where $\vartheta = 0$ or $\vartheta = \pi$ and the value of φ becomes irrelevant.

Finally, examine

$$r = R, \quad (2c)$$

where again $\{r, \vartheta, \varphi\}$ are spherical polar coordinates, but due to the high symmetry of a sphere, we simply state that the radius be of some particular value.

These three parametrizations are very different. The first one involves a square root, together with some onerous restrictions on the set of permitted values for x and y , and an ugly \pm -symbol (ugly, since it chops the sphere in half at the equator, with no differentiable connection linking the two parts). The second parametrization removes the square root at the price of trigonometric functions. The third one, pleasingly, involves none of that, but it describes the surface “in one go,” without the possibility to single out a specific point—for which we would have to go back to something like (2b).

The square root in (2a) reminds us that Cartesian coordinates are a graceless way to describe a sphere. As universal and simple as these coordinates are, they usually do not reflect the geometry of whatever it is they are striving to describe. Accordingly, square roots show up whenever distances not aligned with the axes play a geometric role. Of course, this does not mean that the geometry is difficult, it only means that a Cartesian parametrization does not naturally capture it, and this problem is not at all unique to spheres. The second and third parametrization explicitly use a coordinate system adapted to the sphere, and yet the second one is still nonlinear. However, as already stated, the trigonometric functions only matter if we wish to identify individual points on the sphere, and to be fair, these are then identified only with respect to an arbitrarily fixed set of axes that the spherical polar system first had to prescribe (“where is the north pole?”, “where is the Greenwich meridian?”). The third parametrization, even though we can view it as using spherical polar coordinates, really comes closest to a description that is coordinate free, since it describes the surface of a sphere through its defining *geometric* property: the locus of all points having a fixed distance from some given center.

It is no coincidence that stripping the parametrization away clarifies the true geometry. Granted, the example of a sphere was almost misleadingly simple, since it gave a description of the whole surface in one fell swoop, a luxury we cannot usually expect. But at least *locally* it ought to be possible to describe surfaces by their true geometric properties (say, their local curvature) instead of hobbling

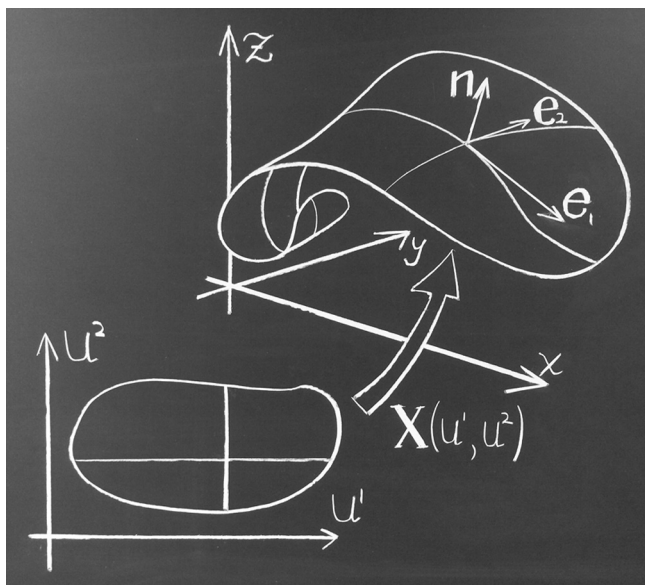


Fig. 1. Illustration of the surface parametrization described by Eq. (3). A region in the two-dimensional (u^1, u^2) -space is mapped to a surface in three-dimensional space. The vectors \mathbf{e}_1 and \mathbf{e}_2 arise as tangent vectors to the coordinate lines $u^2 = \text{const.}$ and $u^1 = \text{const.}$, respectively. The normal vector is perpendicular to both \mathbf{e}_1 and \mathbf{e}_2 .

on the crutches of some more or less clumsy parametrization. The extent to which we succeed in this endeavor will determine how well we can disentangle nonlinearities of the underlying physics of lipid membranes from those sneaking in through a specific mathematical description.

These remarks should suffice to convince the reader that substantial benefits can be reaped by diving a bit deeper into the elegant framework of differential geometry, the mathematical tool by which we will largely overcome the arbitrariness of parametrizations. To boost the morale, it is worth mentioning ahead of time that the efficiency by which just a little bit of extra mathematics does away with a large number of awkward problems is nothing short of amazing.

2.2. A general purpose surface parametrization

While abolishing parametrizations is our ultimate goal, we first have to start with one. Many possibilities exist, but we will begin with a fairly general and common parametrization reminiscent of Eq. (2b), but without the built-in spherical symmetry. The idea is to adopt a local (evidently two-dimensional) coordinate system $\{u^1, u^2\}$ for the surface we wish to describe and find a mapping that assigns each coordinate pair (u^1, u^2) to some point in three-dimensional space (which we describe by its Cartesian coordinates):

$$\mathbf{r} = \mathbf{X}(u^1, u^2) = \begin{pmatrix} X(u^1, u^2) \\ Y(u^1, u^2) \\ Z(u^1, u^2) \end{pmatrix}, \quad (3)$$

where $(u^1, u^2) \in G \subset \mathbb{R}^2$. The bold-faced type of \mathbf{r} or \mathbf{X} means that they are vectors in three-dimensional space. Fig. 1 illustrates this mapping, which is called a “chart.” Generally, we cannot hope to parametrize a given surface with a single chart—this does not even work for something as quotidian as the surface of a sphere. Instead, a surface (or, more generally, a differentiable manifold) must usually be constructed as the union of several charts, appropriately called an “atlas.” Where two charts overlap, the mappings must be connected differentiably (Kreyszig, 1991; do Carmo, 1976;

Willmore, 2012; Lovelock and Rund, 1989; Frankel, 2004; Darling, 1994; Schutz, 1980): If the two parametrizations $\mathbf{X}(u)$ and $\mathbf{Y}(v)$ overlap on some patch of the surface, then the mapping $\mathbf{Y}^{-1} \circ \mathbf{X}$ from the u -space to the v -space, as well as its inverse $\mathbf{X}^{-1} \circ \mathbf{Y}$ have to be sufficiently many times differentiable (i.e., constitute a “diffeomorphism”).

Having agreed on a parametrization of a surface à la Eq. (3), we can now construct a coordinate system on every point of the surface in the following way. First, we define the two vectors

$$\mathbf{e}_a := \frac{\partial \mathbf{X}}{\partial u^a} = \partial_a \mathbf{X}, \quad a \in \{1, 2\}. \quad (4)$$

It is fairly obvious that \mathbf{e}_a is tangent to the surface and points into the direction in which the value of the coordinate u^a increases—just imagine that u^a somehow measures “time” along this particular coordinate line, then \mathbf{e}_a would be the velocity vector along this coordinate curve, which must evidently be tangential to it and thus to the surface. The set $\{\mathbf{e}_1, \mathbf{e}_2\}$ then spans the local tangent plane to the surface, provided the two vectors are not collinear (if they are, something went terribly wrong with our choice of the parametrization).

While the coordinates u^a were chosen to have an upper index, the vectors \mathbf{e}_a now have a lower one. This is much more than convention. Before we proceed, we must discuss this seemingly incidental detail.

2.3. Excursion: covariant vs. contravariant

The placement of indices in Eq. (4) (and really for the rest of all that follows) is part of a clever formalism that distinguishes between “covariant” (lower) and “contravariant” (upper) components of geometric objects such as vectors or tensors. These objects live in different mathematical spaces (tangent and cotangent spaces), but physicists prefer to say that they “transform differently.” For instance, if we were to define a new set of coordinates, \bar{u}^b , which are given by some (sufficiently smooth and invertible) functions of the old coordinates u^a , then the differential du^a of the coordinates u^a would obviously transform as follows:

$$du^a = \sum_b \left(\frac{\partial u^a}{\partial \bar{u}^b} \right) d\bar{u}^b, \quad (5a)$$

where we used nothing but the chain rule. Even if the transformation of the coordinates is very nonlinear, the differentials transform linearly, namely with the Jacobian $(\partial u^a / \partial \bar{u}^b)$ of the transformation equations.

The central point to appreciate is that not all one-index-objects transform like Eq. (5a). For instance, the tangent vectors \mathbf{e}_a transform differently:

$$\mathbf{e}_a = \frac{\partial \mathbf{X}}{\partial u^a} = \sum_b \frac{\partial \mathbf{X}}{\partial \bar{u}^b} \frac{\partial \bar{u}^b}{\partial u^a} = \sum_b \left(\frac{\partial \bar{u}^b}{\partial u^a} \right) \bar{\mathbf{e}}_b. \quad (5b)$$

This is again a linear transformation, but the Jacobian $(\partial \bar{u}^b / \partial u^a)$ is the inverse of the one that appeared in the previous case (5a).

The fact that there are two different transformation laws might appear like a nuisance, but it enables something extremely important: the construction of coordinate invariant scalars. To see this, define a product between (the components of) a contravariant vector X^a and (the components of) a covariant vector Y_b by multiplying the components and summing over them: $\sum_a X^a Y_a$. Such an operation is known as a “contraction.” If we now ask how this object transforms under a change of coordinates, two transformation matrices would appear—one for the first factor and one for the second factor. But because of the co- vs. contravariant nature of the

two factors, one of the Jacobians is the inverse of the other, and hence they cancel:

$$\begin{aligned} \sum_a X^a Y_a &= \sum_a \left[\sum_b \left(\frac{\partial u^a}{\partial \bar{u}^b} \right) \bar{X}^b \right] \left[\sum_c \left(\frac{\partial \bar{u}^c}{\partial u^a} \right) \bar{Y}_c \right] \\ &= \sum_{b,c} \bar{X}^b \bar{Y}_c \sum_a \left(\frac{\partial u^a}{\partial \bar{u}^b} \right) \left(\frac{\partial \bar{u}^c}{\partial u^a} \right) = \sum_{b,c} \bar{X}^b \bar{Y}_c \frac{\partial \bar{u}^c}{\partial \bar{u}^b} \\ &= \sum_{b,c} \bar{X}^b \bar{Y}_c \delta_b^c = \sum_b \bar{X}^b \bar{Y}_b, \end{aligned} \quad (6)$$

where δ_b^c are the components of the unit matrix (or the “Kronecker-delta,” which is 1 if $b=c$ and 0 otherwise). This means that the numerical value of the contraction is the same when evaluated in the two different coordinate systems. It is *independent of the coordinates*, or as physicists are wont to say, the expression is *reparametrization invariant*. This is very important, because if such expressions are unaffected by coordinate changes, they express deeper physical or geometric properties than the components they are constructed from. Such a contraction can work its scalar magic only with oppositely transforming components. The placement of indices not only helps us to keep track of this, but also enables the following nifty (“Einstein”-) convention: Whenever you find two identical (“dummy”) indices, one upstairs and one downstairs, a summation is implied over their permissible range (which here is of course from 1 to 2). The previous equation can then succinctly be written as

$$X^a Y_a = \left(\frac{\partial u^a}{\partial \bar{u}^b} \right) \bar{X}^b \left(\frac{\partial \bar{u}^c}{\partial u^a} \right) \bar{Y}_c = \bar{X}^b \bar{Y}_c \left(\frac{\partial u^a}{\partial \bar{u}^b} \right) \left(\frac{\partial \bar{u}^c}{\partial u^a} \right) = \bar{X}^b \bar{Y}_b.$$

2.4. Important geometric objects

In Section 2.2 we have introduced a general-purpose surface parametrization, Eq. (3), and from it defined the two tangent vectors $\mathbf{e}_a = \partial_a \mathbf{X}$. We can complete these into a full local coordinate system in \mathbb{R}^3 by defining the associated normal vector:

$$\mathbf{n} := \frac{\mathbf{e}_1 \times \mathbf{e}_2}{|\mathbf{e}_1 \times \mathbf{e}_2|}. \quad (7)$$

It is customary to normalize \mathbf{n} to unit length. The same is not true for the tangent vectors, which generally are neither of unit length nor in fact perpendicular to each other. It hence makes sense to quantify the “lack of orthonormality” by defining the tensor

$$g_{ab} := \mathbf{e}_a \cdot \mathbf{e}_b, \quad (8)$$

where the dot “ \cdot ” refers to the ordinary scalar product of the two (bold faced!) vectors in the embedding three-dimensional space. This tensor g_{ab} , which is evidently symmetric under an exchange of its two indices, is the first fundamental form of the surface, also called the “metric tensor” or simply the “metric.” Both indices are lower indices, hence g_{ab} are the covariant components of an abstract tensor. The contravariant components g^{bc} are defined by demanding that they contract with the covariant ones to give the unit matrix:

$$g_{ab} g^{bc} = g_a^c \equiv \delta_a^c. \quad (9)$$

Using the metric tensor we can create co- and contravariant versions of any vector or tensor by “raising” or “lowering” indices, for instance

$$X^a = g^{ab} X_b \quad \text{or} \quad Y_a{}^c = Y_a{}^{dc} g_{bd}. \quad (10)$$

The reader might want to check that the cancellation of Jacobians works just fine with these definitions.

At this point maybe a little side note is appropriate: When tensors with more than one index occur, their sometimes elaborate positions tend to confuse a young padawan of differential geometry, but it is really quite simple: from left to right the ordering enumerates the argument of the tensor—one, two, three, and so on. Just as the rows and columns of a matrix must be distinguished, so must the index referring to a given argument or “slot” of a tensor. Upstairs vs. downstairs, in contrast, refers to contravariant and covariant components. For instance, the notation $K_a{}^b$ refers to the components of a second-rank tensors, the first of which, labeled for now with “ a ”, is a covariant component, and the second one, “ b ”, is a contravariant one. We can obtain this tensor from its twofold covariant components by raising the second index. If we instead were to raise the first component, we would get a different object:

$$K_a{}^b = K_{ac} g^{cb} \quad \text{not the same as} \quad K^a{}_b = K_{bc} g^{ca}. \quad (11a)$$

Which of the components is labeled “ a ” and which one is labeled “ b ” is a different matter still, since it is the choice of the user how to name them. In that sense, the following two tensors can be identical:

$$K_a{}^b = K_{ac} g^{cb} \quad \text{vs.} \quad K_b{}^a = K_{bc} g^{ca}; \quad (11b)$$

both emerge from the twofold covariant components of a second rank tensor after lifting the second component—they are simply differently labeled. These two examples also show that generally $K^a{}_b \neq K_b{}^a$. The exception is if the tensor is symmetric in its two indices when they are both co- or contravariant. In that case one generally does not bother to shift them into their first and second position and simply writes them on top of each other:

$$\text{if } K_{ab} = K_{ba} \quad \text{then} \quad K^a{}_b = K_b{}^a \equiv K_b^a. \quad (12)$$

Conversely, writing K_b^a implies that we know that the tensor is symmetric—for if it were not, it would be unclear whether lowering the index “ a ” should make it the first or the second one.

So much for index ordering. Let us return to the metric tensor g_{ab} . Its *determinant* is written as g . We can connect it to the tangent vectors as follows: using the antisymmetric ϵ -symbol to express the determinant, we can calculate

$$\begin{aligned} g &= \frac{1}{2} \epsilon^{ac} \epsilon^{bd} g_{ab} g_{cd} = g_{11} g_{22} - g_{12} g_{21} \\ &= g_{11} g_{22} - (\mathbf{e}_1 \cdot \mathbf{e}_2)^2 = g_{11} g_{22} [1 - \cos^2(\angle(\mathbf{e}_1, \mathbf{e}_2))] \\ &= |\mathbf{e}_1|^2 |\mathbf{e}_2|^2 \sin^2(\angle(\mathbf{e}_1, \mathbf{e}_2)) = |\mathbf{e}_1 \times \mathbf{e}_2|^2. \end{aligned} \quad (13)$$

Since $\mathbf{e}_1 du^1$ and $\mathbf{e}_2 du^2$ span the local infinitesimal area element on our surface, this means that the covariant area element can be written as

$$dA = |\mathbf{e}_1 du^1 \times \mathbf{e}_2 du^2| = \sqrt{g} du^1 du^2, \quad (14)$$

an identity that explains why the metric determinant is so important; $dA = \sqrt{g} du^1 \dots du^d$ is actually true in any dimension and does not rely on a cross product.

If there is a first fundamental form, there is probably also a second one. It is defined as⁴

$$K_{ab} = \mathbf{e}_a \cdot \partial_b \mathbf{n}^* = -\mathbf{n} \cdot \partial_b \mathbf{e}_a = -\mathbf{n} \cdot \partial_{ab} \mathbf{X}. \quad (15)$$

The equality at “ $*$ ” follows from differentiating the obvious identity $\mathbf{e}_a \cdot \mathbf{n} = 0$, and the last equality shows that K_{ab} is a symmetric tensor under index exchange, just like the metric. The tensor K_{ab}

⁴ The mathematical literature tends to define the curvature tensor K_{ab} with the opposite minus sign. There is no deeper significance in that choice, it is convention whether one chooses curvature away from the normal vector as positive or as negative. The present convention chooses the former, such that a sphere with outward pointing normal vector has a positive curvature.

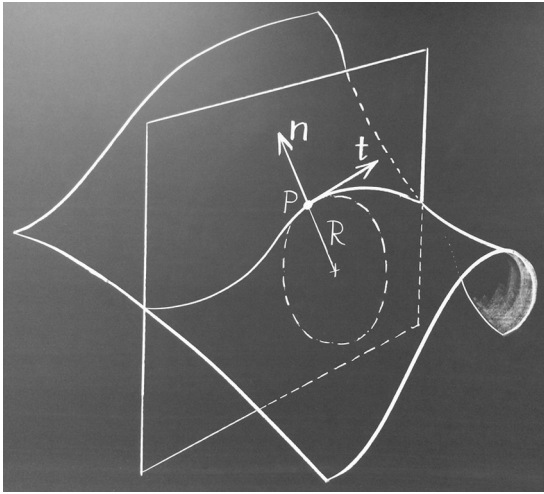


Fig. 2. Illustration of normal curvature: Pick a point P on a surface and select a direction by specifying a tangent vector \mathbf{t} . The plane spanned by \mathbf{t} and the surface's normal vector \mathbf{n} intersects the surface in a planar curve, whose local curvature $K_{||} = 1/R$ is the normal curvature of the surface at P into the direction \mathbf{t} .

is the “extrinsic curvature tensor” (actually, its covariant components), and it quantifies the extent of local curvature of the surface in the embedding three-dimensional space. This is intuitive, since it essentially measures how the normal vector changes as one moves along the surface. Unlike the metric tensor g_{ab} , the tensor K_{ab} can only be defined if we have a normal vector, and therefore it requires an “embedding” of the surface into some higher-dimensional space (here, just three-dimensional space). This is why K_{ab} is called the “extrinsic” curvature tensor. The counterpart, objects that do not require the normal vector for their definition, are called “intrinsic.” We will soon meet a different curvature tensor, the “Riemann tensor,” which is intrinsic.

More specifically, consider a point P on the surface and a unit vector $\mathbf{t} = t^a \mathbf{e}_a$ at P that is tangent to the surface (see Fig. 2). If we cut the surface with a plane that contains both \mathbf{n} and \mathbf{t} , we create a cross-sectional curve, whose curvature at P (up to possibly a minus sign) is given by $K_{||} = K_{ab} t^a t^b$ and which is called the *normal curvature* of the surface at P into the direction \mathbf{t} . Hence, the local normal curvature is a quadratic form, and this means that there will be two directions along which the curvature is extremal. These so-called principal directions $\mathbf{p}_i = p_i^a \mathbf{e}_a$ correspond to the eigenvectors of K_{ab} , and the associated eigenvalues K_i are called the principal curvatures:

$$K_{ab} p_i^b = K_i g_{ab} p_i^a, \quad (16a)$$

or after lifting one index:

$$K_b^a p_i^b = K_i p_i^a. \quad (16b)$$

Hence, the *trace* K of the extrinsic curvature tensor is a scalar invariant, called the (total) extrinsic curvature:⁵

$$K := g^{ab} K_{ab} = K_a^a = K_1^1 + K_2^2 = K_1 + K_2. \quad (17)$$

Also, since the principal directions are the eigenvectors of the symmetric curvature tensor, they are necessarily orthogonal:

$$\mathbf{p}_1 \cdot \mathbf{p}_2 = p_1^a \mathbf{e}_a \cdot p_2^b \mathbf{e}_b = p_1^a p_2^b g_{ab} = 0. \quad (18)$$

Knowing the principal curvatures, we can easily compute any normal curvature, if we know the angle ϑ of the cutting direction with

respect to the principal directions. To see this, let us assume without loss of generality that $\{\mathbf{p}_1, \mathbf{p}_2\}$ are normalized, and define our arbitrary cutting direction \mathbf{t} as

$$\mathbf{t} = \cos \vartheta \mathbf{p}_1 + \sin \vartheta \mathbf{p}_2. \quad (19)$$

The normal curvature $K_{||}$ along \mathbf{t} is then given by

$$\begin{aligned} K_{||} &= t^a t^b K_{ab} \\ &= (\cos \vartheta p_1^a + \sin \vartheta p_2^a)(\cos \vartheta p_1^b + \sin \vartheta p_2^b) K_{ab} \\ &= \cos^2 \vartheta p_1^a p_1^b K_{ab} + \sin^2 \vartheta p_2^a p_2^b K_{ab} \\ &= \cos^2 \vartheta K_1 + \sin^2 \vartheta K_2. \end{aligned} \quad (20)$$

This result is known as the Theorem of Euler (Kreyszig, 1991; do Carmo, 1976).

A second invariant of the curvature tensor, this time quadratic, is obtained by taking the *determinant* of the matrix K_a^b . The associated scalar is called the Gaussian curvature and given by

$$K_G = \det(K_a^b) = K_1 K_2. \quad (21)$$

Let us make a brief example: Consider a sphere of radius R , parametrized according to Eq. (2b). We find

$$\mathbf{e}_\vartheta = R \begin{pmatrix} \cos \vartheta \cos \varphi \\ \cos \vartheta \sin \varphi \\ -\sin \vartheta \end{pmatrix}, \quad \mathbf{e}_\varphi = R \begin{pmatrix} -\sin \vartheta \sin \varphi \\ \sin \vartheta \cos \varphi \\ 0 \end{pmatrix}, \quad (22a)$$

and with the enumeration ϑ = first coordinate and φ = second coordinate we get the metric⁶

$$g_{ab} = R^2 \begin{pmatrix} 1 & 0 \\ 0 & \sin^2 \vartheta \end{pmatrix}, \quad g^{ab} = \frac{1}{R^2} \begin{pmatrix} 1 & 0 \\ 0 & \sin^{-2} \vartheta \end{pmatrix}. \quad (22b)$$

The normal vector is given by

$$\mathbf{n} = \frac{\mathbf{e}_\vartheta \times \mathbf{e}_\varphi}{|\mathbf{e}_\vartheta \times \mathbf{e}_\varphi|} = \begin{pmatrix} \sin \vartheta \cos \varphi \\ \sin \vartheta \sin \varphi \\ \cos \vartheta \end{pmatrix} = \frac{1}{R} \mathbf{r}. \quad (22c)$$

Since $\partial_\vartheta \mathbf{n} = R^{-1} \mathbf{e}_\varphi$ and $\partial_\varphi \mathbf{n} = R^{-1} \mathbf{e}_\vartheta$, we find $K_{ab} = R^{-1} g_{ab}$. The curvature tensor is diagonal and both eigenvalues are R^{-1} —quite plausible for a sphere of radius R .

2.5. Covariant differentiation

Not everything with a bunch of indices is a tensor—in the sense that it would transform according to Eq. (5a) with one Jacobian ($\partial u^a / \partial \bar{u}^b$) for every upper index and Eq. (5b) with one inverse Jacobian ($\partial \bar{u}^b / \partial u^a$) for every lower index. Consider for instance the

⁶ The dot over the equation sign should remind us of the following subtlety: Writing the metric tensor g_{ab} as a 2×2 matrix is slightly misleading, because g_{ab} is not a matrix. It is a twofold covariant tensor which, if contracted with a contravariant vector results in a covariant vector. Matrices, in contrast, should take a contravariant vector and turn it into another contravariant vector (or a covariant vector into another covariant vector). Given this, a second-rank tensor with one covariant and one contravariant index is a proper matrix. Still, we might want to succinctly write the components of g_{ab} , and we can of course do this in the form of a 2×2 number scheme. We should just remember that this is a slight misuse of notation.

⁵ Historically, people often consider the quantity $H = (1/2)K = (1/2)(K_1 + K_2)$, which is called the “mean curvature.” Since nothing is gained by the extra factor of $1/2$, I will avoid this notation here.

partial coordinate derivative of a tangent vector, $\partial_a \mathbf{e}_b$. How does this object transform? Let us check:

$$\begin{aligned} \partial_a \mathbf{e}_b &= \frac{\partial}{\partial u^a} \frac{\partial \mathbf{X}}{\partial u^b} = \frac{\partial}{\partial u^a} \left(\frac{\partial \mathbf{X}}{\partial \bar{u}^d} \frac{\partial \bar{u}^d}{\partial u^b} \right) \\ &= \left(\frac{\partial}{\partial \bar{u}^c} \frac{\partial \mathbf{X}}{\partial \bar{u}^d} \right) \frac{\partial \bar{u}^c}{\partial u^a} \frac{\partial \bar{u}^d}{\partial u^b} + \frac{\partial \mathbf{X}}{\partial \bar{u}^d} \frac{\partial^2 \bar{u}^d}{\partial u^a \partial u^b} \\ &= \partial_c \bar{\mathbf{e}}_d \left(\frac{\partial \bar{u}^c}{\partial u^a} \right) \left(\frac{\partial \bar{u}^d}{\partial u^b} \right) + \bar{\mathbf{e}}_d \frac{\partial^2 \bar{u}^d}{\partial u^a \partial u^b}. \end{aligned} \quad (23)$$

The first term looks alright, two Jacobians for the two indices, but the additional second term spoils the correct transformation law— $\partial_a \mathbf{e}_b$ is not a tensor!

Not only have we just seen that innocent looking objects with indices need not be tensors, we have found that this can happen to very important objects: derivatives of vectors (and, generally, tensors). But the notion of a derivative is essential, and we need rescue it. The origin of this problem is that on a curvilinear manifold (such as our surface) not just the tensors living on it but also the coordinate system itself is position dependent, thus a coordinate derivative will drag the arbitrariness of a parametrization into the tensor's derivative, spoiling its covariant nature. This can be fixed by defining a *covariant derivative* ∇_a which—in some sense—simply subtracts out the offending bit. The correction works differently for covariant and contravariant components and has the following form:

$$\nabla_a X^b = \partial_a X^b + X^c \Gamma_{ac}^b, \quad (24a)$$

$$\nabla_a Y_b = \partial_a Y_b - Y_c \Gamma_{ab}^c, \quad (24b)$$

where the new object Γ_{ab}^c is called the Christoffel symbol of the second kind. It is not a tensor either, in fact, it better not be, for otherwise it could not subtract out the non-covariant remnant of the first term. It is defined as

$$\Gamma_{abc} = \frac{1}{2} [\partial_a g_{bc} + \partial_b g_{ca} - \partial_c g_{ab}], \quad (25a)$$

$$\Gamma_{ab}^c = g^{cd} \Gamma_{abd}, \quad (25b)$$

and the symbol Γ_{abc} is sometimes called the Christoffel symbol of the first kind. Evidently, Γ_{abc} is symmetric in its first two indices, and hence Γ_{ab}^c is symmetric in its lower two indices. Observe that the Christoffel symbols can be calculated in a fully intrinsic way, since they only depend on the metric and its partial derivatives. The concept of covariant differentiation is therefore intrinsic: it does not require an embedding.

If we have tensors with more indices, then every upper index gets an extra Christoffel-term such as the one in Eq. (24a), and every lower index get an extra term like the one in Eq. (24b). For instance, the covariant derivative of the third-rank tensor T_{ab}^c is given by

$$\nabla_d T_{ab}^c = \partial_d T_{ab}^c - T_{ib}^c \Gamma_{da}^i - T_{ai}^c \Gamma_{db}^i + T_{ab}^i \Gamma_{di}^c. \quad (26)$$

If there is no index, then no extra Christoffel term is necessary, because partial and covariant derivative are the same for scalars: $\nabla_a \phi = \partial_a \phi$, or $\nabla_a \mathbf{X} = \partial_a \mathbf{X}$.

It can be verified by direct calculation that the thus defined operation on a tensor produces a new object that again transforms like a tensor (with one more lower index), but verifying this does not answer a number of obvious and deep questions that arise at this point, such as: where does this construction come from? Why can it generalize the notion of a derivative to curved surfaces? And is this the only way it could be done? Exploring these issues quickly leads to concepts which lie at the heart not only of differential geometry but of modern physics (for instance the foundations of gauge theory), but of course the present review cannot follow up on any of this. The interested reader will find answers

to all these questions in the more mathematics-oriented literature (Kreyszig, 1991; do Carmo, 1976, 1992; Willmore, 2012; Spivak, 1970, 1975a,b; Lovelock and Rund, 1989; Frankel, 2004; Schutz, 1980; Darling, 1994; Flanders, 1989), but for now knowing them will not be necessary to follow the rest of this review.⁷

It seems that the prescription is now this: Whenever we want to differentiate tensors, we first determine the Christoffel symbols and amend the partial derivatives with the appropriate extra terms. Yet, nothing could be further from the truth. Christoffel kerfuffle is messy and intrinsically parametrization-laden, so the aim really should be to rewrite all partial derivatives by covariant ones and from then on exclusively work with the latter throughout the rest of the calculation. This indeed works rather well, since covariant derivatives have nice properties that make them easier to work with than the ordinary partial coordinate derivatives. The Lemma of Ricci for instance states that (Kreyszig, 1991)

$$\nabla_a g_{bc} = 0, \quad \nabla_a g^{bc} = 0, \quad \nabla_a g = 0. \quad (27)$$

In other words, the metric and the metric determinant behave like constants with respect to covariant differentiation. This in particular means that *raising and lowering indices commutes with taking covariant derivatives*, something that is enormously useful.⁸

But how do we get hold of covariant derivatives in the first place? Fortunately, we usually do not have to do anything at all: they naturally “happen” to us without any particular effort, because covariant derivatives are the physically meaningful ones. They are “natural,” while partial ones are not, for the latter are contaminated by the arbitrariness of one's specific parametrization. Hence, if in the process of generalizing a known physical equation to curved space a derivative is needed, virtually always the correct way to proceed is to simply replace all ordinary derivatives by covariant ones.

Another useful property is that covariant differentiation, combined with integration over covariant area elements, follows the usual rules of partial integration. Let us illustrate this by proving one example. Using the definition of the Christoffel symbol, one can verify that⁹

$$\partial_a \sqrt{g} = \sqrt{g} \Gamma_{ba}^b. \quad (28)$$

⁷ As a little teaser: apparently the offending bit in Eq. (23) is symmetric in the indices a and b . This suggests one way of eliminating it, namely to *antisymmetrize* one's expressions. This path leads to the Cartan Calculus of antisymmetric differential forms and the exterior derivative (Frankel, 2004; Schutz, 1980; Darling, 1994; Flanders, 1989). Alternatively, one could use a given vector field on a surface and the “flow” it induces as a means to drag tensors along a surface, which enables one to compare objects that live in different tangent or cotangent spaces. Applying this to nearby tensors leads to the Lie derivative (Frankel, 2004; Schutz, 1980; Darling, 1994), a very natural construct for instance in variational problems. Both derivatives are more “basic” than the covariant derivative we have defined, since they do not require the manifold to have a metric.

⁸ Conversely, one is asking for trouble if one were to define a partial derivative with an upper index, ∂^a . Besides the non-tensor issues (which one could fix by bringing in more Christoffels), we have a definition problem: since $g^{ab}[\partial_b(\dots)] \neq \partial_b[g^{ab}(\dots)]$, raising the index on ∂_a does not commute with differentiation, and so it is not even clear what the symbol ∂^a would mean: is the index raised before or after the operator differentiates?

⁹ For completeness: This equation shows that there is one more subtlety we have skipped: Clearly, \sqrt{g} has no index, so its covariant derivative ought to coincide with its partial derivative. But Ricci's lemma tells us that $\nabla_a \sqrt{g} = 0$, while Eq. (28) now claims that the partial derivative does not vanish. What went wrong? The answer is that \sqrt{g} is a tensor *density* (of weight 1), for which the transformation laws are slightly different. We shall not go into details here, but the curious reader will find more information for instance in Lovelock and Rund (1989).

Hence, we also have

$$\begin{aligned} \frac{\partial_a(X^a\sqrt{g})}{\sqrt{g}} &= \frac{\sqrt{g}\partial_a X^a + X^a\partial_a\sqrt{g}}{\sqrt{g}} \\ &= \partial_a X^a + X^a\Gamma_{ba}^b = \nabla_a X^a. \end{aligned} \quad (29)$$

Using this, let us rewrite the following surface integral

$$\begin{aligned} \int dA Y \nabla_a X^a &= \int d^2u \sqrt{g} Y \frac{\partial_a(X^a\sqrt{g})}{\sqrt{g}} \\ &= \int d^2u Y \partial_a(X^a\sqrt{g}) \\ &\stackrel{*}{=} - \int d^2u (\partial_a Y)(X^a\sqrt{g}) \\ &= - \int dA X^a \nabla_a Y, \end{aligned} \quad (30)$$

where at “*” we integrated by parts using the rules for “ordinary” derivatives and integrals (and also ignored a boundary term) and where in the last step we used $\partial_a Y = \nabla_a Y$, which is true because Y is a scalar and requires no extra Christoffels to switch between partial and covariant derivatives. Notice that the overall transformation simply mirrors integration by parts on the covariant level. This also works for higher order tensors.

If we do not want to discard the boundary terms, we can rewrite them in a way that is completely equivalent to the three-dimensional version of Gauss’ theorem. If we have a surface patch \mathcal{P} , then a total divergence of a vector v^a can be rewritten as

$$\int_{\mathcal{P}} dA \nabla_a v^a = \oint_{\partial\mathcal{P}} ds l_a v^a, \quad (31)$$

where ds is the line element on the boundary $\partial\mathcal{P}$ and l_a is the outward pointing unit normal that is tangential to the surface and normal to the integration contour.

From two covariant first order derivatives we can construct a scalar second order one:

$$\Delta = \nabla_a \nabla^a = g^{ab} \nabla_a \nabla_b. \quad (32)$$

This is nothing but the generalization of the Laplace operator to curved space (sometimes called the “Laplace–Beltrami operator”). If we insist on applying it in coordinates, we need to decide what object we apply it on. For instance, if we want to apply it on a scalar ϕ , then using the special choice $X^a = \nabla^a \phi = g^{ab} \nabla_b \phi = g^{ab} \partial_b \phi$ in Eq. (29), we find

$$\Delta \phi = \frac{1}{\sqrt{g}} \frac{\partial}{\partial u^a} \left[\sqrt{g} g^{ab} \frac{\partial}{\partial u^b} \phi \right], \quad (33)$$

which the reader might recognize as the expression for how the Laplacian acts on a scalar function in general curvilinear coordinates.

While covariant derivatives seem to work just like ordinary partial ones, there are differences as well. Arguably the most important one is that, generally, *covariant derivatives do not commute*. Instead, when applied to a vector, the commutator of covariant derivatives turns out to be (Spivak, 1970; do Carmo, 1992; Schutz, 1980)

$$[\nabla_a, \nabla_b]V_c = \nabla_a \nabla_b V_c - \nabla_b \nabla_a V_c = R_{abcd}V^d, \quad (34)$$

where the tensor R_{abcd} is the so-called Riemann curvature tensor, which we will meet again in a short while.

2.6. Gauss, Weingarten, Codazzi, Mainardi

Having a coordinate system $\{\mathbf{e}_1, \mathbf{e}_2, \mathbf{n}\}$ on the surface is useful, since we can expand any vector in this local basis. But once we perform derivatives, we then also need to differentiate the coordinate system. This is closely related to the problem we have solved

in the previous section, and as a consequence, the solution is now very easy. Consider for instance the derivative of \mathbf{n} . It will again be a vector in three-dimensional space, and so we can expand it in the local coordinate system. It will also have one more index (from the differentiation), and so we can write it as $\nabla_a \mathbf{n} = X^c{}_a \mathbf{e}_c + Y_a \mathbf{n}$ with some as yet undetermined tensors $X^c{}_a$ and Y_a . Since $\mathbf{n}^2 = 1$ we know that $0 = \nabla_a \mathbf{n}^2 = 2 \mathbf{n} \cdot \nabla_a \mathbf{n}$, and so we must have

$$0 = \mathbf{n} \cdot \nabla_a \mathbf{n} = \mathbf{n} \cdot (X^c{}_a \mathbf{e}_c + Y_a \mathbf{n}) = Y_a, \quad (35)$$

because $\mathbf{n} \cdot \mathbf{e}_c = 0$. And from the definition of the (extrinsic) curvature tensor in Eq. (15) we know

$$K_{ab} = \mathbf{e}_a \cdot \nabla_b \mathbf{n} = \mathbf{e}_a \cdot (X^c{}_b \mathbf{e}_c + Y_b \mathbf{n}) = g_{ac} X^c{}_b = X_{ab}. \quad (36)$$

We thereby arrive at the equation of Weingarten:

$$\nabla_a \mathbf{n} = K_a^b \mathbf{e}_b. \quad (37a)$$

Similarly, we can derive the equation of Gauss:

$$\nabla_a \mathbf{e}_b = -K_{ab} \mathbf{n}. \quad (37b)$$

This brings us to our last point: In the theory of curves, any choice of curvature and torsion functions results in a unique space curve (modulo rotations and translations, and ignoring some subtle degeneracy issues) (Kreyszig, 1991; do Carmo, 1976; Kamien, 2002). Is the same also true for surfaces, meaning, if we pick some (suitably differentiable) metric and curvature tensors, g_{ab} and K_{ab} , do they describe a surface? The answer is in general no, since further integrability conditions must be satisfied. As usual, they derive from the need of some second (partial) derivatives to commute,¹⁰ in this case

$$\partial_a \partial_b \mathbf{e}_c \stackrel{\perp}{=} \partial_b \partial_a \mathbf{e}_c. \quad (38)$$

Evaluating the two derivatives gives rise to a lengthy equation, both sides of which have components along \mathbf{n} and along \mathbf{e}_i . The normal component yields a condition known as the Codazzi–Mainardi equation, which using covariant derivatives can be written as follows:

$$\nabla_a K_{bc} - \nabla_b K_{ac} = 0. \quad (39)$$

The tangential component results in an equation that (also) goes under the name equation of Gauss:

$$K_{ac} K_{bd} - K_{ad} K_{bc} = R_{abcd}, \quad (40)$$

where R_{abcd} is again the Riemann tensor, for which one now arrives at the following explicit representation:¹¹

$$R_{abcd} = \partial_c \Gamma_{bda} - \partial_d \Gamma_{bca} + \Gamma_{bc}^e \Gamma_{ade} - \Gamma_{bd}^e \Gamma_{ace}. \quad (41)$$

Eq. (40) should come as a big surprise. Notice that its right hand side, the Riemann tensor, can be calculated by only knowing the metric (since the Christoffel symbols can, see Eqs. (25a,b)). This means that it is an intrinsic quantity—there is no need for an embedding. This is different from the curvature tensor K_{ab} , which is extrinsic because it needs the normal vector for its definition. And yet, Eq. (40) states that a suitable combination of the extrinsic curvature tensor is equal to the intrinsic Riemann tensor.

We can contract the Gauss equation twice, thus also introducing two more objects, the Ricci tensor R_{ab} and the Ricci scalar R :

$$R_{bd} = g^{ac} R_{abcd} = K K_{bd} - K_{ba} K_d^a, \quad (42a)$$

¹⁰ As a better-known example, think of thermodynamics, where the Maxwell-relations are integrability conditions resulting from the fact that second derivatives of thermodynamic potentials must commute.

¹¹ To be fair, to prove that this tensor is indeed identical to the one which earlier occurred in Eq. (34) requires some further math.

$$R = g^{bd}R_{bd} = K^2 - K_a^b K_b^a = 2K_G. \quad (42b)$$

This shows that the Gaussian curvature K_G , defined in Eq. (21) as the determinant of the extrinsic curvature tensor, is in fact fully intrinsic. Gauss was so impressed when he discovered this fact, that he called it the *Theorema Egregium*, the “outstanding theorem.”

For two-dimensional surfaces the Gaussian curvature is the *only* independent component of the Riemann tensor: Despite its impressive set of indices, it contains no more information than the Ricci scalar, since we have

$$R_{abcd} \stackrel{d=2}{=} K_G [g_{ac}g_{bd} - g_{ad}g_{bc}], \quad (43a)$$

$$R_{ab} \stackrel{d=2}{=} \frac{1}{2} R g_{ab} = K_G g_{ab}. \quad (43b)$$

This is no longer true in higher dimensions, which matters greatly for general relativity.

2.7. Monge gauge

Even though the central aim of this section is to avoid specific parametrizations, some of them occur so frequently that it is useful to understand how to translate between them and a purely geometric language. The by far most popular parametrization is *Monge gauge*, which describes a surface as a height function $h(x, y)$ above a flat reference plane. For instance, Eq. (2a) describes the surface of a sphere in Monge gauge.

Using the results derived so far, we can calculate the geometric surface objects as they derive from this specific parametrization, which we can formalize as

$$\mathbf{r} = \mathbf{X}(x, y) = \begin{pmatrix} x \\ y \\ h(x, y) \end{pmatrix}. \quad (44)$$

The local tangent vectors are then given by

$$\mathbf{e}_x = \begin{pmatrix} 1 \\ 0 \\ h_x \end{pmatrix}, \quad \mathbf{e}_y = \begin{pmatrix} 0 \\ 1 \\ h_y \end{pmatrix}, \quad (45)$$

where we used the abbreviation $h_x = \partial_x h$. The metric is now given by

$$g_{ab} \stackrel{\cdot}{=} \begin{pmatrix} 1 + h_x^2 & h_x h_y \\ h_x h_y & 1 + h_y^2 \end{pmatrix}, \quad (46a)$$

$$g^{ab} \stackrel{\cdot}{=} \frac{1}{1 + h_x^2 + h_y^2} \begin{pmatrix} 1 + h_y^2 & -h_x h_y \\ -h_x h_y & 1 + h_x^2 \end{pmatrix}. \quad (46b)$$

These matrices are not diagonal: even though the coordinates on the base plane are Cartesian, the metric on the surface is clearly not. Its determinant is given by

$$g = 1 + h_x^2 + h_y^2 = 1 + (\nabla h)^2, \quad (47)$$

where we defined the two-dimensional gradient operator on the base plane, $\nabla = (\partial_x, \partial_y)$.¹² Hence, the area element in Monge gauge is

$$dA = \sqrt{1 + (\nabla h)^2} dx dy. \quad (48)$$

The normal vector is found to be

$$\mathbf{n} = \frac{\mathbf{e}_x \times \mathbf{e}_y}{\sqrt{g}} = \frac{1}{\sqrt{1 + (\nabla h)^2}} \begin{pmatrix} -h_x \\ -h_y \\ 1 \end{pmatrix}, \quad (49)$$

which leads to the second fundamental form

$$K_{ab} \stackrel{\cdot}{=} -\frac{1}{\sqrt{1 + (\nabla h)^2}} \begin{pmatrix} h_{xx} & h_{xy} \\ h_{xy} & h_{yy} \end{pmatrix}. \quad (50)$$

From this we can finally calculate the total and the Gaussian curvature:

$$K = -\nabla \cdot \left(\frac{\nabla h}{\sqrt{1 + (\nabla h)^2}} \right), \quad (51a)$$

$$K_G = \frac{\det[\partial^2 h]}{(1 + (\nabla h)^2)^2}, \quad (51b)$$

where $\partial^2 h$ is the Hessian of the function $h(x, y)$.

A particularly important case occurs if the surface deviates only weakly from the flat reference plane, such that $|\nabla h| \ll 1$ and a number of convenient approximations are possible. In particular, we find

$$\sqrt{g} = \sqrt{1 + (\nabla h)^2} \approx 1 + \frac{1}{2} (\nabla h)^2, \quad (52)$$

which removes the square root from the area element. Also, the two curvatures in Eq. (51a,b) simplify to

$$K = -\text{Tr}[\partial^2 h] = -\nabla^2 h, \quad (53a)$$

$$K_G = \det[\partial^2 h]. \quad (53b)$$

This particular approximation is called “linearized Monge gauge,” and it is the framework within which the majority of all theoretical membrane science is done.

3. The Helfrich Hamiltonian

If we take a chemical or atomistic point of view, lipid membranes are assemblies with numerous inner degrees of freedom that give rise to larger-scale membrane behavior. Many quantitative models can be (and have been) developed to account for the local physics inside a lipid bilayer, and so it might appear surprising that on sufficiently large scales they all reduce to the same claim: the soft modes of membranes are curvature deformations. This, however, is nothing but scale-separation in action. If the local physics inside a bilayer is sufficiently well disentangled from the larger whole-membrane scale, then the energy, expressed at that larger scale, will only depend on observables definable on that larger scale. Almost every detail at the small scale, even though it is ultimately responsible for the very existence of the membrane, vanishes from the description. It will, however, restrict the types of large-scale theories that can be written down (for instance by imposing symmetry constraints), and it will ultimately determine the values of material parameters which emerge on the large scale but whose values cannot be predicted on that scale.

The Helfrich Hamiltonian is a perfect example for constructing an effective energy functional on the emergent scale of the whole membrane based on large-scale phenomenological considerations. Whatever the local physics might be, the form of the large scale Hamiltonian is essentially determined—kudos to the remarkable power of physical symmetry principles. In fact, Helfrich himself largely derived the Hamiltonian this way (Helfrich, 1973). In this section we will briefly revisit the reasoning, using the language

¹² The parametrization free expressions such as $g = 1 + (\nabla h)^2$ also hold if the base-plane is not represented in Cartesian coordinates but, say, in polar ones.

Table 1
Independent geometric surface scalars ordered by the number of derivatives, modulo boundary terms, taken from Ref. (Capovilla et al., 2003).

Order L^{-n}	Full set of independent surface scalars
$n=0$	1
$n=1$	K
$n=2$	K^2, K_G
$n=3$	K^3, KK_G
$n=4$	$K^4, K^2K_G, K_G^2, (\nabla_a K)(\nabla^a K)$

developed in the previous section, and then discuss a number of implications and ramifications.

3.1. What symmetry permits

As a first step, we must decide on the permissible and relevant physics at the local scale of the lipids. Let us revisit the most crucial aspects:

1. *Fluidity.* If lipids can laterally diffuse past each other but not easily escape the membrane, one's energy functional cannot contain the equivalent of in-plane shear stresses.
2. *Stretching.* Changing the area per lipid is a valid deformation and will cost energy, but thin plate theory shows that curvature deformations are lower in energy (Landau and Lifshitz, 1999)—see also Eq. (61). The modes we must understand first are therefore bending deformations.
3. *Tilting.* If lipids can tilt, this degree of freedom can couple to the shape. We may think of it as a vector-field defined on the curved surface that couples to the geometry. This term is typically regarded as small, but it would give rise to modifications with physical implications (Nelson and Powers, 1993; Powers and Nelson, 1995; Seifert et al., 1996; Selinger et al., 1996; Müller et al., 2005a; Tu and Seifert, 2007).
4. *Bilayer.* Whether membranes are bilayers or monolayers does not matter for the form of the large-scale Hamiltonian, save for one crucial point: One must know whether lipids can exchange between the two leaflets of a bilayers, for if they cannot, this creates a globally conserved quantity (the area difference between the two leaflets) to which the large-scale Hamiltonian will couple. This problem was not originally considered by Helfrich but investigated by later authors (Svetina and Žekš, 1989; Heinrich et al., 1993; Kralj-Iglić et al., 1993; Miao et al., 1994).

Since the energy is a scalar, it must be constructed from other scalars, and in the present case from objects associated with the membrane geometry. Fluidity implies that the membrane can have no memory of any previous shape, nor can the energy functional be sensitive to in-plane deformations. As such, the energy can only be a function of its current geometry.

While constructing an approximate large-scale Hamiltonian, one usually writes it as a series expansion in some smallness parameter. Here, we want the curvature of the membrane to be small compared to its inverse thickness, and this naturally leads to an expansion in terms of the number of derivatives needed to define a surface scalar, or equivalently, the power n in the dimension $1/\text{length}^n$ of the scalar. The objects we can work with are the two fundamental tensors of the surface, the Riemann tensor, and the covariant derivative.

Capovilla et al. (2003) have investigated this question, and their answers up to $1/\text{length}^4$ are collected in Table 1. At first sight, this table seems to be missing quite a number of obvious scalars, but others one could write are either not independent of the ones written down, or they are equivalent to them up to a boundary term that is usually irrelevant. For instance, the quadratic invariant $K_{ab}K^{ab}$ is equal to $K^2 - 2K_G$, see Eq. (42b), or by using the set of

identities derived in Section 2.6, one can show that $K_{ab}R^{ab} = KK_G$ or $K_a^b K_b^c K_c^a = K^3 - 3KK_G$, leading to no new invariant. Also, the fourth order term $K\Delta K$ is equivalent to the term $(\nabla_a K)(\nabla^a K)$ up to a boundary term, since $K\Delta K = \nabla_a(K\nabla^a K) - (\nabla_a K)(\nabla^a K)$, and the first term on the right hand side is a total derivative that can be moved to a boundary upon integrating by parts.

Based on this set of scalars, a natural expansion for a geometric Hamiltonian would be

$$H = \int dA \{ C^{(0)} + C^{(1)}K + C^{(2,1)}K^2 + C^{(2,2)}K_G + C^{(3,1)}K^3 + C^{(3,2)}KK_G + C^{(4,1)}K^4 + C^{(4,2)}K^2K_G + C^{(4,3)}K_G^2 + C^{(4,4)}(\nabla_a K)(\nabla^a K) + \mathcal{O}(\text{length}^{-5}) \}. \quad (54)$$

In the standard theory one actually caps the expansion at the order $1/\text{length}^2$, or squared curvature, even though higher order theories have in fact been proposed (Goetz and Helfrich, 1996; Fournier and Galatola, 1997; Siegel, 2010). With the relabeled constants

$$C^{(0)} = \sigma + \frac{1}{2}\kappa K_0^2, \quad C^{(1)} = -\kappa K_0, \quad (55a)$$

$$C^{(2,1)} = \frac{1}{2}\kappa, \quad C^{(2,2)} = \bar{\kappa}, \quad (55b)$$

the Hamiltonian takes the well known form (Helfrich, 1973)

$$H = \int dA \left\{ \sigma + \frac{1}{2}\kappa(K - K_0)^2 + \bar{\kappa}K_G \right\}. \quad (56)$$

The meaning of the four phenomenological constants in this expression will be discussed in Section 3.3.

3.2. Model-dependent derivations

The considerations in the previous section used the microscopic basis of a lipid membrane only inasmuch as they affected general construction principles of an effective large-scale Hamiltonian. To contrast this with the opposite viewpoint, this brief section will show how some actual physical models reproduce the general form of the Helfrich energy functional, while additionally providing information about the phenomenological material parameters. Of course, such models are neither guaranteed to be correct in all their extra detail, nor are they in fact unique, because the observable macrophysics does not fully determine the underlying microphysics (a constant source of distress for physicists of the first-principles couleur).

Let us begin by considering stretching. If we have a flat membrane of area A_0 , we can (isotropically) stretch it into a membrane of area $A > A_0$, and to lowest order (linear elasticity) the energy should behave as

$$E = \frac{1}{2}K_A \frac{(A - A_0)^2}{A_0} = \frac{1}{2}K_A A_0 u^2, \quad (57)$$

where u is the area strain and K_A is called area expansion modulus, which typically has a value around 240 mN/m for many lipid bilayers (Rawicz et al., 2000).¹³ Unlike for a liquid–fluid surface tension, the resulting stress Σ_s is not constant but indeed linear in the area strain,

$$\Sigma_s = \frac{\partial E}{\partial A} = K_A \frac{A - A_0}{A_0} = K_A u. \quad (58)$$

¹³ Membrane fluctuations add an entropic contribution to the overall membrane tension, which needs to be subtracted out before the “ground state” term characterized by K_A can be assigned.

This linear stress–strain relation holds until the membrane ruptures. The rupture tension depends not only on the lipid, but also on the loading rate: it can be as low as a few mN/m, and reach values of up to 25 mN/m for long-tailed lipids and fast loading rates (Evans et al., 2003). But as long as the membrane is pulled gently, the rupture strain is very low, just a few percent. Balancing the stretching energy (57) against the edge energy of a rupture pore of radius r , $E_{\text{rim}} = 2\pi r\Gamma$, where Γ is the free energy of a membrane edge (“edge tension”), shows that in the constant tension ensemble membrane rupture is a classical nucleation process: a pore with a radius smaller than the critical radius $R_c = \Gamma/\Sigma_s$ will self-heal, while a bigger one will rupture the membrane (Litster, 1975). At the critical size, the pore energy is $E_c = \pi\Gamma^2/\Sigma_s$. With $\Gamma \sim 10$ pN (Chernomordik et al., 1985; Zhelev and Needham, 1993; Genco et al., 1993; Karatekin et al., 2003) and $\Sigma_s \sim 1$ mN/m we get $R_c \sim 10$ nm and $E_c \sim 80k_B T$. The constant area ensemble gives a more curious result: both the rupture strain and the rupture stress depend weakly on the total membrane area: both are proportional to $A_0^{-1/3}$ (Farago, 2003; Tolpekina et al., 2004; Cooke and Deserno, 2005).

The possibly simplest model for such an elastic film is thin plate theory in the framework of linear elasticity (Landau and Lifshitz, 1999). If the film has a thickness d and is composed of a material with Young modulus E and Poisson ratio ν , this model predicts

$$K_A = \frac{Ed}{2(1-\nu)}. \quad (59)$$

Dimensional analysis necessitates $K_A \propto Ed$, and the factor 2 arises because the isotropic area strain is twice bigger than the linear strain to which the Young modulus typically refers (the Poisson-ratio-correction is hard to explain intuitively).¹⁴ The same model also predicts the two bending rigidities (Landau and Lifshitz, 1999):

$$\kappa = \frac{Ed^3}{12(1-\nu^2)}, \quad \bar{\kappa} = -\frac{Ed^3}{12(1+\nu)} \quad (\text{one sheet}). \quad (60)$$

Since a membrane of thickness d consists of two sheets of thickness $d/2$ that can slide and hence cannot transmit tangential stress, the bending modulus of a bilayer is the sum of the moduli of the two individual layers.¹⁵ Accounting for this, and combining Eq. (59) with Eq. (60), then leads to

$$\kappa = \frac{K_A d^2}{24(1+\nu)} \quad (\text{two thin solid sheets}). \quad (61)$$

Interestingly, the value of the Poisson ratio vanishes from the frequently encountered combination

$$2\kappa + \bar{\kappa} = \frac{K_A d^2}{24} \quad (\text{two thin solid sheets}). \quad (62)$$

Moreover, Eq. (60) implies

$$\frac{\bar{\kappa}}{\kappa} = \nu - 1, \quad (63)$$

and since experiments seem to indicate that $\bar{\kappa}/\kappa$ typically lies in the range $[-1, -0.7]$ (Lorenzen et al., 1986; Templer et al., 1998; Siegel and Kozlov, 2004; Baumgart et al., 2005; Siegel, 2006, 2008; Semrau et al., 2008), the Poisson ratio should typically fall within the range $\nu \in [0, 0.3]$, in turn implying a denominator in Eq. (61) around 24 . . . 31, consistent with experiments (Rawicz et al., 2000;

Bloom et al., 1991). A more sophisticated polymer brush theory predicts the denominator 24 (Rawicz et al., 2000), which is formally equivalent to $\nu = 0$ but really arises from different physics.

Of course, real membranes are two-dimensional fluids, so the above argument can at most apply to weak bending. We cannot fix the calculation trivially by setting the shear modulus μ to zero, though, because $E \propto \mu$ and thus all moduli would vanish (Evans, 1974). Goetz et al. (1999) suggest to alternatively think of a bilayer as stacks of two-dimensional uncoupled fluid sheets, so one can restrict fluidity to within the sheets. The area expansion modulus and the bending rigidity of such a two-dimensional layer can be written as $\lambda_{2d} + \mu_{2d}$ and $(\lambda_{2d} + 2\mu_{2d})d^2/12$, respectively, where λ_{2d} and μ_{2d} are the two-dimensional Lamé-coefficients, and where $\mu_{2d} = 0$ in the fluid case. Assuming this, and again decoupling the two leaflets, they find (Goetz et al., 1999)

$$\kappa = \frac{K_A d^2}{48} \quad (\text{two thin } 2d\text{-fluid sheets}). \quad (64)$$

This seems to be slightly too small compared to experiment, but it describes their numerical simulations well (Goetz et al., 1999), and there is at any rate a certain leeway (both in simulation and in experiment) in the definition of d . Unfortunately, it is not clear how one can derive the Gaussian modulus from this analysis.

Since $\kappa/K_A \propto d^2$, bending rigidities vanish more quickly in the limit $d \rightarrow 0$ than the stretching modulus, and hence the soft modes of thin plates are bending deformations. This is how we can derive Eq. (1), used in the introduction to illustrate in what sense bending is lower in energy than stretching: Set the stretching energy (57) equal to the energy of a closed spherical vesicle, which is $8\pi\kappa + 4\pi\bar{\kappa}$. Using $\kappa \propto K_A d^2/\mathcal{N}$, one can further sharpen Eq. (1). With Eq. (62) we get $R_s \approx d/(2\sqrt{3}s)$, which for $s = 1\%$ becomes $R_s \approx 30d$, showing how the stretching-comparable curvature radius is a few tens times the membrane thickness, and thus remarkably small.

This simple continuum theory is still fairly crude, for membranes are neither thin continuum solids nor layered isotropic liquids. Attempts to account for their underlying structural physics come in a number of different flavors. For instance, the tilt degree of freedom of individual lipids adds bend- and splay-contributions to the local elastic energy (Hamm and Kozlov, 1998, 2000; May and Ben-Shaul, 1999; May, 2000; Kozlovsky and Kozlov, 2002), whose relation to the curvature-elastic moduli has recently found a renewed interest (May et al., 2007a,b; Watson and Brown, 2010; Watson et al., 2011). A few years back a systematic procedure to derive a fluid membrane Hamiltonian by dimensional reduction has been proposed (Zurlo, 2007; Deseri et al., 2008), starting from a fluid surface of finite thickness but internal structure. Unsurprisingly, large-scale curvature elastic behavior is recovered, but the material’s micro-physics adds new terms. For instance, a fluid–gel transition would change the thickness d of the bilayer, which incurs an energetic contribution proportional to $(\nabla d)^2$, and this term is especially relevant at domain boundaries between phases, contributing to the line tension (Deseri and Zurlo, 2013). Such terms could be added “by hand” as additional fields to the Helfrich functional, but here they follow naturally from the model, because the physics to describe them is part of the microscopic Hamiltonian. The approaches in Lomholt and Miao (2006), Bitbol et al. (2012) and Maleki et al. (2013) follow a similar spirit, and Rangamani et al. (2013) adds the tilt degree of freedom to this framework.

3.3. The phenomenological constants

3.3.1. Surface tension

The first constant in the Helfrich Hamiltonian, σ , is seemingly the simplest one; and yet this “surface tension” term is fraught with a number of curious subtleties worth unraveling. Since σ is a constant, this term can simply be written as σA , where A is the total

¹⁴ Some work seems to implicitly assume $K_A = Ed$, but this only holds for incompressible materials for which $\nu = 1/2$. Distressingly, I have fallen into the same trap, and hence Eq. (61) in the present review will supersede the incorrect Eq. (13) in Deserno (2009).

¹⁵ A proof of this will follow below, see Eq. (75c). The point is not trivial, since the statement is not true for the Gaussian modulus if the individual leaflets have a nonvanishing spontaneous curvature.

area of the membrane, and so it looks like a classical thermodynamic surface tension. But if the area per lipid is constant, then the total area is also constant and proportional to the total number of lipids, in which case σ is directly proportional to their chemical potential.

It has therefore been pointed out (Brochard et al., 1976; David and Leibler, 1991) that one ought to distinguish the total membrane area A from the *projected* membrane area A_p . The latter can be pictured as the area of a planar frame that spans the membrane, and the membrane tension really is the thermodynamic variable conjugate to A_p . Usually this is discussed within Monge gauge (see Section 2.7), where both views give rise to the same equation, but a different interpretation. Since the difference (or “excess area”) ΔA between total area and projected area can be written as

$$\begin{aligned} \Delta A &= \int dA_p \{\sqrt{g} - 1\} = \int dA_p \left\{ \sqrt{1 + (\nabla h)^2} - 1 \right\} \\ &\approx \int dA_p \frac{1}{2} (\nabla h)^2, \end{aligned} \quad (65)$$

one usually finds a term $(1/2)\sigma(\nabla h)^2$ in linearized Monge gauge, irrespective of whether the projected area is constant and the total area is varying, or vice versa.

Unlike the surface tension of water, the tension σ of a bilayer is not a material parameter but reflects its intrinsic isotropic tangential stress, and this depends on mechanical constraints the bilayer is subject to—such as its boundary conditions, or whether a closed vesicle is osmotically swollen. For instance, a piece of bilayer spread across a hole in some substrate is subject to a (usually large) tension, the origin of which is the adhesion energy of the bilayer to the substrate surrounding the hole. Notice also that the constant term $C^{(0)}$ in Eq. (55a) has a contribution from the spontaneous membrane curvature. Its role as a “spontaneous tension” has recently been discussed by Lipowsky (2013, 2014), and we will come back to it in Section 4.6.1.

In the functional (56) the parameter σ can also be interpreted as a Lagrange multiplier that helps to fix the overall area A , for instance if one tries to find solutions minimizing the energy. In that case σ becomes a function of all other constraints, such as total area or volume of the vesicle. If, on the other hand, σ is prescribed as the independent thermodynamic variable, it is considered a constant. In that case the surface tension term σA or $\sigma \Delta A$ is *linear* in the area, meaning if one pulls in twice the area from some lipid reservoir, one pays twice the energetic cost. This is very different from the bilayer tension (57) that ensues if one actually stretches a bilayer such that the area per lipid begins to change.

Finally, it is important to note that the tension σ does *not* coincide with the stress that resides in the membrane. What types of forces a material can transduce depends on its constitutive equation, and curvature elastic surfaces permit a much richer behavior than what one is used to from fluid interfaces or soap films. All this will become clearer when we deal with the membrane stress tensor in Section 4.

3.3.2. Spontaneous curvature

The second term in the Helfrich Hamiltonian quadratically penalizes the deviation of the total curvature K from the spontaneous curvature K_0 , a constant of dimension 1/length. Looking at Eq. (55a), this term stems from the linear order in the expansion (54), and it can only occur when the bilayer-leaflet (“up-down”) symmetry is broken. Recall that the definition of the curvature tensor K_{ab} includes an arbitrary sign convention, deciding whether the curvature of a sphere with outward pointing unit normal is counted as positive or negative. If both sides of the membrane are indistinguishable, this choice of the normal vector \mathbf{n} cannot have physically observable consequences, and so the linear term (which would

flip its sign if we swapped the irrelevant convention) must vanish. Hence, $K_0 = 0$ for up-down symmetric membranes. However, if we can distinguish the two sides, the two possible normal vectors are no longer equivalent. For instance, one of the two leaflets might be enriched in a particular lipid species, or the composition of the solvent is not identical on the two sides (Döbereiner et al., 1999), allowing us to fix the direction of \mathbf{n} based on a physical observable. Of course, this again requires an arbitrary choice, but now the two different choices are *physically distinguishable*, hence there is no need for the Hamiltonian to be invariant when swapping the sign of \mathbf{n} , and this permits the linear term to show up.

Annoyingly, two different conventions exist for quantifying the spontaneous curvature. Expressed in terms of the principal curvatures, one encounters the total curvature term in one of two different forms:

$$\begin{aligned} \frac{1}{2}\kappa(K_1 + K_2 - K_0)^2 &\longleftrightarrow \frac{1}{2}\kappa(K_1 + K_2 - 2H_0)^2 \\ \frac{1}{2}\kappa(K - K_0)^2 &\longleftrightarrow 2\kappa(H - H_0)^2, \end{aligned} \quad (66)$$

where $H = K/2$ and $H_0 = K_0/2$. To avoid misunderstandings, it is therefore vital to find out, whether by “spontaneous curvature” a given author refers to the spontaneous *total* curvature K_0 or the spontaneous *mean* curvature H_0 . Sadly, not all authors make this entirely clear, so the reader should be wary of analytical or numerical discrepancies involving factors of two. To make matters worse, the different sign conventions for the curvature K also result in different ways for including the spontaneous curvature term, so that one also finds it written as $(c + c_0)^2$, for instance in Tu and Ou-Yang (2003).

Observe that no spontaneous Gaussian curvature is possible on the quadratic level: a term proportional to $(K_G - K_{G,0})^2$ would be quartic. However, does the spontaneous curvature have to be a scalar or could we have a spontaneous curvature *tensor* $K_{ab}^{(0)}$? Such a new tensor would offer the possibility of a linear term $K^{ab}K_{ab}^{(0)}$, but the physics that would give rise to the spontaneous curvature tensor would have to be investigated more closely. For instance, since lipids are not axisymmetric (they have two tails), any local ordering of the vectors joining the two tails would break the local rotational symmetry, something that could be captured by a traceless tensor whose larger eigenvector aligns with the direction of ordering and whose magnitude captures the order parameter—much as one would do in the Landau-de Gennes theory for liquid crystals (de Gennes and Prost, 1993). In a slightly simpler (but symmetrically not entirely equivalent) way one could distinguish that direction with a tangential director field $\mathbf{m} = m^a \mathbf{e}_a$, now mimicking the Frank–Oseen theory for liquid crystals (de Gennes and Prost, 1993). Such vectors would permit a number of extra terms in the free energy functional. Some terms would couple the direction with the geometry, most notably $K_{ab}m^a m^b$, others would capture the physics of the order itself, for instance in the form of a classical Ginzburg–Landau expansion, à la

$$\begin{aligned} E[\mathbf{m}] &= \frac{1}{2}r(\nabla_a m^a)^2 + \frac{1}{2}r'(\nabla_a m^b)(\nabla^a m_b) \\ &\quad + \frac{1}{2}t(m_a m^a) + \frac{1}{4!}u(m_a m^a)^2. \end{aligned} \quad (67)$$

Indeed, theories of this second type have been investigated in the past (Nelson and Powers, 1993; Powers and Nelson, 1995; Seifert et al., 1996; Selinger et al., 1996; Müller et al., 2005a; Tu and Seifert, 2007). However, since the vector \mathbf{m} can also be viewed as indicating lipid *tilt*, these theories have been devised to understand tilt–curvature coupling, not whether untilted but not axisymmetric lipids endow a membrane with a different local anisotropy.

3.3.3. Curvature moduli

The two curvature moduli κ and $\bar{\kappa}$ multiply the two independent quadratic curvature scalars K^2 and K_G (the first one shifted by K_0). The parameter κ is usually referred to as the *bending modulus* or the *bending rigidity*, while $\bar{\kappa}$ is called *Gaussian curvature modulus* or *saddle splay modulus*.¹⁶ Notice that K_G has no fixed sign; it is not positive definite, but of course the entire Hamiltonian has to be. Since this feature does not involve the constant and linear term, we can consider it based on the two quadratic invariants alone. Using the two principal curvatures K_1 and K_2 , we can write

$$\begin{aligned} E &= \frac{1}{2}\kappa K^2 + \bar{\kappa}K_G = \frac{1}{2}[\kappa(K_1 + K_2)^2 + 2\bar{\kappa}K_1K_2] \\ &= \frac{1}{2}(K_1, K_2) \begin{pmatrix} \kappa & \kappa + \bar{\kappa} \\ \kappa + \bar{\kappa} & \kappa \end{pmatrix} \begin{pmatrix} K_1 \\ K_2 \end{pmatrix} \stackrel{!}{\geq} 0. \end{aligned} \quad (68)$$

For this inequality to hold, we need the eigenvalues $\lambda_{\pm} = \kappa \pm (\kappa + \bar{\kappa})$ of the matrix to be non-negative, and this implies

$$-2\kappa \leq \bar{\kappa} \leq 0. \quad (69)$$

The bending modulus is positive, while the Gaussian curvature modulus is negative but larger than -2κ .¹⁷ The model-dependent result from Eq.(63) implies the stronger constraint $-2 \leq \bar{\kappa}/\kappa \leq -1/2$ (because $-1 \leq \nu \leq 1/2$ (Landau and Lifshitz, 1999)), and typically $-1 \leq \bar{\kappa}/\kappa \leq -1/2$ (because ν is virtually always positive), but these limits should not be taken too seriously given the crudeness of solid thin plate theory for the present situation. Making more physical assumptions about the shapes of lipids, the range $-1 \leq \bar{\kappa}_m/\kappa_m \leq 0$ for the monolayer moduli has been derived (Templer et al., 1998).¹⁸

There is no physical reason for $\bar{\kappa}$ to be close to zero, and indeed $|\bar{\kappa}|$ and κ tend to be comparable in magnitude (Lorenzen et al., 1986; Templer et al., 1998; Siegel and Kozlov, 2004; Baumgart et al., 2005; Siegel, 2006, 2008; Semrau et al., 2008). From this one might incorrectly conclude that both moduli affect a membrane's shape about equally strongly, but in truth the Gaussian term has often no influence. The reason for this is a fascinating result from differential geometry, known as the Gauss–Bonnet theorem. If \mathcal{P} is a membrane patch and $\partial\mathcal{P}$ is its boundary, then this theorem states that

$$\int_{\mathcal{P}} dA K_G + \int_{\partial\mathcal{P}} ds k_g = 2\pi\chi_{\mathcal{P}}, \quad (70)$$

where k_g is the so-called *geodesic curvature* along the membrane's boundary (a covariant geometric definition of this quantity will be given in Eq.(107) below) and $\chi_{\mathcal{P}}$ is the *Euler characteristic* of the patch \mathcal{P} (Kreyszig, 1991; do Carmo, 1976; Spivak, 1975a; Kamien, 2002). The important point is that the surface integral over the Gaussian curvature can be decomposed into a boundary contribution (which in particular vanishes if there is no boundary, such as for closed vesicles), and a term proportional to $\chi_{\mathcal{P}}$, which is a topological invariant that is independent of the actual shape. As

¹⁶ The name “saddle splay modulus” stems from the following observation: Consider a local curvature deformation for which the principal curvatures satisfy $K_1 = -K_2 \neq 0$. The membrane bends up along one principal direction and equally strongly down along the perpendicular direction, thereby locally acquiring the shape of a saddle. Since $K_G = K_1K_2 < 0$, the Gaussian curvature term contributes to the energy of this saddle, but the normal bending term does not if $K_0 = 0$ (since $K = K_1 + K_2 = 0$). However, the Gaussian curvature term also contributes at non-saddle-like deformations, so the notion that it is particularly relevant for saddles is misleading. By the same logic, one could call κ the “cylindrical rigidity”, since it contributes at locally cylindrical deformations ($K_1 \neq 0, K_2 = 0$) at which K_G vanishes. (In fact, Landau and Lifshitz do just that (Landau and Lifshitz, 1999).)

¹⁷ This argument is presented in Safran (1994), but the final result given there is unfortunately incorrect.

¹⁸ Section 3.4 will discuss in more detail the question how bilayer and monolayer parameters are related.

a consequence, both the shape equation for membranes and the stresses transmitted through them do not depend on $\bar{\kappa}$, as we will see in Section 4, and this makes it hard to find the value of the Gaussian curvature modulus, both in experiment (Lorenzen et al., 1986; Templer et al., 1998; Siegel and Kozlov, 2004; Baumgart et al., 2005; Siegel, 2006, 2008; Semrau et al., 2008) and in simulation (Brannigan and Brown, 2007; den Otter, 2009; Hu et al., 2012, 2013a). There are still important situations where $\bar{\kappa}$ matters, though, most prominently membrane fission and fusion, which happen for biomembranes all the time, since these change the topology: Fission increases $\chi_{\mathcal{P}}$ by 2, fusion reduces it by 2, thus giving rise to an energy change of magnitude $|4\pi\bar{\kappa}|$. With $\bar{\kappa} \approx -\kappa \approx -20k_B T$ (Seifert and Lipowsky, 1995; Evans et al., 2003; Nagle, 2013), this amounts to a total energy change of plus (fusion) or minus (fission) $250k_B T$ from the topological term alone—anything but negligible.

The Gauss–Bonnet theorem also shows why for many practical cases the Hamiltonian originally proposed by Canham (1970) is equivalent to the one proposed by Helfrich (1973). Canham also wanted to express the energy in terms of the principal curvatures, so he wrote a term proportional to $(K_1)^2 + (K_2)^2 = K_a^b K_b^a$, which is equal to the trace of the square of the curvature tensor and hence obviously a scalar. Since the twice contracted equation of Gauss, Eq. (42b), states that $K_a^b K_b^a = K^2 - 2K_G$, we see that for the common case $K_0 = 0$ Canham's Hamiltonian differs from Helfrich's one only by the often irrelevant Gaussian contribution, and if additionally $\bar{\kappa} = -\kappa$, the two Hamiltonians are actually identical.

Since σ is not material dependent, K_0 frequently vanishes for symmetry reasons, and $\bar{\kappa}$ largely restricts to topological effects, the bending modulus κ emerges as the probably single most important phenomenological parameter necessary to characterize and describe membranes on large scales. How do we find its value? One possible way would be to predict it based on finer-scale theories of lipid bilayers. For instance, theories amending the bilayer shape by a lipid orientation degree of freedom (Hamm and Kozlov, 1998, 2000; May et al., 2007a,b; Watson and Brown, 2010; Watson et al., 2011, 2012) provide connections between the smaller scale moduli coupling to orientation and tilt and the bending moduli. At even higher resolution mean-field techniques adapted from polymer theory have been used to describe the lipid tails and infer large-scale elastic properties (Ben Shaul et al., 1985; Szeleifer et al., 1985, 1988, 1990; Rawicz et al., 2000; Uline and Szeleifer, 2012). The highest possible resolution is molecular modeling, and at this level analytical predictions give way to results obtained from computer simulations, which study a variety of physical observables that are sensitive to the bending rigidity. This includes monitoring membrane shape undulations (Goetz et al., 1999; Lindahl and Edholm, 2000; Marrink and Mark, 2001; Aytton and Voth, 2002; Hofsäß et al., 2003; Farago, 2003; Marrink et al., 2004; Brannigan et al., 2004, 2005; Wang and Frenkel, 2005; Cooke et al., 2005; Cooke and Deserno, 2005; May et al., 2007a,b; Wang and Deserno, 2010a,b; Watson and Brown, 2010; Watson et al., 2011; Brandt et al., 2011; Shiba and Noguchi, 2011), pulling tethers (Harmandaris and Deserno, 2006; Arkhipov et al., 2008; Shiba and Noguchi, 2011; Baoukina et al., 2012), or buckling membranes (Noguchi, 2011; Hu et al., 2013b). Alternatively, one can measure the bending rigidity in experiments (Nagle, 2013; Dimova, 2014; Bassereau et al., 2014), for instance by monitoring shape undulations by optical (Brochard and Lennon, 1975; Brochard et al., 1976; Schneider et al., 1984a,b; Faucon et al., 1989; Henriksen et al., 2004) or scattering (Liu and Nagle, 2004; Pan et al., 2008a, 2008, 2009) techniques, pulling tethers (Cuvelier et al., 2005; Tian and Baumgart, 2008; Heinrich et al., 2010; Baumgart et al., 2011), or measuring the low-tension stress–strain relation (Evans and Rawicz, 1990).

Without bending rigidity, the surface is only characterized by a surface tension σ . Conversely, if the tension vanishes, we have

the pure bending case. If both terms are present, the problem is more complicated, but the pure-bending and pure-tension cases emerge as limits for small and large length scales, respectively, with a characteristic crossover length given by

$$\lambda := \sqrt{\kappa/\sigma}. \quad (71)$$

On length scales smaller than λ the tension contribution to the energy becomes subdominant to the bending terms, and on length scales large than λ it is the other way around and the tension term dominates. For instance, taking the value of the surface tension typical for cell membranes, $\sigma \sim 0.02$ mN/m (Morris and Homann, 2001), and $\kappa \sim 20k_B T$ (Seifert and Lipowsky, 1995; Evans et al., 2003; Nagle, 2013), we get $\lambda \sim 64$ nm. Hence, for the high curvature deformations that occur during cellular events such as endocytosis, budding, or vesiculation, the bending terms are very much relevant, but on the micron scale such biomembranes are essentially surface tension dominated structures. Under substantially higher tensions, say $\sigma \sim 1$ mN/m, the characteristic length drops below 10 nm, and bending terms only matter on length scales that are comparable to membrane thickness. In other words, they matter on scales for which the very idea that quadratic bending theory is sufficient becomes questionable itself.

3.4. Bilayer vs. monolayer

Lipid bilayers consist of two lipid monolayers which can slide past each other without a cost in free energy. Hence, the same arguments that apply to the bilayer also hold for each single monolayer, and so there must be a monolayer Hamiltonian of the form

$$H_m = \int dA' \left\{ \sigma_m + \frac{1}{2} \kappa_m (K' - K_{m,0})^2 + \bar{\kappa}_m K'_G \right\}, \quad (72)$$

where the subscripts “m” on the parameters and the primes on the geometric scalars indicate that these quantities refer to a monolayer. We now want to explore how monolayer and bilayer parameters are related.

The most straightforward difference is that monolayers have no obvious up-down symmetry, hence the spontaneous monolayer curvature $K_{m,0}$ is typically nonzero. Since this parameter originates from the asymmetric shape of the lipids, it is also sometimes referred to as the lipid curvature. The same unpleasant factor-of-two confusion discussed for the bilayer case (see Eq. (66)) also beleaguers the monolayer spontaneous curvature. As far as the sign is concerned, the usual convention is that a lipid with a positive spontaneous curvature is one with a large head, so that it prefers to reside in a leaflet whose hydrophilic side is convex (curved like the outside of a sphere).

What about tension and curvature moduli? Given that a bilayer is a stack of two relatively independent monolayers, one might naïvely think that the bilayer values are simply the sum of the monolayer values, or if the two leaflets are identical, that the bilayer values are twice as big. This is not generally true, though, for quite an interesting reason: When writing equations such as (56) or (72) we represent a physical surface of finite thickness with an idealized mathematical surface. Where within the actual physical surface do we place the idealized mathematical one? For a bilayer the surface between the two leaflets (“midplane”) is the obvious choice. For monolayers the situation is more subtle. Imagine bending a monolayer, or for that matter, any thin plate of finite thickness. Upon bending, the “outside” surface is stretched, while the “inside” surface is compressed, and in fact the total volume integral of this elastic energy ought to result in the overall curvature energy. Clearly, between the outside and the inside there will be a surface where neither stretching nor compression happens, and this surface is called the “surface of inextension” or sometimes also the

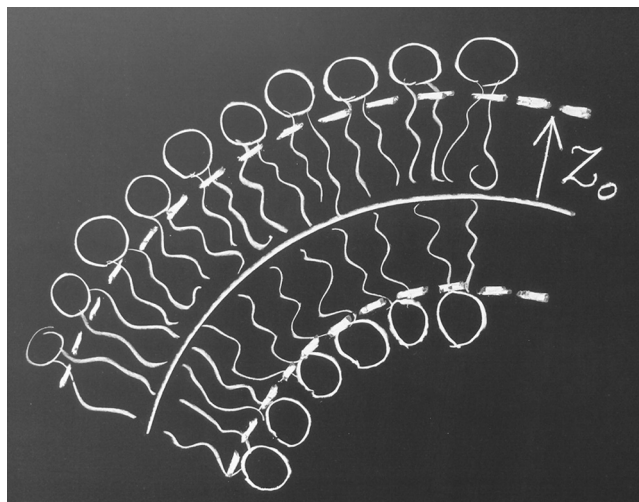


Fig. 3. The pivotal plane (or surface of inextension) for each of the two monolayers in a bilayer (dashed curves) is located a distance z_0 away from the bilayer's midplane (solid curve).

“pivotal plane.” It is a frequently followed convention to refer to this surface when discussing bending of monolayers.¹⁹ However, the pivotal plane of a bilayer's leaflet is a finite distance z_0 away from the midplane—see Fig. 3. This matters because area elements dA and the curvatures K and K_G depend on that reference. Picture two spheres with radii R and $R' = R + z_0$, with $z_0 > 0$. The area element dA' of the bigger sphere is larger than the element dA of the smaller one, namely by a factor $(1 + z_0/R)^2$; moreover, its total curvature is different by a factor $(1 + z_0/R)^{-1}$, and its Gaussian curvature differs by a factor $(1 + z_0/R)^{-2}$. More generally, if we construct a new “parallel surface” $\mathbf{Y}(u^1, u^2) = \mathbf{X}(u^1, u^2) + z_0 \mathbf{n}(u^1, u^2)$, there exists a beautiful exact relation between the area elements and the curvatures on these two surfaces (Spivak, 1975a; Willmore, 2012; do Carmo, 1976):

$$\frac{dA'}{dA} = 1 + Kz_0 + K_G z_0^2, \quad (73a)$$

$$\frac{K'_G}{K_G} = \frac{1}{1 + Kz_0 + K_G z_0^2}, \quad (73b)$$

$$\frac{K'}{K} = \frac{1 + (2K_G/K)z_0}{1 + Kz_0 + K_G z_0^2}. \quad (73c)$$

These identities generalize the special case of spheres mentioned above. Observe the curious fact that $dA K_G = dA' K'_G$, meaning that the Gaussian curvature combined with the area element stays invariant when moving along layers of parallel surfaces.²⁰

Using the identities (73a–c)—in fact, their expansions to first order in z_0 suffices—we can rewrite the monolayer energy from Eq. (72), which refers to the surface of inextension (the “primed”

¹⁹ It is not the only possible choice, though. Recall that the energy of a membrane contains both quadratic bending (56) and stretching (57) terms, so a general quadratic ought to include a cross term of the form $\kappa_s(A - A_0)K$. It turns out that there is a special choice, called the “neutral surface,” at which the cross term vanishes, but unfortunately this surface does not coincide with the pivotal plane (Kozlov and Winterhalter, 1991).

²⁰ Lest the reader thinks this is trivial: If we perform a simple scaling of the surface by some factor, both $dA K_G$ and $dA K^2$ remain invariant. But parallel surfaces do not just differ by an overall scaling factor. The special example of a sphere is misleading in this regard, and the reader might want to contemplate instead what parallel surfaces of a torus would look like.

quantities), while expressing the geometry with respect to the bilayer's midplane. A straightforward calculation gives

$$\begin{aligned} H_m &= \int dA' \left\{ \sigma_m + \frac{1}{2} \kappa_m (K' - K_{m,0})^2 + \bar{\kappa}_m K'_G \right\} \\ &= \int dA \left\{ \left[\sigma_m + \frac{1}{2} \kappa_m K_{m,0}^2 \right] \right. \\ &\quad + \left[-\kappa_m K_{m,0} + \left(\sigma_m + \frac{1}{2} \kappa_m K_{m,0}^2 \right) z_0 \right] K \\ &\quad + \frac{1}{2} \kappa_m K^2 + [\bar{\kappa}_m - 2\kappa_m K_{m,0} z_0] K_G \\ &\quad \left. + \text{higher order curvature terms} \right\}. \end{aligned} \quad (74)$$

The total bilayer energy is the sum of two such contributions. If the two monolayers are identical, the elastic constants and the value of z_0 (which is also a material parameter) are the same, provided we choose the normal vector of the opposite leaflet also in the opposite directions. This flip in \mathbf{n} leaves K^2 and K_G invariant, but switches the sign of K . After adding the two leaflets, a comparison with the bilayer energy (56) and the identifications from Eq. (55a,b) leads to

$$\sigma = 2 \left[\sigma_m + \frac{1}{2} \kappa_m K_{m,0}^2 \right], \quad (75a)$$

$$K_0 = 0, \quad (75b)$$

$$\kappa = 2\kappa_m, \quad (75c)$$

$$\bar{\kappa} = 2[\bar{\kappa}_m - 2\kappa_m K_{m,0} z_0]. \quad (75d)$$

As expected, the spontaneous curvature vanishes, and the bilayer bending modulus is twice the monolayer bending modulus.²¹ But two possibly unexpected things happened. First, the Gaussian curvature modulus picks up an additional correction due to the monolayer spontaneous curvature (Helfrich, 1994), which is proportional to z_0 and thus reveals its origin to be the difference between the two reference surfaces. Second, the tension picks up a contribution that may be viewed as the “zero-point energy” of a flat monolayer, the elastic energy it has due to the spontaneous curvature of its constituent lipids. It is the monolayer equivalent of the “spontaneous tension” discussed by Lipowsky (2013, 2014), but notice that it contributes to the bilayer tension even though it does not create a bilayer spontaneous curvature. Its magnitude is typically small; for instance, membranes composed of the lipid DOPC (1,2-dioleoyl-*sn*-glycero-3-phosphatidylcholine) have a monolayer rigidity of $\kappa_m = \kappa/2 \approx 10k_B T$ (Nagle et al., 2014) and a spontaneous curvature of $K_{m,0} \approx 0.05 \dots 0.07 \text{ nm}^{-1}$ (Szule et al., 2002), from which we get an extra contribution of about 0.01 mN/m. Taking an area per lipid of about $a_\ell = 0.72 \text{ nm}^2$ (Liu and Nagle, 2004) this translates to an extra energy per lipid of about $E_{m,0,\ell} = (1/2)\kappa_m K_{m,0}^2 a_\ell \approx 0.01 k_B T$, which is much smaller compared to the thermal energy, let alone the aggregation free energy per lipid. In fact, one can check that $E_{m,0,\ell} \sim k_B T$ requires $K_{m,0}^{-1}$ to become comparable to the membrane thickness, in which case the preferred aggregate shape is likely not a planar membrane (Israelachvili et al., 1976).

Evidently, the term $(1/2)\kappa_m K_{m,0}^2$ by construction leads to a contribution that is always proportional to the total area or indeed the number of lipids, so in line with the discussion in Section 3.3.1 it seems most appropriate to regard it as part of the chemical potential of the lipids, the elastic contribution to the condensed state.

Since it only shifts the zero-point energy of the bilayer, it can be disregarded if one only cares about an already existing bilayer and its shape changes. However, integrated over the entire membrane this contribution need not be small, especially if $K_{m,0}$ is not as small as the value given above for DOPC, and it has been suggested to play a role in the total energetics of a cell's membrane stock (Hague et al., 2013).

Finally, let us comment on condition (4) discussed at the beginning of Section 3. If lipids cannot change between the two leaflets of a bilayer, the lipid number in the two monolayers is individually conserved. This matters because shape changes will change the areas of the two leaflets and thus create nonlocal stretching terms. From Eq. (73a) we find the area of the outer (“+ z_0 ”) or inner (“- z_0 ”) leaflet, as measured at the pivotal plane:

$$\begin{aligned} A'_\pm &= \int dA'_\pm = \int dA (1 \pm Kz_0 + K_G z_0^2) \\ &= A \pm z_0 \int dA K + z_0^2 \int dA K_G, \end{aligned} \quad (76)$$

and so the *area difference* between the two leaflets is

$$\Delta A = A'_+ - A'_- = 2z_0 \int dA K. \quad (77)$$

It is worth observing that this equation rests on exact results for parallel surfaces and hence makes no smallness assumption about z_0 .

In the bilayer couple model (Svetina and Žekš, 1989; Heinrich et al., 1993; Kralj-Iglič et al., 1993; Miao et al., 1994) ΔA is penalized by a stretching term analogous to Eq. (57). Since the resulting expression does not involve the integral over the square of K but rather the square of the integral over K , it amounts to a *nonlocal* bending contribution.

3.5. Higher order corrections

Constructing a phenomenological energy functional for membranes based on their surface geometry naturally leads to the expansion in Eq. (54). Terminating it at quadratic order yields the Helfrich Hamiltonian (56), but there is no reason to assume that higher order terms vanish, and indeed such terms and their physical implications have been investigated previously (Goetz and Helfrich, 1996; Fournier and Galatola, 1997; Siegel, 2010). The question is, how relevant are the energetic contributions associated with it under “normal” circumstances?

Since Eq. (54) is ultimately a small-curvature-expansion, one must expect higher order corrections to become relevant at strong bending. Dimensional analysis shows that the ratio of the moduli multiplying the quartic terms to the moduli multiplying the quadratic terms is the square of a length, and the most obvious natural length that could be involved here is the bilayer thickness (or z_0 , which is about 2–3 times smaller). If this is true, it implies that quartic terms will only compete with the quadratic ones at curvature radii comparable to the membrane thickness. Indeed, experiments on highly curved membrane tethers suggest that quadratic Helfrich theory is applicable down to this highly curved regime (Cuvelier et al., 2005; Tian and Baumgart, 2008; Heinrich et al., 2010; Baumgart et al., 2011). In simulations of coarse grained models a slight softening has been reported (Harmandaris and Deserno, 2006; Hu et al., 2013b; Shiba and Noguchi, 2011),²²

²¹ Still, $\kappa = 2\kappa_m$ is not trivial at all. The fact that in Eq. (74) the prefactor in front of the K^2 term is simply $\kappa_m/2$ arises due to an intriguing cancellation between the shifts in dA and $(K - K_{m,0})^2$.

²² The accuracy of the results in Harmandaris and Deserno (2006) was not good enough to justify the inclusion of quartic terms, but later more precise measurements (Hu et al., 2013b) more convincingly support their existence. Re-analyzing the old results in Harmandaris and Deserno (2006) including a quartic term in the

while self consistent field theory calculations of block-copolymer membranes have found a slight stiffening (Li et al., 2013a).

Higher order terms must enter the scene once we push the Helfrich Hamiltonian beyond its stability limit, for instance by violating the constraint in Eq. (69). From Eq. (75d) we see that the “easiest” way to do this is to change the lipid spontaneous curvature (or to look at a sequence of amphiphiles for which $K_{m,0}$ varies). At sufficiently large positive values of $K_{m,0}$ the value of $\bar{\kappa}/\kappa$ might drop below -2 , and then the bilayer disintegrates in favor of cylindrical or even spherical micelles, in accord with simple geometric arguments for how the packing of amphiphiles determines the aggregate geometry (Israelachvili et al., 1976). Conversely, the lipid curvature might render the Gaussian curvature modulus $\bar{\kappa}$ positive. In this case membranes do not structurally disintegrate but assume bicontinuous phases. The reason is that for $\bar{\kappa} > 0$ the Gaussian curvature term $\bar{\kappa}K_G$ prefers saddle shapes (for which $K_G < 0$), and bicontinuous phases (or their highly symmetric realizations as triply periodic (almost) minimal surfaces, such as the gyroid) essentially consist only of saddles. Hence, the total curvature term $\frac{1}{2}\kappa K^2$ becomes very small and the Gaussian term very negative. What then stops a finite membrane from creating infinitely many saddles? The physical answer is that it has a finite thickness. In terms of the Hamiltonian, the answer is that additional quartic terms can solve the problem that for $\bar{\kappa} > 0$ the quadratic functional is no longer bounded below, thus solving the problems that led to the inequality (69) (Siegel, 2010). Both answers are essentially equivalent if, indeed, the thickness of the membrane is the physical reason for the quartic terms.

It is interesting to note that higher order terms enter the Hamiltonian of lipid bilayer membranes for two different reasons. For one thing, they naturally arise in the expansion of the energy (54). But they also emerge from the monolayer–bilayer connection explored in Section 3.4. Even if, miraculously, the Helfrich Hamiltonian for a monolayer were strictly quadratic in the curvatures, the geometric translation from two monolayers into a single bilayer would create numerous higher order curvature corrections to Eq. (74). Indeed, Siegel points out that a consistent theory for understanding the stability of bicontinuous phases needs both the “physical” and the “geometric” corrections in order to quantitatively explain experimental data (Siegel, 2010).

Finally, it is worthwhile to remember that whenever we said “quadratic,” we meant “quadratic in the curvatures.” This does not mean that the Hamiltonian, once translated into a particular parametrization, is also quadratic and hence “simple.” For instance, the area element dA and the total curvature K in Monge gauge are pretty nonlinear functions—see Eqs. (48) and (51a)—and only upon expanding them for small gradients do we arrive at a Hamiltonian that is also quadratic in the parametrization. Pushing the expansion of $\sqrt{g}K^2$ to higher order, one finds (Kleinert, 1986)

$$\int dA K^2 = \int d^2x \left\{ (h_{ii})^2 - \frac{1}{2}(h_{ii})^2 h_j h_j - 2h_{ii} h_j h_{jk} h_k + \mathcal{O}(h^6) \right\}, \quad (78)$$

where the indices are abbreviations for partial derivatives ($h_i = \partial h / \partial x_i$, etc.) and we sum over repeated ones.²³ Curiously, these higher order terms also affect the lower order ones, since their

analysis indeed gives results for the ordinary bending modulus κ that agree better with independent measurements.

²³ Why do we sum even though the indices are not upstairs–downstairs? Because for Cartesian coordinates the difference between covariant and contravariant components vanishes, and hence one generally does not bother to distribute the indices up and down.

thermal fluctuations renormalize the curvature moduli (Helfrich, 1985; Kleinert, 1986; Förster, 1986).

4. The stress tensor of lipid membranes

Now that we have a Hamiltonian describing the energy of membranes, we can predict their physical behavior under a great number of circumstances, provided we can mathematically analyze the implications of the functional (56). Two questions are most pressing: First, if membranes strive to minimize that functional, what are the shapes they should assume? And second, what are the stresses that are associated with curvature deformations? Since equilibrium shapes should have their stresses “relaxed,” we expect these questions to be related, and indeed they are: For equilibrium shapes the local force density vanishes, which is the covariant divergence of the local surface stress. To translate these statements into useful equations, we first need to understand what surface stresses are.

The aim of this review is to introduce the concept of the stress tensor geometrically, without entangling it to a specific parametrization. However, it is possible to derive both stress- and torque tensor within Monge gauge (Fournier, 2007). This requires less mathematical preparation than to do it covariantly, but the geometric connections are more difficult to spot. In any case, it is a worthwhile exercise to translate back and forth between these two formulations, which ultimately clarifies both.

4.1. The meaning of surface stresses

The surface tension of liquids or soap films is the prime example of surface stresses. It is equal to the force per unit length acting along any randomly chosen cut across such a surface or film. For instance, imagine cutting the lower half of a soap bubble away. What forces are required to keep the upper half unaffected? To prevent the film from snapping back, we need to pull it with a force σ per unit length along the open edge that is constant, tangential to the surface, and perpendicular to the cut. Since in the present situation the cut is along the equator of the soap bubble, a great circle of radius R , the total force in the downward direction equals $2\pi R\sigma$. Also, the gas inside the soap bubble is under a slightly higher pressure than the gas outside (since the tension in the soap film contracts the bubble and thus compresses the gas inside). To keep the situation in equilibrium, we also need to keep the gas from rushing out, which requires a “piston” of area πR^2 to push upwards against the (excess) pressure P . In equilibrium, both forces balance, and from $\pi R^2 P = 2\pi R\sigma$ we get the well-known Young–Laplace relation for spherical surfaces,

$$P = \frac{2\sigma}{R}. \quad (79a)$$

It is easy to relax the condition of sphericity: imagine a stable tension-dominated surface with local curvature K and area element dA . If we perform a parallel displacement of that area element by a distance δz along the local normal, Eq. (73a) tells us that the change in area element is $\delta dA = K\delta z dA$. This translation also implies a change of the enclosed volume, which is evidently given by $\delta V = \delta z dA$. The necessary balance between the two work-contributions, namely tension–area ($\sigma\delta A$) and pressure–volume ($P\delta V$), implies the generalized Young–Laplace relation

$$P = \sigma K. \quad (79b)$$

The product of tension and curvature is given by the (usually) constant pressure difference between the two sides of the surface, so wherever the curvature becomes smaller, the tension increases. This is for instance why burritos, if amateurishly rolled up while

applying too much pressure, tend to rip along the weakly curved sides and not at the more strongly curved ends.

This type of reasoning shows how convenient it can be to use surface stress arguments. Unfortunately, the surface tension is not particularly well suited to serve as a guiding example, because it has so many special properties: it is tangential, isotropic, and independent of the surface geometry. General surface stresses, including those of membranes, are more complicated, hence the question “with what force per unit length do I have to pull along an open edge to prevent it from snapping back?” will involve a more complex answer. Moreover, this answer will not just involve forces: for surfaces more complicated than tension-dominated films surface *torques* are also important.

4.2. A straightforward functional variation

To find the “shape equation” resulting from a minimization of the Helfrich energy functional (56), as well as the associated surface stresses and torques, let us take a step back and contemplate what ought to be calculated. Minimizing the geometric surface functional requires a functional variation, or setting the first Fréchet derivative of the functional to zero (Lovellock and Rund, 1989; Spivak, 1975b). The thing being varied is the shape, which we characterized by a parametrization $\mathbf{X}(u^1, u^2)$. A general functional variation can therefore be written as (Jenkins, 1977a,b; Ou-Yang and Helfrich, 1989; Capovilla et al., 2003; Spivak, 1975b)

$$\mathbf{X} \rightarrow \mathbf{X}' = \mathbf{X} + \delta\mathbf{X} \quad \text{with} \quad \delta\mathbf{X} = \phi\mathbf{n} + \phi^a\mathbf{e}_a, \quad (80)$$

where we have decomposed the variation $\delta\mathbf{X}$ into a normal and a tangential part, specified by three functions ϕ and ϕ^a . To first order, the tangential variation describes nothing but a reparametrization, and so it contains no interesting physical information (Capovilla et al., 2003).²⁴ We can thus restrict to normal variations. Observe that this is a generalization of the concept of parallel surfaces, for which $\phi(u^1, u^2) = z_0 = \text{const}$.

What renders a “brute-force” functional variation relatively tedious is the fact that the energy is constructed from geometric scalars, such as K , which depend in a very intricate way on the original parametrization $\mathbf{X}(u^1, u^2)$. Varying \mathbf{X} first tells us how the tangent vectors vary, from there we find how the metric and the normal vector vary, from there how the curvature tensor varies. We then need to find the variation of the inverse metric, and the metric determinant, the trace of the curvature tensor, and the Gaussian curvature (which we could either do intrinsically, by varying the Riemann tensor, or extrinsically, by exploiting the Gauss–Codazzi–Mainardi equations). For instance, the variation of the tangent vectors is found to be

$$\begin{aligned} \delta\mathbf{e}_a &= \delta\nabla_a\mathbf{X} = \nabla_a(\phi\mathbf{n}) = (\nabla_a\phi)\mathbf{n} + \phi\nabla_a\mathbf{n} \\ &= (\nabla_a\phi)\mathbf{n} + \phi K_a^b\mathbf{e}_b, \end{aligned} \quad (81)$$

where in the last step we used the equation of Weingarten (37a). The first order variation of the metric then follows as

$$\begin{aligned} \delta g_{ab} &= \delta(\mathbf{e}_a \cdot \mathbf{e}_b) = \delta\mathbf{e}_a \cdot \mathbf{e}_b + \mathbf{e}_a \cdot \delta\mathbf{e}_b \\ &= [(\nabla_a\phi)\mathbf{n} + \phi K_a^c\mathbf{e}_c] \cdot \mathbf{e}_b + \mathbf{e}_a \cdot [(\nabla_b\phi)\mathbf{n} + \phi K_b^c\mathbf{e}_c] \\ &= 2\phi K_{ab}. \end{aligned} \quad (82)$$

Working through like this, one finds (in a series of increasingly more tedious calculations) the following first order normal variations

(Jenkins, 1977a,b; Ou-Yang and Helfrich, 1987, 1989; Capovilla et al., 2003; Spivak, 1975b):

$$\delta\mathbf{e}_a = (\nabla_a\phi)\mathbf{n} + \phi K_a^b\mathbf{e}_b, \quad (83a)$$

$$\delta\mathbf{n} = (\nabla^a\phi)\mathbf{e}_a, \quad (83b)$$

$$\delta g_{ab} = 2\phi K_{ab}, \quad (83c)$$

$$\delta g^{ab} = -2\phi K^{ab}, \quad (83d)$$

$$\delta g = 2gK\phi, \quad (83e)$$

$$\delta K_{ab} = (-\nabla_a\nabla_b - KK_{ab} + K_G g_{ab})\phi, \quad (83f)$$

$$\delta K = (-\Delta - K^2 + 2K_G)\phi, \quad (83g)$$

$$\delta K_G = -KK_G\phi. \quad (83h)$$

The Laplacian occurring in Eq. (83g) is the covariant Laplacian from Eq. (32). From these pieces we can now construct variations of geometric surface functionals. Given an arbitrary Hamilton density \mathcal{H} , we find

$$\begin{aligned} \delta \int dA \mathcal{H} &= \delta \int d^2u \sqrt{g} \mathcal{H} \\ &= \int d^2u [(\delta\sqrt{g})\mathcal{H} + \sqrt{g}\delta\mathcal{H}] \\ &= \int d^2u \left[\frac{1}{2\sqrt{g}} \delta g \mathcal{H} + \sqrt{g} \delta \mathcal{H} \right] \\ &= \int d^2u \sqrt{g} [\mathcal{H} K \phi + \delta \mathcal{H}] \\ &= \int dA [\mathcal{H} K \phi + \delta \mathcal{H}]. \end{aligned} \quad (84)$$

Applying this to the Helfrich functional (56), we get

$$\begin{aligned} \delta H &= \delta \int dA \left\{ \sigma + \frac{1}{2} \kappa (K - K_0)^2 + \bar{\kappa} K_G \right\} \\ &= \int dA \left\{ \left[\sigma + \frac{1}{2} \kappa (K - K_0)^2 + \bar{\kappa} K_G \right] K \phi \right. \\ &\quad \left. + [\kappa (K - K_0)(-\Delta - K^2 + 2K_G)] \phi - \bar{\kappa} K K_G \phi \right\} \\ &= \int dA \left\{ \sigma K - \kappa \Delta K + \frac{1}{2} \kappa (K - K_0) \right. \\ &\quad \left. \times [(K - K_0)K - 2K^2 + 4K_G] \right\} \phi \end{aligned} \quad (85)$$

where in the last step we integrated the term $(K - K_0)\Delta\phi$ twice by parts and ignored the boundary terms.

Since we frequently deal with vesicles, one might want to keep the volume which they enclose fixed during the functional variation. If one adds a Lagrange-multiplier term $-PV$ to the free energy, this means we also need to know the variation of the volume, but to first order the answer is obviously given by

$$\delta V = \int dA \phi. \quad (86)$$

Hence, setting the functional derivative of $H - PV$ to zero results in the shape equation (Ou-Yang and Helfrich, 1987, 1989; Capovilla et al., 2003)

$$\sigma K - \kappa \left\{ \Delta K - \frac{1}{2} (K - K_0) [(K - K_0)K - 2K^2 + 4K_G] \right\} = P. \quad (87)$$

As written, this equation is fully covariant. When expressed in terms of the original surface parametrization $\mathbf{X}(u^1, u^2)$, it is a fourth order partial differential equation that is highly nonlinear and thus extremely hard to solve analytically. Notice that in the limit where the bending rigidity vanishes, $\kappa = 0$, the equation reduces

²⁴ This is no longer true at second order. However, for a second variation around the equilibrium solution the tangential part becomes a total divergence, i.e., it only contributes a boundary term (Capovilla et al., 2003).

to $\sigma K = P$. We thereby recover the generalized Young–Laplace law from Eq. (79b) as a very special case. Its solutions are evidently constant mean curvature surfaces, and if there is not even a pressure difference between the two sides, the equation simplifies further to $K = 0$, which is the equation for minimal surfaces. Knowing how much beautiful and nontrivial mathematics is hidden in this innocuous equation $K = 0$ lets one maybe appreciate better how much more complicated the full shape equation (87) is.

Obviously, any constant mean curvature surface with $K = K_0$ is a solution of Eq. (87), provided only that $\sigma K_0 = P$; in particular, for $K_0 = 0$ (and thus $P = 0$) any minimal surface solves the shape equation. That does not mean, though, that in a given situation these special solutions are the right ones, because the set of solutions of Eq. (87) is much bigger than that of $K = \text{const}$.

Since the Gauss–Bonnet theorem (70) delegates the surface integral over the Gaussian curvature to topology and boundary, it is no surprise that the term $\bar{\kappa}K_G$ leaves no trace in the shape equation. In fact, the variation of the “densitized” Gaussian curvature is given by (Capovilla et al., 2003)

$$\delta\sqrt{g}K_G = -\sqrt{g}G_{ab}K^{ab}\phi, \quad (88)$$

where $G_{ab} = R_{ab} - (1/2)Rg_{ab}$ is the Einstein tensor, which vanishes identically in two dimensions, as Eq. (43b) shows. Compare this to the special case we encountered for parallel surfaces, where dAK_G was invariant under constant (but arbitrarily large) variations $\phi = z_0$. Here we see that constancy is not required if we are willing to restrict to a first order variation.

In closing this section, it is worthwhile to point out that surfaces endowed with curvature functionals have also been investigated by mathematicians, independently and in fact earlier than physicists. In particular, in the mathematical literature the functional $(1/4)\int dAK^2$ is connected with the mathematician Thomas Willmore. He proved in 1965 that it is bounded below by 4π and conjectured the better lower bound $2\pi^2$ for surfaces of genus $g > 0$ (Willmore, 1965). This conjecture was proved only very recently (Marques and Neves, 2012). The Willmore functional and its variation has a long and fruitful mathematical history, dating back almost 200 years (Thomsen, 1924; Blaschke, 1929; Willmore, 1965, 1982; White, 1973; Pinkall and Sterling, 1987).

4.3. A more elegant functional variation

The “brute force” functional variation leading to the shape equation (87) is not only cumbersome (the pain really being hidden in the work leading to Eqs. (83a–h)); it also does not provide much insight into what the shape equation in fact says. Both clarity and understanding are gained by reformulating the variation in a way proposed by Guven (2004). The key idea is this: instead of working through all the geometric relations individually while performing the variations, one enforces them by additional Lagrange multiplier functions, resulting in the extended functional

$$\tilde{H} = H + \int dA \left\{ \mathbf{f}^a \cdot (\mathbf{e}_a - \nabla_a \mathbf{X}) + \lambda_{\perp}^a (\mathbf{e}_a \cdot \mathbf{n}) + \lambda_n (\mathbf{n}^2 - 1) + \lambda^{ab} (g_{ab} - \mathbf{e}_a \cdot \mathbf{e}_b) + \Lambda^{ab} (K_{ab} - \mathbf{e}_a \cdot \nabla_b \mathbf{n}) \right\}, \quad (89)$$

where H is any surface functional (e.g. the usual Helfrich energy (56)) and the extra terms define the geometry. In particular, the Lagrange multiplier function \mathbf{f}^a enforces the definition of the tangent vectors, λ_{\perp}^a enforces that the normal vector is perpendicular on both tangent vectors and λ_n enforces its normalization, while the two functions λ^{ab} and Λ^{ab} take care of the definitions of the first and second fundamental form, respectively. In the new functional all geometric quantities can be varied *independently*, which greatly simplifies the math. For instance, if the functional H does not depend explicitly on the parametrization \mathbf{X} (like the Helfrich

functional, which only depends implicitly on it through the geometric scalars), the only occurrence of \mathbf{X} in the extended functional \tilde{H} is in the term that defines the tangent vectors. Performing the variation, we find

$$\begin{aligned} \delta_{\mathbf{X}} \tilde{H} &= - \int dA \mathbf{f}^a \cdot \nabla_a \delta \mathbf{X} \\ &= - \int dA [\nabla_a (\mathbf{f}^a \cdot \delta \mathbf{X}) - (\nabla_a \mathbf{f}^a) \cdot \delta \mathbf{X}] \\ &= - \oint ds l_a \mathbf{f}^a \cdot \delta \mathbf{X} + \int dA (\nabla_a \mathbf{f}^a) \cdot \delta \mathbf{X}, \end{aligned} \quad (90)$$

where for once we did not disregard the boundary term but turned it into a line integral around the boundary over which we performed the variation, using the two-dimensional analog of Gauss’ theorem—see Eq. (31).

In equilibrium, both the bulk and the boundary term of $\delta_{\mathbf{X}} \tilde{H}$ must vanish. As far as the bulk term is concerned, this gives rise to the condition

$$\nabla_a \mathbf{f}^a = 0. \quad (91)$$

This equation makes the remarkable statement that for every equilibrium surface there exists an object, \mathbf{f}^a , which is covariantly conserved.²⁵ Nothing in the shape equation (87) readily suggests the existence of such a conservation law. Clearly, we should now be very curious to find out what \mathbf{f}^a is! This is fairly easy to work out, though, because the remaining four variations with respect to \mathbf{e}_a , \mathbf{n} , g_{ab} and K_{ab} give us a closed expression for \mathbf{f}^a in terms of the surface geometry. Through calculations much simpler than the ones leading to Eqs. (83a–h), one finds (Guven, 2004; Müller, 2007)

$$\mathbf{f}^a = (T^{ab} - \mathcal{H}^{ac} K_c^b) \mathbf{e}_b - (\nabla_b \mathcal{H}^{ab}) \mathbf{n}, \quad (92)$$

where we have defined the functional derivatives of the Hamiltonian density with respect to the two fundamental forms as

$$T^{ab} = - \frac{2}{\sqrt{g}} \frac{\delta(\sqrt{g}\mathcal{H})}{\delta g_{ab}} = -\mathcal{H}g^{ab} - 2 \frac{\delta \mathcal{H}}{\delta g_{ab}}, \quad (93a)$$

$$\mathcal{H}^{ab} = \frac{\delta \mathcal{H}}{\delta K_{ab}}. \quad (93b)$$

In Eq. (93a) we also used the identity $\partial g / \partial g_{ab} = g g^{ab}$ for the derivative of the metric determinant. For the case $\mathcal{H} = K^n$ we now find

$$T^{ab}[K^n] = -K^n g^{ab} + 2nK^{n-1} K^{ab}, \quad (94a)$$

$$\mathcal{H}^{ab}[K^n] = nK^{n-1} g^{ab}, \quad (94b)$$

and for the Hamiltonian density $\mathcal{H} = K_G$ we get

$$T^{ab}[K_G] = K_G g^{ab}, \quad (95a)$$

$$\mathcal{H}^{ab}[K_G] = K g^{ab} - K^{ab}. \quad (95b)$$

Combining these results, we find that the conserved quantity \mathbf{f}^a for the case of the Helfrich energy density $\mathcal{H} = \sigma + (\kappa/2)(K - K_0)^2 + \bar{\kappa}K_G$ is given by

$$\mathbf{f}^a = \left\{ \kappa(K - K_0) \left[K^{ab} - \frac{1}{2}(K - K_0)g^{ab} \right] - \sigma g^{ab} \right\} \mathbf{e}_b - \kappa(\nabla^a K) \mathbf{n}. \quad (96)$$

If we now calculate the divergence $\nabla_a \mathbf{f}^a$, we discover that it coincides with the left hand side of Eq. (87); in other words, *the shape equation is equivalent to the fact that \mathbf{f}^a is covariantly conserved*. This should now makes us really curious about the physical meaning of this conserved quantity.

²⁵ If we include the pressure constraint $-PV$ in the functional, the right hand side turns into $P \mathbf{n}$, stating that P acts as a constant normal source term.

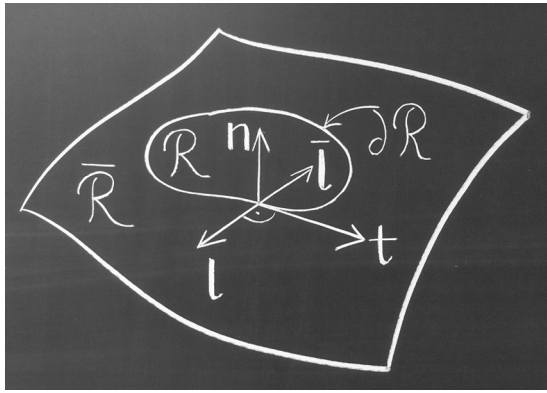


Fig. 4. A patch \mathcal{R} on a membrane with boundary $\partial\mathcal{R}$. Along its contour it has an outward pointing unit vector \mathbf{l} , tangent to the surface. The outward pointing unit vector of the complement $\bar{\mathcal{R}} = \mathcal{M} \setminus \mathcal{R}$ has an outward pointing unit normal $\bar{\mathbf{l}} = -\mathbf{l}$.

4.4. Interpretation of \mathbf{f}^a as the stress tensor

The object \mathbf{f}^a has been introduced by Capovilla and Guven in a series of papers (Capovilla and Guven, 2002a,b, 2004; Capovilla et al., 2002) and identified as the surface stress tensor. They first encounter it as a consequence of Noether's theorem: every continuous symmetry of a variational problem implies a conservation law for the solution. Here, translational symmetry implies a conserved current for equilibrium shapes, and that current is \mathbf{f}^a . Its relation to translational symmetry indeed reveals its connection to stresses and forces.

Let us now consider a mechanical argument that sheds light onto the nature of \mathbf{f}^a (Müller et al., 2005a; Müller, 2007). Imagine a membrane \mathcal{M} , and on it a compact region \mathcal{R} . We will refer to the membrane *without* the region \mathcal{R} as the complement of \mathcal{R} , or $\bar{\mathcal{R}} = \mathcal{M} \setminus \mathcal{R}$ —see Fig. 4. Assume now that the membrane outside of \mathcal{R} is in equilibrium, such that $\nabla_a \mathbf{f}^a = 0$ holds on $\bar{\mathcal{R}}$. We will make no such assumption about \mathcal{R} , but we postulate that the whole membrane \mathcal{M} is stationary (if need be, by the application of extra forces). Across the boundary $\partial\mathcal{R}$ we have a tug of war between the surface stresses of the two patches \mathcal{R} and $\bar{\mathcal{R}}$, but at any given point along the contour they must precisely cancel. If we translate the boundary $\partial\mathcal{R}$ by an infinitesimal amount $\delta\mathbf{a}$, the energy of the complement $\bar{\mathcal{R}}$ must change, but since the shape equation holds on $\bar{\mathcal{R}}$, this change only results from the boundary term of Eq. (90), and we get

$$\delta\tilde{H}[\bar{\mathcal{R}}] = -\delta\mathbf{a} \cdot \oint_{\partial\mathcal{R}} ds \bar{\mathbf{l}}_a \mathbf{f}^a = \delta\mathbf{a} \cdot \mathbf{F}_{\text{ext}}[\bar{\mathcal{R}}], \quad (97)$$

where ds is the line element on $\partial\mathcal{R}$ and $\bar{\mathbf{l}}_a$ is the normal vector on $\partial\mathcal{R}$ (tangential to the membrane) which points out of $\bar{\mathcal{R}}$ (and thus *into* \mathcal{R}). Since the change in energy of $\bar{\mathcal{R}}$ is given by a translation $\delta\mathbf{a}$ dotted into some other expression, this other expression must be the external force acting on $\bar{\mathcal{R}}$. To clarify the sign: Picture a situation in which the translation proceeds in the opposite direction as the external force, $\delta\mathbf{a} \cdot \mathbf{F}_{\text{ext}}[\bar{\mathcal{R}}] < 0$. Clearly, the system $\bar{\mathcal{R}}$ has done work on its surrounding. Since the situation was assumed to be globally in equilibrium, the only source of energy to perform that work could have come from the system, which therefore must have lowered its energy, and so we also have $\delta\tilde{H}[\bar{\mathcal{R}}] < 0$.

Eq. (97) shows that the line integral over $\bar{\mathbf{l}}_a \mathbf{f}^a$ is equal to the *negative* of the external force on $\bar{\mathcal{R}}$ (the patch to which $\bar{\mathbf{l}}_a$ is the outward pointing normal vector). In other words, it is equal to the force which $\bar{\mathcal{R}}$ exerts on its surrounding. This is the same construction by which in classical elasticity the stress tensor is defined (Landau and Lifshitz, 1999): The force per unit area across a two-dimensional cut through a material is given by $n_a \sigma^{ab}$, where σ^{ab} is the three-dimensional stress tensor and n_a is the outward pointing normal

vector of the area element.²⁶ In three dimensional elasticity theory the stress tensor has two indices (it is essentially a 3×3 matrix), but our stress tensor seems to have only one index—what is going on? It turns out that our stress tensor also has two indices, but they run over different ranges: The first index a labels the two *surface* coordinates u^1 and u^2 , and the second index should label the three *space* coordinates x, y , and z , so we could write it as f^{ai} , where $a \in \{1, 2\}$ and $i \in \{1, 2, 3\}$ —the surface stress tensor is a 2×3 matrix! Evidently, this is prone to much confusion, and so it is more convenient to combine the three space coordinates into one (bold-faced space-)vector.

If we know the force with which $\bar{\mathcal{R}}$ acts on its surrounding, then by Newton's third law the force by which \mathcal{R} acts back on $\bar{\mathcal{R}}$ must simply be the negative of that. We can account for that extra minus sign by also flipping the normal vector and use $\mathbf{l}^a = -\bar{\mathbf{l}}^a$, which is the outward pointing unit normal vector to $\partial\mathcal{R}$. Hence, we get the important result for the force by which a patch \mathcal{R} acts on its surrounding:

$$\mathbf{F}[\mathcal{R}] = \oint_{\partial\mathcal{R}} ds \mathbf{l}^a \mathbf{f}^a. \quad (98)$$

The seemingly labyrinthine reasoning with a detour over $\bar{\mathcal{R}}$ served to show that in Eq. (98) we do *not* have to assume that the patch \mathcal{R} is in equilibrium. In fact, all we really need is that the shape equation holds in a small stripe around the contour $\partial\mathcal{R}$.

To add some intuition to this important physical interpretation of the stress tensor, a comparison with an analogous but much more familiar situation from electrostatics might be useful. Poisson's equation states that the divergence of the electric field $\mathbf{E}(\mathbf{r})$ equals the charge density $\rho(\mathbf{r})$, times some constant that depends on the system of units; in SI units we get $\nabla \cdot \mathbf{E} = \rho/\epsilon_0$. Away from charges the electric field is thus divergence free—but of course not necessarily zero. Imagine a region of space \mathcal{R} that contains a total charge Q inside it. By integrating Poisson's equation over that region and using Gauss' law, we find

$$\begin{aligned} \int_{\mathcal{R}} dV \nabla \cdot \mathbf{E} &= \frac{1}{\epsilon_0} \int_{\mathcal{R}} dV \rho \\ \oint_{\partial\mathcal{R}} d\mathbf{A} \mathbf{n} \cdot \mathbf{E} &= \frac{1}{\epsilon_0} Q, \end{aligned} \quad (99)$$

where \mathbf{n} is the outward pointing unit vector of the surface $\partial\mathcal{R}$. In other words, by calculating the flux of the electric field through a closed surface, we can determine the total charge inside. The stress tensor analogy is now obvious: By integrating the flux of the stress through a closed contour $\partial\mathcal{R}$ we can determine the total force with which \mathcal{R} acts on the membrane surrounding it. This is precisely what Eq. (98) states. Of course, this integral can only be nonzero if $\nabla_a \mathbf{f}^a = 0$ does *not* hold everywhere, just like in the electrostatic analogy $\nabla \cdot \mathbf{E} = 0$ cannot hold everywhere. In electrostatics we need a charge density to source an electric field, and here we need a force density to source the stress.

The fact that in the absence of an explicit force density the stress tensor is covariantly conserved is the key reason why it is so

²⁶ Alas, up to a minus sign again: The convention followed for instance in Landau and Lifshitz (1999) has the stress tensor describe the force of the exterior region $\bar{\mathcal{R}}$ onto the inner region \mathcal{R} rather than the force of that region onto its surrounding. This for instance implies that an isotropic pressure has a stress tensor proportional to $-P$ (see [Landau and Lifshitz, 1999, Eq. (2.6)]), while in the convention to be adopted here an isotropic surface tension has the surface stress tensor proportional to $-\sigma$ (see Eq. (112) below). The situation is analogous to the question what sign "work" has in thermodynamics: is it the work done by the system on its surroundings or of the surroundings onto the system? There seems little hope that the literature will converge on a single convention, and so one simply has to make sure one understands the convention followed by some author before taking any sign serious.

immensely useful. If this statement is still not obvious, let us illustrate it with one final analogy, this time from classical mechanics. Imagine you fire a bullet into a freely suspended block of wood so that it gets stuck in it. Question: with what speed does the bullet-plus-woodblock system move afterwards? This could potentially be a completely unanswerable problem, given that we have no idea how the bullet deformed upon impact, what grain structure the woodblock had, how much kinetic energy was turned into heat, and that we would never be able to calculate these things anyways. And yet, we give problems of this sort to high school seniors, since the answer, of course, follows easily by considering momentum conservation. The moral is this: in the absence of additional external forces the momentum of a closed system is a first integral of the equations of motion: $\dot{\mathbf{p}} = \mathbf{F} = 0$ implies that \mathbf{p} is conserved, and hence we do not need to solve the equations of motion in order to answer this particular question. Likewise, in the absence of additional force densities the stress tensor \mathbf{f}^a is covariantly conserved, and hence there exist numerous questions which we can readily answer without ever having to solve the complicated nonlinear shape equations.

4.5. Stress tensor in the Darboux frame

The stress tensor, as defined in Eqs. (92) or (96) is fully covariant, but it is expressed in the local coordinate system $\{\mathbf{e}_1, \mathbf{e}_2, \mathbf{n}\}$, and the two tangent vectors are a last remnant of our coordinate choice. Ultimately, the goal is to express it in geometrically intuitive quantities that do not refer to coordinates at all. Since the stress tensor answers questions about force densities along contours \mathcal{C} , it would be much more natural to use the tangent vector \mathbf{t} to such a contour as well as the (outward pointing) normal vector $\mathbf{l} = \mathbf{t} \times \mathbf{n}$ as a replacement for the two tangent vectors $\{\mathbf{e}_1, \mathbf{e}_2\}$. In other words, we want to use the coordinate system $\{\mathbf{l}, \mathbf{t}, \mathbf{n}\}$ on the surface, which is called the “Darboux frame” of the curve \mathcal{C} (do Carmo, 1976). It differs from the usual Frenet frame of a curve by a rotation around \mathbf{t} , because the two normal vectors to the curve are constructed from the characteristic surface vectors \mathbf{n} and \mathbf{l} rather than the normal vector of the curve itself and its associated binormal vector.

To connect \mathbf{t} and \mathbf{l} to the tangent vectors \mathbf{e}_1 and \mathbf{e}_2 from the parametrization, let us expand them as follows:

$$\mathbf{t} = t^a \mathbf{e}_a \quad \text{and} \quad \mathbf{l} = l^a \mathbf{e}_a. \quad (100)$$

Since we use the convention that $\{\mathbf{l}, \mathbf{t}, \mathbf{n}\}$ is a right-handed coordinate system, this implies that the direction by which a patch is looped around is right-handed with respect to the normal vector.²⁷ Because \mathbf{l} and \mathbf{t} are normalized and orthogonal, their components satisfy completeness on the surface:

$$\delta_a^b = l_a^b + t_a^b, \quad (101)$$

which also implies

$$\mathbf{e}_a = t_a \mathbf{t} + l_a \mathbf{l}. \quad (102)$$

We can now define the components of the curvature tensor within this coordinate system:

$$K_{\perp} = K_{ab} l^a l^b, \quad K_{\parallel} = K_{ab} t^a t^b, \quad K_{\perp\parallel} = K_{ab} l^a t^b. \quad (103)$$

This means that K_{\parallel} is the normal curvature of the surface if it is cut along \mathbf{t} , or along the contour to which \mathbf{t} is the tangent vector. K_{\perp} is the normal curvature tangential to \mathbf{l} or perpendicular to \mathbf{t} , and $K_{\perp\parallel}$ is the off-diagonal component, which is nonzero if $\{\mathbf{l}, \mathbf{t}\}$ do not coincide with the principal directions. The curvature $K_{\perp\parallel}$ is

sometimes also referred to as the “geodesic torsion,” because it is equal to the torsion of a geodesic that locally has the tangent vector \mathbf{t} (Kreyszig, 1991; Spivak, 1975a; Willmore, 2012).

In the same way we can also define directional derivatives along \mathbf{t} and \mathbf{l} :

$$\nabla_{\perp} = l_a \nabla^a, \quad \nabla_{\parallel} = t_a \nabla^a. \quad (104)$$

Let us look at an important example in order to practice these equations. Consider a curve \mathcal{C} on the surface and its Darboux frame $\{\mathbf{l}, \mathbf{t}, \mathbf{n}\}$. As we move along \mathcal{C} , the normal vector \mathbf{n} changes as follows:

$$\nabla_{\parallel} \mathbf{n} = t^a \nabla_a \mathbf{n} = t^a K_a^b \mathbf{e}_b = t^a K_a^b (t_b \mathbf{t} + l_b \mathbf{l}) = K_{\parallel} \mathbf{t} + K_{\perp\parallel} \mathbf{l}. \quad (105)$$

For the change of the tangent vector \mathbf{t} we find

$$\begin{aligned} \nabla_{\parallel} \mathbf{t} &= t^a \nabla_a (t^b \mathbf{e}_b) = t^a t^b \nabla_a \mathbf{e}_b + t^a \mathbf{e}_b \nabla_a t^b \\ &= -t^a t^b K_{ab} \mathbf{n} + (t_b \mathbf{t} + l_b \mathbf{l}) \nabla_{\parallel} t^b = -K_{\parallel} \mathbf{n} + (l_b \nabla_{\parallel} t^b) \mathbf{l} \\ &= -K_{\parallel} \mathbf{n} - k_g \mathbf{l}. \end{aligned} \quad (106)$$

At “*” we used the fact that differentiating $t_b t^b = 1$ implies $t_b \nabla_{\parallel} t^b = 0$. The abbreviation $k_g = -l_b \nabla_{\parallel} t^b$ introduced in the last line is the geodesic curvature of the curve. It is the curvature of a surface curve projected back onto the surface, i.e., that part of the curve’s curvature that is not due to the fact that the surface itself might be curved. Since $\mathbf{t} \cdot \mathbf{t} = 1$, differentiation shows that $\mathbf{t} \cdot \nabla_{\parallel} \mathbf{t} = 0$, and so $\nabla_{\parallel} \mathbf{t}$ cannot have a component along \mathbf{t} . Projecting into the plane therefore means projecting onto \mathbf{l} , and if we do this using Eq. (106), we obtain a coordinate free expression for the geodesic curvature:

$$k_g = -\mathbf{l} \cdot \nabla_{\parallel} \mathbf{t}. \quad (107)$$

This gives a clean geometric definition for the quantity that enters the Gauss–Bonnet theorem (70). The sign convention is such that a planar circle of radius R with outward pointing normal \mathbf{n} has a positive geodesic curvature $1/R$. As an example, a great circle on a sphere of radius R has a curvature $1/R$ but no geodesic curvature, since $\nabla_{\parallel} \mathbf{t}$ points towards the center of the sphere but \mathbf{l} is tangential to it, so that $k_g = -\mathbf{l} \cdot \nabla_{\parallel} \mathbf{t} = 0$. Curves with a vanishing geodesic curvature are called geodesics. They generalize straight lines to curved geometries.

Finally, since $\mathbf{l} \cdot \mathbf{n} = 0$, we know that $\mathbf{l} \cdot \nabla_{\parallel} \mathbf{n} = -\mathbf{n} \cdot \nabla_{\parallel} \mathbf{l}$, and since $\mathbf{l} \cdot \mathbf{t} = 0$, we know that $\mathbf{l} \cdot \nabla_{\parallel} \mathbf{t} = -\mathbf{t} \cdot \nabla_{\parallel} \mathbf{l}$. This helps us to get the projections of $\nabla_{\parallel} \mathbf{l}$ onto \mathbf{n} and \mathbf{t} from Eqs. (105) and (106), respectively:

$$\nabla_{\parallel} \mathbf{l} = -K_{\perp\parallel} \mathbf{n} + k_g \mathbf{t}. \quad (108)$$

Notice that we can combine Eqs. (105), (106) and (108) in the following elegant way (Spivak, 1975a):

$$\nabla_{\parallel} \begin{pmatrix} \mathbf{l} \\ \mathbf{t} \\ \mathbf{n} \end{pmatrix} = \begin{pmatrix} 0 & k_g & -\tau_g \\ -k_g & 0 & -k_n \\ \tau_g & k_n & 0 \end{pmatrix} \begin{pmatrix} \mathbf{l} \\ \mathbf{t} \\ \mathbf{n} \end{pmatrix}, \quad (109)$$

where we used the more common symbols $k_n = K_{\parallel}$ for the normal curvature along the curve and $\tau_g = K_{\perp\parallel}$ for the geodesic torsion. Eq. (109) is a compact notation for the Frenet–Serret equations of the Darboux-frame, i.e., the answer to the question how the Darboux-frame changes as one moves along the curve \mathcal{C} .²⁸ They nicely illustrate how to work with the decompositions defined in Eqs. (100)–(104), but they do not feature prominently if one only considers the surface itself. However, once one cares about physical curves on surfaces, such as semiflexible polymers, these

²⁷ This unfortunately happens to differ from the convention followed in the mathematical literature, which defines \mathbf{l} pointing in the opposite direction, such that now $\{\mathbf{t}, \mathbf{l}, \mathbf{n}\}$ is right-handed.

²⁸ Again, due to different sign conventions, these equations look differently in the mathematical literature.

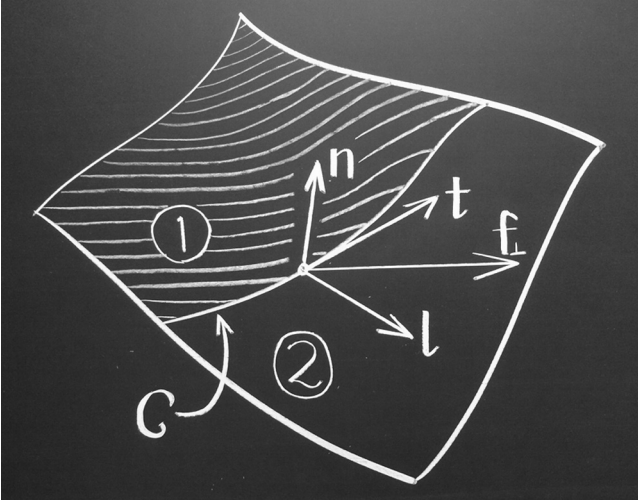


Fig. 5. Stress tensor in the Darboux frame: We are interested in the stress across a curve C , which separates a membrane region 1 from a membrane region 2. The curve has a local tangent vector \mathbf{t} , normal vector \mathbf{l} tangent to the surface, and surface normal vector \mathbf{n} . Let \mathbf{l} be oriented such that it is the outward pointing normal to the region 1. The stress through the curve, $\mathbf{f}_\perp = l_a \mathbf{f}^a$, answers the question: What force per length does patch 1 exert onto patch 2 through the curve C ?

equations become extremely important (Nickerson and Manning, 1988; Guven and Vázquez Montejo, 2012).

Using the Darboux frame as our reference, we can rewrite the force per unit length $l_a \mathbf{f}^a$ for the Helfrich stress tensor from Eq. (96) in the following way:²⁹

$$\begin{aligned} \mathbf{f}_\perp := l_a \mathbf{f}^a &= \kappa(K - K_0) \left[l_a K^{ab} (l_b l^c + t_b t^c) \mathbf{e}_c \right. \\ &\quad \left. - \frac{1}{2} (K - K_0) l_a g^{ab} (l_b l^c + t_b t^c) \mathbf{e}_c \right] \\ &= \kappa(K - K_0) \left[K_\perp \mathbf{l} + K_{\parallel} \mathbf{t} - \frac{1}{2} (K - K_0) \mathbf{l} \right] \\ &\quad - \sigma \mathbf{l} - \kappa(\nabla_\perp K) \mathbf{n} \\ &= \left\{ \frac{1}{2} \kappa [K_\perp^2 - (K_{\parallel} - K_0)^2] - \sigma \right\} \mathbf{l} \\ &\quad + \kappa(K - K_0) K_{\parallel} \mathbf{t} - \kappa(\nabla_\perp K) \mathbf{n}, \end{aligned} \quad (110)$$

where in the last step we used the fact that $K = K_\perp + K_{\parallel}$. In the important special case $K_0 = 0$ this simplifies to

$$\mathbf{f}_\perp = \left[\frac{1}{2} \kappa (K_\perp^2 - K_{\parallel}^2) - \sigma \right] \mathbf{l} + \kappa K K_{\parallel} \mathbf{t} - \kappa(\nabla_\perp K) \mathbf{n}. \quad (111)$$

Fig. 5 illustrates the geometry of our definition of the force density in the Darboux frame.

We now have gained a much better position from which to judge the physical meaning of the stress tensor. Begin by considering the simple special case in which $\kappa = 0$, so the surface Hamiltonian is really only characterized by a surface tension σ . In that case the stress tensor is $\mathbf{f}^a = -\sigma \mathbf{e}^a$, and the force per unit length is

$$\mathbf{f}_\perp = -\sigma \mathbf{l} \quad (112)$$

in the Darboux frame. This force is seen to be independent of the surface geometry, isotropic, tangential, and normal to the cut. The negative sign tells us that for positive surface tension the force *pulls*: A patch of membrane with outward pointing unit normal \mathbf{l} pulls *inward*. But as Eqs. (110) or (111) show, the transmitted forces are more complicated in the presence of curvature elasticity:

1. The force depends on the surface geometry through the local curvature.
2. The occurrence of the curvature tensor K_{ab} (instead of the scalar K) also shows that the force is generally not isotropic (in which case it could only be proportional to g_{ab}).
3. If the curvature K is not constant, the last term $-\kappa(\nabla_\perp K) \mathbf{n}$ shows that the resulting force is no longer tangential to the surface.
4. If the cut is not along a principal direction, the off-diagonal component $K_{\perp\parallel}$ does not vanish and a force component tangential to the cutting direction emerges.³⁰

As far as the force component normal to the cut (along \mathbf{l}) is concerned, we can observe an interesting pattern: The curvature K_\perp perpendicular the cut leads to a repulsive force of magnitude $(1/2)\kappa K_\perp^2$, while the curvature K_{\parallel} parallel to the cut increases the tensile force of the surface tension term by an additional amount $(1/2)\kappa(K_{\parallel} - K_0)^2$. It is quite curious that only the latter term involves the spontaneous curvature K_0 .

The slightly convoluted discussion in Section 4.4 shows that understanding the correct sign of the force from first principles can easily turn into a nerve-wracking exercise one does not wish to go through each and every time one needs to know the direction of the force. In the experience of the author, a reliable shortcut is to calibrate one's expectation of the sign against the surface tension term, for which intuition will give the right direction. For instance, since σ and $(1/2)\kappa(K_{\parallel} - K_0)^2$ both occur with the same sign in Eq. (110), and since we know that a positive surface tension leads to a tensile force, we know that the parallel curvature term does so, too.

Finally, observe that, again, the Gaussian term has dropped out of the stress tensor: \mathbf{f}^a does not involve $\bar{\kappa}$. We have previously seen that the shape equation is independent of the Gaussian modulus; now we find that even surface stresses do not involve the Gaussian curvature term in the Hamiltonian.

4.6. Simple examples for the stress tensor

It is instructive to look at a few special cases for the stress tensor, and below we will investigate the simple but nevertheless important special cases of planes, spheres, and cylinders.

4.6.1. Plane

If the membrane is flat, all curvatures (and of course their gradients) vanish, and so the stress tensor (110) greatly simplifies:

$$\mathbf{f}_\perp = - \left[\sigma + \frac{1}{2} \kappa K_0^2 \right] \mathbf{l}. \quad (113)$$

The first contribution, $-\sigma \mathbf{l}$, is nothing but the surface tension term. The second contribution, $-(1/2)\kappa K_0^2 \mathbf{l}$, is the *spontaneous tension* recently described by Lipowsky (2013, 2014). Its sign is such that it always pulls, exactly like an ordinary positive surface tension.³¹

²⁹ Guven and Vázquez Montejo (2013) define $\mathbf{f}_\perp = -l_a \mathbf{f}^a$, presumably to get closer to the conventional sign definition of the stress tensor. Here I rather stay with the convention that the subscript “ \perp ” indicates a projection onto l_a , without any minus signs that may or may not happen, and have the same convention for the sign of \mathbf{f}^a and \mathbf{f}_\perp .

³⁰ Given that the off-diagonal component of the curvature tensor is involved, it is tempting to interpret this force as a shear, but this view is misleading: The surface is fluid and cannot support shear.

³¹ Notice, though, that the sign of σ does not necessarily have to be positive: Membranes under compression can have a negative tension, as we will see in Section 6.3.

Both terms together result in what might be called the *isotropic tension* Σ with which a flat membrane pulls:

$$\Sigma := \sigma + \frac{1}{2}\kappa K_0^2 = \sigma \left[1 + \frac{1}{2}(K_0\lambda)^2 \right], \quad (114)$$

where λ is the characteristic length defined in Eq. (71). As we have seen, this length scale can be many tens of nanometers for membranes at low cellular tensions, and so it does not take much of a spontaneous curvature K_0 before the spontaneous tension begins to contribute significantly to the isotropic tension.

The view that, as far as stresses are concerned, a spontaneous curvature K_0 simply leads to a spontaneous tension $(1/2)\kappa K_0^2$ that shifts the value of the bare surface tension σ would be incorrect, though. Yes, for *flat* membranes the term $(1/2)\kappa K_0^2$ indeed contributes additively, but for *curved* membranes the spontaneous curvature enters the overall membrane stress in a more complicated fashion: it only affects the K_{\parallel} part in Eq. (110) and will therefore generally *not* act isotropically, unlike the usual surface tension. Of course, even in the curved case a term $(1/2)\kappa K_0^2$ exists that shifts σ , and so the sum of both terms, Σ , can be viewed as a tension independent of the shape—which is why the term “isotropic tension” seems fitting: a tension that acts irrespective of the local state of curvature. However, expanding the square shows that there generally is an *additional* geometry dependent stress $\kappa K_0 K_{\parallel} \mathbf{l}$. The moral is: the spontaneous curvature creates stresses beyond the spontaneous tension. Its effects are generally not isotropic, even though the scalar K_0 has no direction built into it, because it can entangle the local geometry into the stresses, and the local geometry is generally anisotropic.

4.6.2. Sphere

A sphere's curvature is not just constant but also isotropic: $K_{\perp} = K_{\parallel}$, $K_{\perp\parallel} = 0$ and $\nabla_{\perp} K = 0$. For $K_0 = 0$ we get the very simple result $\mathbf{f}_{\perp} = -\sigma \mathbf{l}$, showing that the stresses in a spherically curved Helfrich membrane do not depend on curvature terms at all. Cutting a spherical vesicle with $K_0 = 0$ into half at the equator means that the force density required to hold the rim is the same as that for a soap film, *i.e.*, the discussion seems identical to that leading to Eq. (79a)—but this is not quite true, because at the open edge of a vesicle it will not be enough to only supply a force. We will also need to supply a torque, as Section 5 will show.

The result $\mathbf{f}_{\perp} = -\sigma \mathbf{l}$ for spherical vesicles is counterintuitive also for a different reason: it does not involve the vesicle's size. One might have expected more highly curved vesicles to experience bigger curvature stresses, but this is not so. The curvature stresses vanish (at least on the quadratic Helfrich level). Of course, the bending energy per lipid, ε_{ℓ} , increases for smaller vesicles: since for a sphere the bending energy is $8\pi\kappa + 4\pi\bar{\kappa}$, we find approximately

$$\varepsilon_{\ell} \approx \frac{a_{\ell}}{2R^2}(2\kappa + \bar{\kappa}). \quad (115)$$

With $2\kappa + \bar{\kappa} \approx 20k_{\text{B}}T$, $a_{\ell} \approx 0.7 \text{ nm}^2$ and even a very small vesicle radius of $R = 5 \text{ nm}$, we get $\varepsilon_{\ell} \approx 0.3k_{\text{B}}T$, which is almost two orders of magnitude smaller than the aggregation free energy per lipid. Hence, there is little reason to suspect that internal curvature energies or stresses destabilize small vesicles: the former are small, the latter are zero.

If the spontaneous curvature K_0 does not vanish, a bending contribution to the surface stress remains:

$$\mathbf{f}_{\perp} = \left\{ \frac{1}{2}\kappa K_0 \left(\frac{2}{R} - K_0 \right) - \sigma \right\} \mathbf{l} = \left\{ \frac{\kappa K_0}{R} - \Sigma \right\} \mathbf{l}. \quad (116)$$

The bending term vanishes if $K_0 = 2/R$, *i.e.*, when the spontaneous curvature equals the vesicle's curvature. If the vesicle is bigger than $2/K_0$, the bending stresses are contractile (same sign as the σ -term!) and hence try to reduce the radius of the vesicle. If the vesicle radius is smaller than $2/K_0$, the bending stresses instead try to swell the

vesicle. In either case, there are no normal stresses, even though there is a normal *force density*, which is the divergence of the stress tensor and which is equal to the excess pressure in the vesicle's interior.

Notice that for closed vesicles we will also have a Young–Laplace pressure to deal with, so the *complete* force balance involves more than surface stresses. If we cut a spherical vesicle at the equator, we get a rim-contribution from the force density in Eq. (116), but this will be balanced by a pressure term that is equal to the excess pressure P of the interior vesicle times the cross-sectional area πR^2 of that cut. Hence, a generalization of the argument that led to Eq. (79a) now yields

$$2\pi R \left[\frac{1}{2}\kappa K_0 \left(\frac{2}{R} - K_0 \right) - \sigma \right] = -\pi R^2 P, \quad (117)$$

or slightly rewritten

$$\frac{2\Sigma}{R} = P + \frac{2\kappa K_0}{R^2}. \quad (118)$$

It is easy to see that this is equivalent to the shape equation (87) specialized to a sphere. It is a quadratic equation in R which only has real solutions if $\Sigma^2 > 2P\kappa K_0$, namely

$$R_{1,2} = \frac{1}{P} \left[\Sigma \pm \sqrt{\Sigma^2 - 2P\kappa K_0} \right]. \quad (119)$$

4.6.3. Cylinder

Imagine pulling a cylindrical tether of radius R and length L out of a flat membrane which is under tension σ and has a spontaneous curvature K_0 . What is the force with which we need to hold the tether?

The two natural directions in which to decompose the stress tensor are along the axis and along the circumference. For symmetry reasons these coincide with the principal directions, and hence no off-diagonal (tangential) force emerges at the cut. Since furthermore the curvature is constant (except maybe at the tip of the tether and where it connects to the flat membrane), the normal stresses vanish, too. Hence for the directions along and around the cylinder, we find the following tangential force per unit length:

$$\text{along:} \quad \mathbf{l} \cdot \mathbf{f}_{\perp} = -\frac{1}{2}\kappa \left(\frac{1}{R} - K_0 \right)^2 - \sigma, \quad (120a)$$

$$\text{around:} \quad \mathbf{l} \cdot \mathbf{f}_{\perp} = \frac{1}{2}\kappa \left(\frac{1}{R^2} - K_0^2 \right) - \sigma. \quad (120b)$$

We cannot control the radius of the cylinder, it instead freely adjusts such that the circumferential stress (120b) vanishes (Fournier, 2007), leading to (Bukman et al., 1996; Hochmuth et al., 1996; Waugh et al., 1992)

$$R = \sqrt{\frac{\kappa/2}{\sigma + \kappa K_0^2/2}} = \sqrt{\frac{\kappa}{2\Sigma}}. \quad (121)$$

The axial force F_{Σ} along the tether pulled from a flat membrane subject to the isotropic tension Σ now arises from multiplying the stress from Eq. (120a) with the circumference of the tether:

$$\begin{aligned} F_{\Sigma} &= 2\pi R \left[\frac{1}{2}\kappa \left(\frac{1}{R} - K_0 \right)^2 + \sigma \right] \\ &= 2\pi \left[\frac{\kappa}{2R} - \kappa K_0 + \Sigma R \right] \\ &= 2\pi \left[\sqrt{2\kappa\Sigma} - \kappa K_0 \right] = 2\pi\kappa \left[\frac{1}{R} - K_0 \right]. \end{aligned} \quad (122)$$

The spontaneous curvature K_0 affects tether radius R and tether force F_{Σ} in different ways: Any non-zero K_0 decreases R ; but the additional shift in F_{Σ} by $-2\pi\kappa K_0$ reduces the force if K_0 prefers the curvature of the tether, while it increases the force otherwise. The

force vanishes if $1/R = K_0$, or equivalently $\sigma = 0$. Hence, for $\sigma < 0$ (or if the isotropic tension Σ is smaller than the spontaneous tension $\frac{1}{2}\kappa K_0^2$) a pre-existing tube will increase its length spontaneously.

We could of course also derive these results using energy arguments. The energy of a tether of radius R and length L pulled from a flat parent membrane is given by

$$E = 2\pi RL \left[\sigma + \frac{1}{2}\kappa \left(\frac{1}{R} - K_0 \right)^2 \right] \quad (123a)$$

$$= 2\pi RL \left[\Sigma + \frac{1}{2}\kappa \left(\frac{1}{R} - K_0 \right)^2 - \frac{1}{2}\kappa K_0^2 \right]. \quad (123b)$$

The condition $0 = (\partial E / \partial R)_\Sigma$ leads to the radius from Eq. (121), and $F_\Sigma = (\partial E / \partial L)_\Sigma$ leads to the force from Eq. (122).

Algebraically, the two expressions (123a) and (123b) are trivially identical; but the interpretation of the terms is subtly different. In Eq. (123a) the first term accounts for the energy of transferring membrane area from the parent membrane into the tether, while the second term is the bending energy of the tether. In Eq. (123b) the first term describes the work required to pull membrane against the isotropic tension Σ of the parent membrane, while the second and third term together account for the *excess* bending energy which a pulled tether possesses compared to the flat parent membrane. Notice how the subtle difference between the price to pay for extra *area* vs. the price to pull against an *isotropic tension* has implications on which form the correct bending term should take (to avoid double-counting). This is one more reminder that the seemingly innocuous term “tension” should be used with great care.

If the tubular membrane is not connected to a flat parent membrane but a curved one (e.g. a vesicle), then the stress balance equations are modified by an additional (Young–Laplace) pressure across the membrane, which can be accounted for by the same reasoning that led to Eq. (79a). For vesicles much bigger than the attached tubes the pressure contribution is a small correction, but it for instance affects stability questions. The numerous ramifications of this situation have recently been discussed by Lipowsky (2013, 2014). Fluctuation corrections are addressed in Ou-Yang and Helfrich (1989), Komura and Lipowsky (1992), Bukman et al. (1996), Fournier and Galatola (2007) and Monnier et al. (2010).

In the situation discussed so far the cylindrical membrane tube was under a fixed tension, which is the experimentally relevant case. However, in computer simulations it is often convenient to simulate cylindrical membranes in the ensemble of constant area, for instance because the tensile force permits access to the bending rigidity κ (Harmandaris and Deserno, 2006; Arkhipov et al., 2008; Shiba and Noguchi, 2011). In this case the membrane radius follows from the tube’s area and length via $R = A / (2\pi L)$ and not from the vanishing of the circumferential stress. It is thus worthwhile to ask whether these tethers are somehow different in terms of their internal stresses.

The area could be fixed with a Lagrange multiplier term σA , but it is easier to enforce this constraint explicitly. The tether force is then seen to be given by

$$\begin{aligned} F_A &= \left(\frac{\partial E}{\partial L} \right)_A = \frac{\partial}{\partial L} \bigg|_A \left[2\pi RL \times \frac{1}{2}\kappa \left(\frac{1}{R} - K_0 \right)^2 \right] \\ &= \frac{\partial}{\partial L} \left[A \times \frac{1}{2}\kappa \left(\frac{2\pi L}{A} - K_0 \right)^2 \right] \\ &= 2\pi\kappa \left(\frac{1}{R} - K_0 \right), \end{aligned} \quad (124)$$

just as in the constant tension case derived in Eq. (122). This answer must equal the result derived from a stress analysis, from which we can determine the unknown bare tension σ :

$$F_A = 2\pi R \left[\frac{1}{2}\kappa \left(\frac{1}{R} - K_0 \right)^2 + \sigma \right]. \quad (125)$$

Inserting Eq. (124) for F_A , we see that this condition is equivalent to Eq. (121), and therefore the value of σ is the same as in the constant-tension ensemble. This in particular implies that the circumferential stress again vanishes, even though the radius does not adjust to do this (instead, the value of σ adjusts). Constant-area and constant-tension tethers are equivalent (at least in their ground state properties).

5. The torque tensor of lipid membranes

In the previous section we have seen how surfaces transmit stresses. If the surface energy is characterized by anything more complicated than an ordinary surface tension, these stresses give rise to more than a constant isotropic tangential force per unit length. But we know from experience that objects that exhibit some rigidity are able to transmit even more than stresses: I can hold a beam horizontally by clamping it at one end, something that does not work with a rope. Beams are able to transmit *torques*, and the same is true for membranes subject to curvature elasticity. In this brief section we will develop the formalism within which this can be simply described. After what we have learned about the stress tensor, the arguments will be very familiar.

5.1. Boundary terms in the functional variation

In Section 4.4 we found the interpretation of the surface stress tensor by looking at the boundary term of the variation of \tilde{H} from Eq. (89). We expected a conserved quantity related to a continuous symmetry—this is how translation symmetry gave rise to the stress tensor. However, there is another obvious continuous symmetry, namely rotations. These would change not only the position of points of the membrane, but also all directions, especially those of the normal vector.

In Eq. (90) we only found one boundary term, namely $-l_a \mathbf{f}^a \cdot \delta \mathbf{X}$, because this is the only one which is nonzero for constant translations. However, it is obvious that in general this is not the only one that could arise upon varying \tilde{H} : for instance, the functional contains the term $\Lambda^{ab}(K_{ab} - \mathbf{e}_a \cdot \nabla_b \mathbf{n})$, which produces a boundary term when varying \mathbf{n} and integrating by parts, namely $-l_b \Lambda^{ab} \mathbf{e}_a \cdot \delta \mathbf{n} = l_b \mathcal{H}^{ab} \mathbf{e}_a \cdot \delta \mathbf{n}$.

Consider again the equilibrated patch \mathcal{R} which we translated in Section 4.4. If we instead perform a constant *rotation* $\delta \mathbf{X} = \delta \boldsymbol{\beta} \times \mathbf{X}$, which implies a concomitant rotation of the normal vector $\delta \mathbf{n} = \delta \boldsymbol{\beta} \times \mathbf{n}$, the boundary change in $\tilde{H}[\mathcal{R}]$ now has a second term from the \mathbf{n} derivative just mentioned, and so we get the slightly more complicated boundary contribution

$$\delta \tilde{H}[\overline{\mathcal{R}}] = -\delta \boldsymbol{\beta} \times \oint_{\partial \mathcal{R}} ds \bar{l}_a \{ \mathbf{X} \times \mathbf{f}^a + \mathcal{H}^{ab} \mathbf{e}_b \times \mathbf{n} \} = \delta \boldsymbol{\beta} \times \mathbf{M}_{\text{ext}}[\overline{\mathcal{R}}]. \quad (126)$$

The integral can now be interpreted as a torque, and the integrand is therefore the torque tensor (Capovilla and Guven, 2002a, 2004)

$$\mathbf{m}^a = \mathbf{X} \times \mathbf{f}^a + \mathcal{H}^{ab} \mathbf{e}_b \times \mathbf{n}. \quad (127)$$

The first term is the obvious external torque: If there is a force density along the edge of the patch \mathcal{R} , then the position crossed into it results in a torque density along the edge. The more interesting term is the second one, the *intrinsic* torque, which arises because the surface itself resists internal rotations around any axis

perpendicular to the surface normal. Since in the special case of the Helfrich Hamiltonian we already know what \mathcal{H}^{ab} is, we quickly get (Capovilla and Guven, 2002a, 2004)

$$\mathbf{m}^a = \mathbf{X} \times \mathbf{f}^a + \bar{\mathbf{m}}^a \quad (128a)$$

$$\text{with } \bar{\mathbf{m}}^a = [\kappa(K - K_0)g^{ab} + \bar{\kappa}(Kg^{ab} - K^{ab})] (\mathbf{e}_b \times \mathbf{n}). \quad (128b)$$

Note that the intrinsic torque is tangential to the surface, meaning that the rotation axis of the couple it corresponds to lies in the plane.

Using again completeness (101), the identities from Section 2.6, the orthonormality of the triad $\{\mathbf{l}, \mathbf{t}, \mathbf{n}\}$, and Eq. (105), the projection of the intrinsic torque on the outward pointing normal \mathbf{l} is (Müller, 2007)

$$\bar{\mathbf{m}}_{\perp} = l_a \bar{\mathbf{m}}^a = -\kappa(K - K_0)\mathbf{t} - \bar{\kappa}(K_{\parallel}\mathbf{t} + K_{\perp}\mathbf{l}) \quad (129a)$$

$$= -\kappa(K - K_0)\nabla_{\parallel}\mathbf{X} - \bar{\kappa}\nabla_{\parallel}\mathbf{n}. \quad (129b)$$

The term proportional to the bending rigidity κ describes a couple around the direction \mathbf{t} of the contour. And the reformulation of the $\bar{\kappa}$ -term in Eq. (129b) reveals the fact that for closed integrals this term must vanish, since $\oint ds \nabla_{\parallel}(\text{anything}) = \oint ds(d/ds)(\text{anything}) = 0$. Whenever K is constant (if we have a so-called “constant mean curvature surface”), the same argument shows that the first term vanishes on closed contours, too. This is certainly always true for the part proportional to K_0 .

5.2. Simple examples for the torque tensor

The nontrivial part in the torque tensor is the intrinsic torque, which is proportional to $\mathcal{H}^{ab} = \delta\mathcal{H}/K_{ab}$. Hence, if the Hamiltonian density of the surface does not depend on its curvature, there is no intrinsic torque. This is evidently true for pure surface tensions: applying a local force couple to an object that feels no bending resistance will not result in the transmission of torques.

For flat membranes all curvatures vanish, and so the intrinsic torque is $\bar{\mathbf{m}}_{\perp} = \kappa K_0 \mathbf{t}$. This expression states that a flat membrane with a spontaneous curvature is under torsional stress: it everywhere wants to “curl down” such that the resulting curvature K more closely corresponds to the spontaneous curvature K_0 .

To get an intuitive feeling about the sign of the intrinsic torque, it is useful to consider a cylindrically curved membrane, such as the one in Fig. 6, for simplicity first in the case $K_0 = 0$. What is the intrinsic torque at its straight edge? From Eq. (129a) we immediately find $\bar{\mathbf{m}}_{\perp} = -\kappa K \mathbf{t}$. The proportionality to \mathbf{t} implies that the intrinsic torque has \mathbf{t} as its axis, and since torques have something to do with local rotations, the following image might be useful: Imagine glueing a rod to the edge of the membrane. If we turn the rod, we would curl the membrane in one direction or the other, thus curving it locally. In equilibrium, the membrane would react by a torque that fights against our attempts to rotate that rod. In Fig. 6 we have to rotate the rod clockwise to curve the membrane the way it is curved; this means that the back-torque exerted by the membrane acts counter-clockwise, as the curled arrow illustrates. Using the right hand rule, we see that this rotation direction corresponds to the (axial) vector $-\mathbf{t}$, just as Eq. (129a) states. Alternatively, consider the formula $\mathbf{r} \times \mathbf{F}$ for a torque, and rewrite $\mathbf{t} = \mathbf{n} \times \mathbf{l}$. If we now identify $\mathbf{n} \leftrightarrow \mathbf{r}$ as a lever arm and exert a force in the direction of $\mathbf{l} \leftrightarrow \mathbf{F}$, we induce the same rotation around the \mathbf{t} -axis. Notice that we need $K > 0$ for this argument, but this is true in the figure, since the membrane bends away from the local normal vector. As usual for torques (and anything else that involves cross-products), the handedness of the coordinate frame matters.

If the edge of the membrane in Fig. 6 were free, nothing there could counterbalance an intrinsic torque, which therefore has to

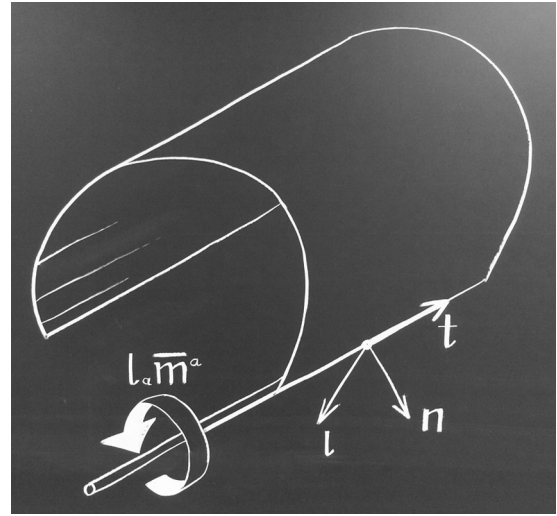


Fig. 6. Geometry along an axial cut of a cylindrical membrane. The “rod” glued to the membrane helps to visualize the rotation necessary to curl the membrane into a given curvature, and in what direction the membrane therefore tries to rotate it back to counteract the imposition of external intrinsic torque—namely in the one indicated by the curved arrow.

vanish. Indeed, $\mathbf{t} \cdot \bar{\mathbf{m}}_{\perp} = 0$, or $\kappa(K - K_0) + \bar{\kappa}K_{\parallel} = 0$, is one of the boundary conditions of an open edge (Capovilla et al., 2002; Tu and Ou-Yang, 2003). In the case of Fig. 6 this would imply $K = 0$, and since here $K_{\parallel} = 0$ anyways, we deduce $K_{\perp} = 0$ at a straight edge, showing that the membrane is planar there. If the curve is not an actual open edge but merely a contour \mathcal{C} drawn on a membrane to separate two regions, just as in Fig. 5, the intrinsic torque does not vanish on \mathcal{C} ; it instead has the magnitude κK and the direction discussed above. As we have seen in Section 4.6.3, the circumferential stress always vanishes for cylindrical membrane tethers, but the axial intrinsic torque generally does not.

For spherical membranes we find the intrinsic torque per unit length

$$\bar{\mathbf{m}}_{\perp} = -\kappa \left(\frac{2}{R} - K_0 \right) \mathbf{t} - \bar{\kappa} \frac{1}{R} \mathbf{t} = - \left[(2\kappa + \bar{\kappa}) \frac{1}{R} - \kappa K_0 \right] \mathbf{t}. \quad (130)$$

The second term is again the torque due to the spontaneous curvature (which in fact never depends on the geometry). The first term counteracts the spontaneous term, and it describes the torque by which a curved membrane resists bending by promoting “uncurling.” Notice that it has a definite sign, because $2\kappa + \bar{\kappa} > 0$ by virtue of the stability condition (69), but the torque balance is indeed curious: Since $\bar{\kappa} < 0$, its contribution alone would make the membrane curl more into the direction it is already curved, but the κ -term always overwhelms this trend.

At this point we can finally complete our analysis of the spherical vesicle (with $K_0 = 0$) cut open at the equator and ask, what do we need to do at the open edge to make up for the missing lower half? We already know that a stress $\mathbf{f}_{\perp} = -\sigma \mathbf{l}$ needs to be balanced. Now we see that also an intrinsic torque $\bar{\mathbf{m}}_{\perp} = -(2\kappa + \bar{\kappa})R^{-1} \mathbf{t}$ must be compensated. In the absence of that, the vesicle would not be able to maintain its curvature at the rim. Interestingly, the intrinsic torque does depend on the vesicle’s size, unlike the stress. If one insists on viewing smaller vesicles as being under a higher stress, then one should have torsional stress in mind.

The equations for the torque finally involve the Gaussian modulus $\bar{\kappa}$ in a nontrivial way. This does not violate the Gauss–Bonnet theorem (70), since the Gaussian term influences the boundary integral over the geodesic curvature. Indeed, Yao et al. (2012) have recently studied how $\bar{\kappa}$ affects the shape of pored membranes.

Flat membranes without spontaneous curvature are torque free. Can spherically curved membranes also be torque free? From Eq. (130) we see that at a given spontaneous curvature this would require the radius

$$R = \frac{2\kappa + \bar{\kappa}}{\kappa K_0}. \quad (131)$$

Interestingly, this is generally not the radius at which the vesicle curvature corresponds to the spontaneous curvature. Instead, it happens to be the radius at which the *energy density* of a spherical vesicle is minimized. The range $-2\kappa \leq \bar{\kappa} \leq 0$ in principle allows $0 \leq R \leq 2/K_0$. Assuming $\bar{\kappa} \simeq -\kappa$ leads to $R \simeq 1/K_0$. Of course, for $R \neq 0$ we will also have curvature stresses and generally a Young–Laplace pressure to reckon with, therefore Eq. (118) must hold, too. Combining this yields a connection between pressure and isotropic tension which a torque-free vesicle would have to satisfy:

$$\Sigma = \frac{(\kappa K_0)^2}{2\kappa + \bar{\kappa}} + \frac{1}{2}P \frac{2\kappa + \bar{\kappa}}{\kappa K_0}. \quad (132)$$

The sign of the first contribution is always positive, while the sign of the second one is not, since both P and K_0 can be either positive or negative. It is therefore possible for the intrinsic torque $\bar{\mathbf{m}}_{\perp}$ and the isotropic tension Σ to *both* vanish, provided the pressure satisfies

$$P = -\frac{2(\kappa K_0)^3}{(2\kappa + \bar{\kappa})^2}. \quad (133)$$

This means that for $K_0 > 0$ the pressure would have to be negative, while for $P > 0$ the spontaneous curvature would have to be opposite to the curvature of the vesicle.

6. Applications

This final section will present four examples that show, how one can efficiently reason with stress and torque tensors that are somewhat less trivial than the cases investigated so far.

6.1. Boundary conditions for adhesion

Consider two membranes, characterized by bending rigidities κ_1 and κ_2 . If they can adhere with an adhesion energy $w > 0$ per unit area, while being able to slide past each other, bending rigidity and tension of the double-membrane are simply the sum of the individual membranes: $\kappa_{12} = \kappa_1 + \kappa_2$ and $\sigma_{12} = \sigma_1 + \sigma_2$ —for exactly the same reason we encountered when transforming between monolayer and bilayer quantities in Section 3.4. We now wish to know what happens at a contact line \mathcal{C} where the two membranes detach, *i.e.*, what can we say about the geometry of the three approaching surfaces if that contact line is in equilibrium.

Since a variation of the contact line (say, some slight un-peeling between the two membranes) does neither affect the topology nor the boundary of either membrane, the Gauss–Bonnet theorem tells us that the Gaussian part in the energy can play no role in this balance. Moreover, in the presence of bending energy the membranes cannot have kinks, so all three surfaces must be tangential at the contact line, and for continuity reasons they must also have the same curvature K_{\parallel} along \mathcal{C} . However, the component K_{\perp} perpendicular to the contact line or its derivative $\nabla_{\perp} K_{\perp}$ need not be the same. In fact, understanding what happens at the contact line boils down to predicting how these curvatures or curvature gradients jump.

In Deserno et al. (2007) this problem is approached using a covariant variation of the contact line. However, the authors point out that the final answer follows readily from a stress- and torque-balance. Since we know the stress- and torque tensors, the conditions can be written down rather quickly. Notice that the only

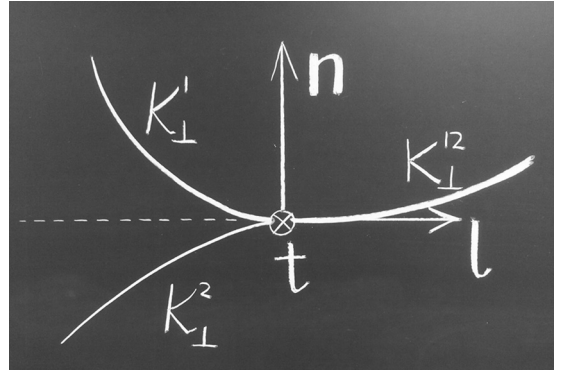


Fig. 7. Geometry along the contact line between two adhering membranes.

meaningful stress is perpendicular to the contact line, but there are two independent directions that would matter: tangential to the surfaces and normal to them. For the torque, the only meaningful direction is along the contact line.

Let us define the vector \mathbf{l} (tangential to the surfaces and normal to \mathcal{C}) such that it points into the direction of the composite membrane—see Fig. 7. The easiest balance is that of the normal force $\mathbf{n} \cdot \mathbf{f}_{\perp}$, which with the help of Eq. (111) results in

$$\kappa_1(\nabla_{\perp} K_{\perp}^1) + \kappa_2(\nabla_{\perp} K_{\perp}^2) = (\kappa_1 + \kappa_2)(\nabla_{\perp} K_{\perp}^{12}), \quad (134)$$

where the superscripts at the curvatures are of course not exponents but indicate the surface, and where the terms involving the parallel curvatures have been omitted because $\nabla_{\perp} K_{\parallel}^i$ is continuous across \mathcal{C} .

The torque balance is fairly straightforward, too. Notice first that stress balance automatically implies the balance of the *external* torques $\mathbf{X} \times \mathbf{f}^a$, so we only need to concern ourselves with the intrinsic torques. Balancing $\mathbf{t} \cdot \bar{\mathbf{m}}_{\perp}$ and ignoring the Gaussian term (as explained above), results in

$$\kappa_1 K_{\perp}^1 + \kappa_2 K_{\perp}^2 = (\kappa_1 + \kappa_2) K_{\perp}^{12}, \quad (135)$$

where the parallel curvatures again cancel because K_{\parallel}^i is continuous across \mathcal{C} .

The final condition to consider is the tangential stress balance, $\mathbf{l} \cdot \mathbf{f}_{\perp}$. The curvature part itself is simple, each membrane pushes back with a force proportional to $(1/2)\kappa_i(K_{\perp}^i)^2$, while the contribution involving $-(1/2)\kappa_i(K_{\parallel}^i - K_0^i)^2 - \sigma_i$ cancels (because the surfaces are all tangential and K_{\parallel}^i is continuous across \mathcal{C}). There is an extra complication, though, originating from the adhesion energy, which changes if we move the contact line along \mathbf{l} . Consider moving \mathcal{C} into the direction of the adhering surfaces. Clearly, the composite membrane, by virtue of its curvature K_{\perp}^{12} will push against such a motion, but moving the contact line into this direction also means *un-peeling* the membranes, *i.e.*, lowering the adhesion energy by $w\delta X \cdot \mathbf{l}$ per unit length along the contact line. This increase in energy must also resist the displacement of the contact line, and since its contribution is simply proportional to the area, it enters the stress tensor exactly like a surface tension term. Taken together, this means that tangential force balance leads to

$$\frac{1}{2}\kappa_1(K_{\perp}^1)^2 + \frac{1}{2}\kappa_2(K_{\perp}^2)^2 = \frac{1}{2}(\kappa_1 + \kappa_2)(K_{\perp}^{12})^2 + w. \quad (136)$$

Eqs. (134)–(136) constitute the contact line conditions for adhering membranes we were looking for. It is possible to symmetrize the two conditions (135) and (136) by alternatively removing K_{\perp}^1 or K_{\perp}^2 between them, resulting in

$$\left(1 + \frac{\kappa_1}{\kappa_2}\right)(K_{\perp}^1 - K_{\perp}^{12})^2 = \frac{2w}{\kappa_1}, \quad (137a)$$

$$\left(1 + \frac{\kappa_2}{\kappa_1}\right) (K_{\perp}^2 - K_{\perp}^{12})^2 = \frac{2w}{\kappa_2}. \quad (137b)$$

From Eq. (135) we see that K_{\perp}^1 and K_{\perp}^2 cannot both be bigger than K_{\perp}^{12} , nor can they both be smaller. Hence, one is bigger and one is smaller than K_{\perp}^{12} , and this means that when we take the square root in Eqs. (137a,b), exactly one of them will receive a minus sign.

Two special cases are interesting. First, if $\kappa_2 \rightarrow \infty$, the second membrane essentially becomes a rigid substrate to which the first membrane adheres. Eq. (137b) then shows that $K_{\perp}^2 = K_{\perp}^{12}$, so the substrate does no longer change its curvature at the contact line (it is too stiff to respond to the adhering membrane). Inserting this condition into Eq. (137a) leads to the well-known contact curvature condition

$$K_{\perp}^1 - K_{\perp}^2 = \sqrt{\frac{2w}{\kappa_1}}, \quad (138)$$

whose axisymmetric version was first quoted by Seifert and Lipowsky (1990, footnote 14) and whose planar version is treated in Landau and Lifshitz (1999, Section 12, Prob. 6). It has been derived in its covariant version by variational considerations as well as exclusively from stress balance by Capovilla and Guven (2002b), but as pointed out by Deserno et al. (2007), this will not work if the substrate is not flat. Indeed, we have seen that Eq. (138) results from an entangled stress-torque condition, and for curved substrates the torque condition is nontrivial, because rotations are enslaved to translations. If one translates the contact line along the substrate, this will generally force the normal vector to rotate, thus exerting an intrinsic torque on the membrane that does work beyond the one due to the stress.

Second, if $\kappa_1 = \kappa_2 = \kappa$, we find

$$(K_{\perp}^1 - K_{\perp}^{12})^2 = (K_{\perp}^2 - K_{\perp}^{12})^2 = \frac{w}{\kappa}, \quad (139)$$

which means that the (squared) curvature jump of $2w/\kappa$ of the rigid substrate case is now evenly shared between the two membranes.

6.2. Micropipette aspiration

Micropipette aspiration is an extremely useful experimental tool for manipulating lipid membrane vesicles (Mitchison and Swann, 1954; Evans and La Celle, 1975; Evans et al., 1976; Kwok and Evans, 1981; Evans, 1983; Evans and Yeung, 1989; Evans and Rawicz, 1990; Rawicz et al., 2000; Hochmuth, 2000; Tian et al., 2007). By partially sucking these vesicles into a pipette, monitoring the required pressure difference, and measuring the radius of the remaining outer vesicle, one can set the membrane's surface tension very precisely. Moreover, changing the pressure difference adds or removes membrane area $\Delta A = 2\pi a \Delta L$ from the outer vesicle part, where a is the inner radius of the pipette and ΔL is the length change of the vesicle's "tongue" inside the pipette. Since a can be quite small, even minute area changes result in values of ΔL that are very noticeable, thus enabling precision experiments of membrane elasticity.

The conventional analysis goes like this (Bukman et al., 1996; Hochmuth et al., 1996; Waugh et al., 1992): If the outer vesicle is a spherical cap of radius R and the end-cap inside the pipette is a hemisphere of radius a (see Fig. 8), we get the Young–Laplace relation (79a) across two spherical interfaces. This permits us to eliminate the pressure P inside the vesicle, resulting in

$$P_0 - P_1 = \Delta P = 2\sigma \left(\frac{1}{a} - \frac{1}{R} \right). \quad (140)$$

However, membranes have a bending rigidity, and the Young–Laplace equation neglects this, so Eq. (140) cannot be exact. In fact, Fournier and Galatola have pointed out the following (Fournier and Galatola, 2008): the contact curvature condition

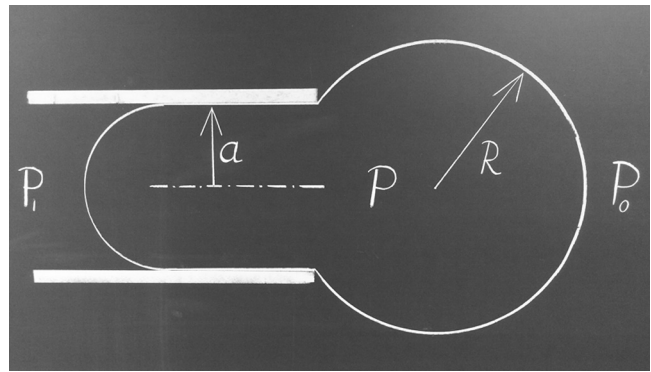


Fig. 8. Illustration of a micropipette aspiration setup: A pipette of inner radius a sucks part of a vesicle into its bore. The pressure P_1 in the pipette is lower than the pressure P_0 in the solution containing vesicles, and the pressure P inside the vesicle is bigger than both, giving $P_1 < P_0 < P$. If the vesicle outside the pipette is not flaccid, it assumes with good accuracy a spherical shape of some radius R .

(138) fixes the curvature with which the membrane inside the pipette detaches from the glass substrate (more precisely, it sets the curvature jump perpendicular to the adhesion contact line). For instance, in the absence of any adhesion energy between membrane and pipette (a situation one usually tries to experimentally ensure by suitably coating the pipette), the curvature jump should be zero, and since the pipette is usually straight along its axis, the normal curvature of the vesicle along the axial direction just after detachment should be zero. However, if that vesicle were a hemispherical cap of radius a , that curvature would instead be $1/a$. Hence, the cap of the vesicle inside the pipette *cannot* be a spherical cap. It seems that in order to work out the exact answer requires us to solve the shape equation *including* the bending terms, which (since we have just seen that K is not constant) is evidently a very difficult task, even under axisymmetry. However, Fournier and Galatola show that the answer can be obtained with great ease from force balance considerations (Fournier and Galatola, 2008). Let us review their elegant argument.

Consider a force balance along the pipette's axis at the circular contact line inside the pipette at which the membrane detaches from the substrate, and let us focus on the cylindrical membrane segment on its right (see Fig. 8). There is a surface term stemming from the membrane stress tensor, and a bulk term stemming from the pressure difference, and these two terms must balance in equilibrium. If we define the vector \mathbf{l} to point along the axis of the pipette and away from the vesicle's main body (to the left in Fig. 8), we get

$$2\pi a(\mathbf{l} \cdot \mathbf{f}_{\perp}) = -\pi a^2(P - P_1). \quad (141)$$

The surface stress in this case is given by

$$\mathbf{l} \cdot \mathbf{f}_{\perp} = -\sigma - \frac{1}{2}\kappa \frac{1}{a^2} + w, \quad (142)$$

where the three terms originate from surface tension, bending, and adhesion, respectively. To clarify their sign, imagine moving the rim to the right: both the surface tension and the bending term pull, so they get a minus sign; however, we lose adhesion energy, so this contribution must be positive. Inserting this result into Eq. (141), we obtain

$$P - P_1 + \frac{2w}{a} = \frac{2\sigma}{a} \left[1 + \frac{1}{2} \left(\frac{\lambda}{a} \right)^2 \right] \quad (143)$$

where we again used the length λ from Eq. (71). Notice that the adhesion contribution acts to increase the pressure difference (thus helping to suck the vesicle into the pipette). Also, the Young–Laplace law gets a correction term that involves the ratio

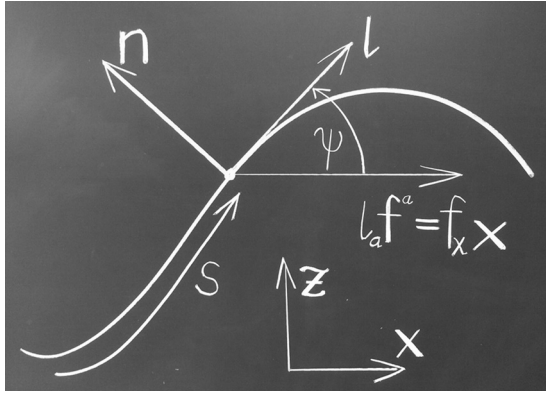


Fig. 9. Geometry along a local planar membrane buckle, which is compressed along the x -direction and translationally invariant along the y -direction. It can be parametrized by giving the angle $\psi(s)$ with respect to the x -direction as a function of arc length s . The buckling force $\mathbf{f}_\perp = l_a \mathbf{f}^a = f_x \mathbf{x}$ has to point along the x -direction.

λ/a and hence matters especially for thin pipettes. Since it is possible to create very small tensions in such experiments (Evans and Rawicz managed to achieve the amazingly low value 10^{-3} mN/m in a controlled fashion (Evans and Rawicz, 1990)), we get $\lambda \sim 300$ nm. Moreover, nanopipettes with diameters less than 200 nm can now be fabricated and have been applied in a soft matter context (Iwata et al., 2007; Schrlau et al., 2008), so we see that there can clearly be experimental situations where the correction term matters or even exceeds the Young–Laplace term, even though this is admittedly not the case for typical micropipettes.

For the large vesicle outside the pipette the conventional Young–Laplace approximation is still very reasonable, since $R \gg \lambda$ implies that its shape is largely tension dominated, and so combining this with Eq. (141) leads to the corrected pipette equation (Fournier and Galatola, 2008)

$$\Delta P = 2\sigma \left[\frac{1}{a} - \frac{1}{R} - \frac{w}{\sigma a} \right] + \frac{\kappa}{a^3}. \quad (144)$$

Up to very minor corrections for the large vesicle part this equation is exact, and it has been derived without solving the shape equation (whose exact solution is quite nontrivial in this case (Fournier and Galatola, 2008)). This worked because all we needed was a stress balance, and the stresses follow from geometric properties that are often known before solving the shape equation, for instance from the boundary condition. This example therefore vividly illustrates why the stress formalism is not just conceptually pleasing but useful in practice.

6.3. Planar membrane buckles

Consider a flat membrane in the xy -plane and exert a compressive force along the x -direction, so that the membrane buckles along the x -direction but remains flat perpendicularly to it. What is the force needed to buckle it, and what is the subsequent stress strain relation? This situation is among the simplest cases in which in-plane stresses lead to an out-of-plane deformation and thus of necessity to a stress tensor that is no longer tangential. It might be too simplified to have an immediate experimental analog, but this clean geometry has recently been exploited in computer simulations as a widely applicable method to probe membrane elasticity, for instance to measure the bending modulus κ (Noguchi, 2011; Hu et al., 2013b).

Consider the geometry as depicted in Fig. 9. If we cut the membrane along any of its straight lines parallel to the y -direction, the

force per unit length, as derived from Eqs. (110) and (114), is evidently given by

$$\mathbf{f}_\perp = \left[\frac{1}{2} \kappa K_\perp^2 - \Sigma \right] \mathbf{l} - \kappa (\nabla_\perp K_\perp) \mathbf{n}. \quad (145)$$

Force balance requires \mathbf{f}_\perp to point along the x -direction and be constant on the membrane: $\mathbf{f}_\perp = f_x \mathbf{x} = \text{const}$. Hence, the buckling force f_x can be determined in two different ways: first as the projection of \mathbf{f}_\perp onto the x -direction, and second as the magnitude of \mathbf{f}_\perp . This gives the following two equations:

$$f_x = \left(\frac{1}{2} \kappa K_\perp^2 - \Sigma \right) \cos \psi + \kappa (\nabla_\perp K_\perp) \sin \psi, \quad (146a)$$

$$f_x^2 = \left(\frac{1}{2} \kappa K_\perp^2 - \Sigma \right)^2 + \kappa^2 (\nabla_\perp K_\perp)^2, \quad (146b)$$

where we used $\mathbf{l} \cdot \mathbf{x} = \cos \psi$ and $\mathbf{n} \cdot \mathbf{x} = -\sin \psi$ (see again Fig. 9). Between these two equations we can eliminate the term $\nabla_\perp K_\perp$ and arrive at a single equation that is one order lower in derivatives:

$$\frac{1}{2} \kappa K^2 - \Sigma = f_x \cos \psi. \quad (147)$$

If we describe the angle ψ of the membrane as a function of the arc length s along the buckle, then $K_\perp = -\dot{\psi}$, and Eq. (147) turns into a differential equation for $\psi(s)$:

$$\frac{1}{2} \kappa \dot{\psi}^2 = f_x \cos \psi + \Sigma, \quad (148)$$

which can be easily solved by separation of variables and leads to a Jacobi elliptic function.

The tricky bit is to enforce constraints. If the membrane has a given total arc length L , and if it is buckled to a maximal extent L_x between its left and right end, these conditions must fix the two remaining unknowns in the problem: First, the integration constant that will emerge upon integrating Eq. (148), and second, the value of the buckling force f_x . The transcendental nature of the solution prevents this from being done in closed form, but Hu et al. (2013b) show how to arrive at an analytical solution of arbitrary precision in the form of a series expansion. If we picture the situation under periodic boundary conditions, such that along the x -direction one periodic buckle of length L fits into the box of length L_x , one finds the buckling force (per unit length)

$$f_x = \kappa \left(\frac{2\pi}{L} \right)^2 \left[1 + \frac{1}{2} \gamma + \frac{9}{32} \gamma^2 + \frac{21}{128} \gamma^3 + \dots \right], \quad (149)$$

where $\gamma = (L - L_x)/L$ is the buckling strain. Notice that f_x does not vanish in the limit $\gamma \rightarrow 0$, which is precisely the hallmark of Euler buckling.

As the area of the membrane was considered fixed, and not its tension, one might think that Σ is also still open, but in fact it follows from the geometry of the solution. Consider an inflection point along the membrane, i.e. a point where $K_\perp = 0$. Calling the angle at that point ψ_i , Eq. (147) now implies

$$\Sigma = -f_x \cos \psi_i. \quad (150)$$

The value of ψ_i follows from the solution (in fact, from the integration constant of Eq. (148)). As long as the buckle does not develop “overhangs” (regions where $|\psi| > 90^\circ$), Eq. (150) and the positivity of the buckling force f_x imply that $\Sigma < 0$, and hence for sure $\sigma < 0$. Here we have a case where the surface tension and even the isotropic tension is negative. The reason for this is, of course, that we compressed the membrane. Buckling is the natural way by which the membrane evades large compressive stresses, but it does not eliminate them entirely. Once overhangs develop, the isotropic tension Σ becomes positive again, and at even larger strains the bare surface tension might turn positive, too.

6.4. Membrane-mediated interactions

When particles adhere to membranes, they exert forces which locally change the membrane's geometry, and the shape equation (87) describes how this perturbation is transmitted to more distant regions. The collective response of a membrane results in an intricate shape, whose energy depends on the positions and orientations of all particles. The membrane therefore exerts forces and torques on them, since slight displacements or rotations of the particles will change the membrane shape and thus its associated energy. These mediated interactions elevate membranes from passive bystanders to active players in the physical interactions of such particles, and they have therefore been studied by a number of authors (Goulian et al., 1993a,b; Park and Lubensky, 1996; Weikl et al., 1998; Fournier and Dommersnes, 1997; Kim et al., 1998; Dommersnes et al., 1998; Dommersnes and Fournier, 1999a,b, 2002; Weikl, 2003; Fournier et al., 2003; Bartolo and Fournier, 2003; Müller et al., 2005b,c, 2007; Yolcu et al., 2011; Yolcu and Deserno, 2012). Since forces feature prominently in this phenomenon, the stress tensor is a natural tool with which to approach it.

First of all, if the membrane indeed exerts forces on the particles, these particles will respond by moving—which they can because the membrane is fluid. In order to study a static situation, we must prevent those motions by applying equal but opposite counter-forces, which fix the particles. These external forces on the particles will be transmitted further onto the membrane, where they become a source term for the stress tensor. Indeed, any closed loop integral of $\mathbf{f}_\perp = I_a \mathbf{f}^a$ around the region where force is added to the surface will give us that force—this is what Eq. (98) taught us.

It might at first sight seem that we have not gained an awful lot, since we do not know the stress tensor numerically for most situations of interest. Finding it might be about as hard as solving the shape equation, so where is the advantage of this reformulation? The answer is that Eqs. (96) or (110) shows us how the stress tensor depends on the membrane geometry, and we might have a fairly good qualitative understanding for how adhering particles change that geometry, while we have probably close to no intuition what happens to the overall energy when we slightly displace the particles.

Another advantage is that we have much freedom in choosing the closed contour. Just as in the electrostatic analogy shown in Eq. (99) we are free to choose any surface that encloses a charge distribution of interest (and *only* that one), we are now free to choose any closed loop, as long as it contains only the source of stress that we care about. This is very useful because we might be able to move the contour such that it conforms to any symmetries we happen to know about, or move it into far-away regions where the membrane is largely unperturbed by particles and where we therefore actually know the stress tensor.

To illustrate this, let us look at the situation of two identical axisymmetric particles adhering to an asymptotically flat membrane with $K_0 = 0$, as illustrated in Fig. 10. This two-particle geometry has two mirror symmetries that will turn out to be useful. According to Eq. (98) the force which the left particle exerts on the membrane can be picked up by a closed loop integral of \mathbf{f}_\perp around the left particle. Let us deform this contour such that it divides into 4 branches. The first one passes along the curve which is the intersection of the membrane and the mirror plane between the particles. Branches 2, 3, and 4 will be moved far away from the two particles, so that the membrane is flat there and the stress tensor given by $\mathbf{f}_\perp = -\sigma \mathbf{l}$. If we place the contours as shown in Fig. 10, the contributions from branch 2 and 4 must exactly cancel, since $\mathbf{l}^{(2)} = -\mathbf{l}^{(4)}$ and both branches have the same shape and length. The contribution from branch 3 will be equal to a surface tension σ per unit length along $-\mathbf{l}^{(3)}$, but it will not cancel the contribution from

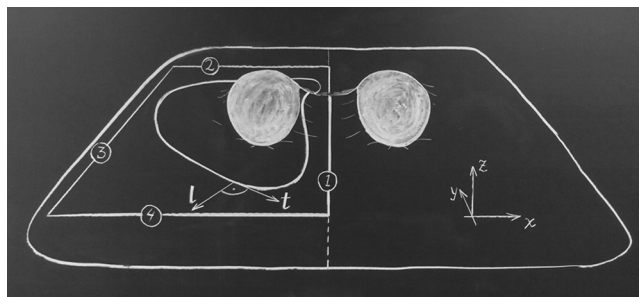


Fig. 10. Geometry of a symmetric mediated-interaction problem involving two spherical particles which partially adhere to an asymptotically flat membrane. The force on the left particle can be determined as the total flux of stress through an arbitrary contour enclosing the left particle. Adapting that contour to the symmetry of the situation will give rise to simple formulas relating the force to the geometry on the midline (branch 1).

branch 1. The mirror symmetry of the midplane ensures that everywhere on branch 1 we have $\mathbf{l}^{(1)} = \mathbf{x}$, and therefore $\mathbf{l}^{(1)} = -\mathbf{l}^{(3)}$, but branch 1 is *longer* than branch 3, because due to the presence of the membrane curving particles it is generally not straight. Its length is by a finite amount ΔL longer than its projection into the xy -plane, and hence the tension-derived force between branch 1 and branch 3 is imbalanced by the term $\sigma \Delta L$. Tracing the sign, we see that this contribution points to the left, into $-\mathbf{x}$ -direction. Since this is ultimately the force with which we fixed the position of the particle, this means that the particle itself pushes to the right, towards the right particle, and so we see that the surface tension contribution induces an attraction between the two particles.

What about the other contributions to the stress tensor? Since these all involve the curvature, they vanish on all branches except the first one. The mirror symmetry between the particles also leads to two convenient results: first, branch 1 is also a line of curvature, and hence $K_{\perp\parallel} = 0$, so the contribution along \mathbf{t} vanishes; and second, $\nabla_\perp K = 0$ there, because the curvature must be an even function when crossing the midline. That only leaves the contribution along \mathbf{l} , which we already know points into the x -direction. The total force picked up by the contour therefore points along the x -direction and has the magnitude (Müller et al., 2005b,c)

$$F = -\sigma \Delta L + \frac{1}{2} \kappa \int_1 ds (K_\perp^2 - K_\parallel^2). \quad (151)$$

We already know that the surface tension term gives rise to an attraction between the particles, and so we see that the K_\parallel contribution in the integral (which is the curvature of the membrane along branch 1) does the same. However, the K_\perp term in the integral (which is due to the membrane curvature perpendicular to branch 1) has the opposite sign. It is not at all obvious which of these two terms “wins” against the others. There is no way to cleverly rewrite this expression so that its sign becomes obvious without first solving the shape equation.

If the two particles perturb the membrane only weakly, one can solve the problem in linearized Monge gauge. This task is still not straightforward, because the classical superposition approximation (Nicolson, 1949) of simply adding up the individual deformations created by the particles separately gives a qualitatively wrong answer. In the case of vanishing tension and for axisymmetric particles we can quickly see what that answer would be: around each particle the membrane takes the shape of a catenoid, which is an axisymmetric minimal surface for which $K = 0$, and hence on the linearized Monge level $\Delta h(x, y) = 0$, such that $h(x, y)$ is harmonic. After superposition of the shapes from the

two particles h is still harmonic and thus the surface still minimal. Now look at the integrand in Eq. (151):

$$K_{\perp}^2 - K_{\parallel}^2 = (K_{\perp} + K_{\parallel})(K_{\perp} - K_{\parallel}) = K(K_{\perp} - K_{\parallel}), \quad (152)$$

which vanishes for a minimal surface, and hence the (bending-associated) force between the particles should vanish—but this is wrong. In a seminal paper, Goulian, Bruinsma and Pincus have calculated an interaction potential which to leading order decays like the fourth power of particle separation (Goulian et al., 1993a). After fixing an incorrect minus sign (Goulian et al., 1993b) and the erroneous occurrence of the Gaussian modulus (Park and Lubensky, 1996; Weikl et al., 1998; Fournier and Dommersnes, 1997), and generalizing to unequal particle radii (Yolcu and Deserno, 2012), the interaction potential takes the form

$$U(r) = 4\pi\kappa(\gamma_1^2 + \gamma_2^2)\frac{R_1^2 R_2^2}{r^4} + \mathcal{O}(r^{-6}), \quad (153)$$

where r is the distance between the centers of the circularly symmetric particles of radii R_i , and γ_i is the detachment angle of the membrane with respect to the horizontal at the rim of particle i . To lowest order, particles repel. Weikl et al. (1998) have generalized this to include tension, but the particles are still found to repel.

Given that this is not only lowest order in particle separation but also linearized Monge gauge, one might wonder whether stronger deformations or a closer distance change the situation. Intuition is no reliable guide for nonlinear physics, so we have little to hold on to. We might notice, though, that linearized Monge gauge for membrane mediated interactions is the equivalent of Newtonian gravity, for which the full theory is space-time mediated interactions between masses à la general relativity. And while many amazing things happen once one crams a lot of mass into a small region of space (black holes come to mind), we know that the force between two masses never changes its sign. Therefore, based on this analogy, we might expect that the membrane-mediated case beyond linear order changes quantitatively but not qualitatively. Alas, this would be wrong. If the particles create detachment angles close to 90° and come close enough together, they will attract, as shown in Reynwar and Deserno (2011) by numerically solving the nonlinear shape equations with the package SURFACE EVOLVER (Brakke, 2012) and deriving asymptotic approximations (based on the stress tensor) valid for close distance and detachment angles close to 90° .

The situation of two compact particles, as illustrated in Fig. 10 is thus quite nontrivial. In contrast, the case of two rods of length L much longer than their cross-section, lying parallel on a membrane, is almost straightforward. Eq. (151) still applies, but some important simplifications happen. First, if the two rods are long enough, we can ignore complications due to their ends and treat the problem as translationally invariant along the rods' axis. Since the curvature on the midplane along the contour now vanishes, $K_{\parallel} = 0$. And since this is the case, the tension contribution vanishes, too, because $\Delta L = 0$. Taken together, the force per length emerges as

$$\frac{F}{L} = \frac{1}{2}\kappa K_{\perp}^2. \quad (154)$$

We still do not know the numerical value of K_{\perp} , but we do know that K_{\perp}^2 is positive, and so we can confidently predict that the two rods will repel. Within linearized Monge gauge the force–distance relation between two parallel cylinders has first been calculated by Weikl (2003); in fact, due to its one-dimensional nature the problem can be solved essentially analytically in terms of elliptic functions and integrals (Müller et al., 2007). But it is still comforting to know that at least the sign can be understood without hardly doing any calculation at all.

7. Conclusions and outlook

In this review we have seen how to describe the stresses and torques transmitted by fluid membranes, and how this formalism can address numerous problems in novel and often illuminating ways. The natural arena to do any of this is differential geometry—a set of powerful and yet not overwhelmingly arcane mathematical tools that strive to describe curved geometries in a way that is not drenched in the arbitrariness of one's choice of a parametrization. The bare bones version presented in Section 2 of this review already gets one surprisingly far, but of course this is only just a beginning. Moreover, there are more abstract versions of it, which use the concept of differential forms (Lovell and Rund, 1989; Frankel, 2004; Schutz, 1980; Darling, 1994; Flanders, 1989), and these have also been applied to describe membranes (Tu and Ou-Yang, 2003, 2004, 2008; Tu et al., 2005; Tu, 2011).

So where do we go from here? The set of topics presented in this review can be expanded in a number of different directions. For instance, little in the introduction of the stress tensor relied on the fact that it was based on the specific example of the Helfrich Hamiltonian. The concept makes sense already for simple tension-dominated surfaces, even though there it is almost trivial. More interestingly, it can be extended to geometric Hamiltonians beyond quadratic curvature elasticity, for instance containing higher powers of the curvatures or higher derivatives. Most aspects generalize straightforwardly, but the possible occurrence of higher derivatives necessarily implies that integration by parts will shovel extra terms onto the boundary, which in the special cases discussed so far do not arise and which we therefore have not paid any attention to. For instance, a term $(1/2)\kappa_{\nabla}(\nabla_a K)(\nabla^a K)$ in the Hamiltonian will modify the contact curvature condition (138) into $\nabla_{\perp}(K_{\perp}^1 - K_{\perp}^2) = \sqrt{2w/\kappa_{\nabla}}$, and these new boundary terms matter in order to arrive at this result (Deserno et al., 2007).

Furthermore, the framework can also be applied to any fields defined on the curved geometry, not just the geometry itself. For instance, if the membrane is mixed, one could define a Ginzburg–Landau type functional on the surface that describes the free energy of mixing, such as $\frac{1}{2}\lambda(\nabla_a\phi)(\nabla^a\phi) + V(\phi) + \beta_{\phi}K\phi$, where ϕ is the composition field and the last term describes a composition–curvature coupling. The same arguments discussed in Section 4 will swiftly lead to the stress tensor associated with this extra field (Capovilla and Guven, 2004). One interesting prediction is that the last term gives rise to normal stresses whenever the field ϕ is spatially varying (Capovilla and Guven, 2004). Since such stresses are also created by curvature gradients, we see that composition–curvature coupling in the Hamiltonian also couples the gradients of these fields on the level of stresses. Alternatively, lipid tilt can be described as a vector field on the membrane, and the associated stress tensor and Euler–Lagrange equations can be derived by completely analogous means (Müller et al., 2005c). Moreover, one can also look at cases of non-fluid membranes, for which shear degrees of freedom matter. In the limiting case of infinite shear resistance we have surfaces akin to paper that are bendable but can only be deformed isometrically (Güven and Müller, 2008; Müller et al., 2008; Güven et al., 2012, 2013).

A different way to make further progress is to exploit additional symmetries of the Hamiltonian. For instance, the Helfrich Hamiltonian (in the absence of a surface tension term) is scale invariant: Scaling all lengths by a factor λ will increase the area element by λ^2 but simultaneously decrease the squared curvatures by the same factor, thus leaving the energy invariant. More interestingly, the Helfrich Hamiltonian is also conformally invariant (Thomsen, 1924; Blaschke, 1929; White, 1973), meaning that—in particular—it is

invariant under inversions at a sphere.³² This implies that special conformal transformations continuously transform a solution of the shape equation into a new one. This is not particularly interesting for spheres, since conformal transformations turn spheres into spheres, but already the torus results in a two-parameter family of degenerate solutions (Seifert, 1991), and higher genus surfaces are even more complex (Jülicher et al., 1993). However, while solutions of the shape equations are turned into new solutions, these new solutions are not necessarily stress free. For instance, if one performs an inversion of a catenoid, one can get discoid-shape solutions if the inversion point lies on the catenoid's axis, but these new shapes require a pair of localized axial point-forces to pin the poles together (Castro-Villarreal and Guven, 2007a,b). If instead one chooses the inversion point close to the surface on the neck of the catenoid, one arrives at solutions of spherical topology which look as if they have the membrane pinched in (or out) by two external point forces (Guven and Vázquez Montejo, 2013). The stress framework turns out to be very well suited to understand the nature of forces and torques necessary to create and stabilize these rather nontrivial shapes.

Even more insight into these connections might be gained by a reformulation of the constrained variational problem discussed in Section 4.3, recently proposed by Guven and Vázquez Montejo (2013): instead of enforcing the geometry of the surface by fixing \mathbf{e}_a , \mathbf{n} , g_{ab} and K_{ab} through their link to the parametrization \mathbf{X} , one instead enforces the integrability conditions of Gauss–Codazzi–Mainardi ((39) and (40)). This way, one can view the surface functional as entirely intrinsic, with the two constraints creating the tensor K_{ab} as an auxiliary field that now just happens to be compatible with an actual surface. The amazing aspect of this is that one can thereby define a curvature functional (such as the Helfrich Hamiltonian) that also involves the extrinsic geometry without ever referring to an actual embedding: the surface becomes an emergent entity. If the Hamiltonian in fact depends on K_{ab} , the multipliers turn out to be generators of conformal transformations, which provides a novel access to study surface instabilities.

The present review has purposefully steered clear of both thermal fluctuations and dynamical phenomena—not because they are not interesting, but because they open a universe of new questions worthy of their own review article. To avoid skipping them entirely, let us close with a few remarks that afford a very brief glance at some of these questions.

In a sense, Helfrich theory already implicitly includes some thermal fluctuations, because integrating out the microscopic degrees of freedom of lipids and solvent molecules essentially implies that the resulting coarse-grained Hamiltonian is actually a *free energy*, and its phenomenological parameters are all temperature dependent.³³ When one talks about thermal fluctuations of membranes it is therefore usually implied that these are fluctuations of the *geometry*, and not of the underlying microscopic constituents. The appropriate language for this problem is statistical field theory, and it is rich in beautiful and nontrivial problems (Nelson et al., 2004). Most theoretical treatments avoid nonlinear nuisances by restricting to quadratic fluctuations around some ground state, almost always the plane, and hence Monge gauge

³² Consider a sphere of radius ρ whose center does not lie on the surface. The inversion $\mathbf{X} \rightarrow \mathbf{X}' = \rho^2 \mathbf{X}/|\mathbf{X}|^2$ is then a conformal transformation. If we perform the sequence “inversion, translation by some vector \mathbf{a} , inversion”, we arrive at the continuous group of special conformal transformations.

³³ For instance, the bending modulus κ depends on temperature, as one would expect from a material parameter. It can therefore also be considered to contain an energetic as well as an entropic “contribution” to its numerical value, and these can be remarkably easily disentangled in a simulation should one be interested to do so (Hu et al., 2013b).

is very popular. Classical topics in this context are membrane shape undulations and strategies to estimate the bending modulus from them (Brochard and Lennon, 1975; Brochard et al., 1976; Schneider et al., 1984a,b; Faucon et al., 1989; Evans and Rawicz, 1990; Komura and Lipowsky, 1992; Goetz et al., 1999; Henriksen et al., 2004; Liu and Nagle, 2004; Imparato et al., 2005), the “Helfrich repulsion” between two undulating membranes (Helfrich, 1978; Helfrich and Servuss, 1984; Safinya et al., 1986; Wennerström and Olsson, 2014), the subtle competition between this repulsion and the shorter-ranged van der Waals attraction between membranes, leading to a continuous unbinding transition (Lipowsky and Leibler, 1986; Milner and Roux, 1992), or fluctuation-mediated interactions between membrane-bound objects (Goulian et al., 1993a,b; Park and Lubensky, 1996; Golestanian et al., 1996a,b; Dommersnes and Fournier, 1999a; Dean and Manghi, 2006; Yolcu et al., 2011, 2014; Yolcu and Deserno, 2012; Lin et al., 2011; Gosselin et al., 2011). Even though the present review has discussed the stress tensor only in static (“ground state”) situations, it remains a very useful tool also in the presence of fluctuations (Fournier and Barbetta, 2008; Gosselin et al., 2011; Hu et al., 2013b).

Dynamical phenomena—*i.e.*, processes that go beyond thermal equilibrium—add a plethora of fascinating aspects to membrane biophysics on basically all length scales, from molecular to macroscopic, and we will give an example at both ends of this spectrum. Let us begin by considering thermally excited membrane undulations of wave vector \mathbf{q} , which have a mean squared amplitude $\langle |h_{\mathbf{q}}|^2 \rangle = k_B T / \kappa q^4$ that does not depend on the specifics of the embedding solvent. However, their *linear relaxation rate* is dictated by the solvent viscosity η , leading to a dispersion relation $i\omega_{\text{u}}(q) = \kappa q^3 / 4\eta$ (Brochard and Lennon, 1975; Zilman and Granek, 1996, 2002; Granek, 1997; Brown, 2008) and thus a dynamic correlation function

$$\langle h_{\mathbf{q}}(t) h_{\mathbf{q}}^*(0) \rangle = \frac{k_B T}{\kappa q^4} \exp \left\{ -\frac{\kappa q^3}{4\eta} t \right\}. \quad (155)$$

The reduction in power $q^4 \rightarrow q^3$ in the “dynamic exponent” (compared to the “static prefactor”) is a consequence of hydrodynamic interactions.

On the level of Helfrich theory, this result holds on all length scales. However, Seifert and Langer (1993) have shown that the need for lipids to laterally redistribute in order to respond to curvature changes implies a small length scale below which one must also account for lipid density changes, a term beyond simple geometry. Briefly, a straightforward dimensional analysis shows that lipid density perturbations relax with a rate $i\omega_{\text{d}} \propto K_A q^2 / b$, where K_A is the membrane's area expansion modulus from Eq. (57) and b the inter-leaflet friction constant. Setting $\omega_{\text{u}} = \omega_{\text{d}}$, and simplifying matters via Eq. (61), leads to the crossover wavevector $q \sim 10^2 \eta / b d^2$. Taking $b \approx 10^8 \text{ Js/m}^4$ (Merkel et al., 1989; Evans and Yeung, 1994; Raphael and Waugh, 1996), we get a crossover wavelength of $\lambda \sim 10^2 \text{ nm}$, which is sub-optical but of the same scale as countless cellular membrane processes. Importantly, the density-bending coupling introduces a renormalized bending rigidity $\tilde{\kappa} = \kappa + K_A z_0^2$, where z_0 is the distance between the bilayer's midplane and a monolayer's pivotal plane, which we discussed extensively in Section 3.4. The extra term $K_A z_0^2 \sim 60 k_B T$ exceeds a membrane's typical bare bending rigidity κ quite substantially. Watson and Brown (2010) have recently argued that this could explain a puzzling discrepancy between values of the bending rigidity measured by conventional equilibrium methods vs. those derived from dynamical neutron-spin-echo techniques, which until then had been “resolved” by assuming that the solvent viscosity is about three times higher than it actually is.

On large scales such density-derived troubles vanish, but if the solvent itself is driven, the resulting shear stresses lead to a very

complex dynamical behavior of any membranes embedded in it, most obviously vesicles. For nearly spherical vesicles one can still treat this analytically using linear stability theory (Misbah, 2006; Vlahovska and Gracia, 2007; Lebedev et al., 2007; Kaoui et al., 2009), but as soon as the vesicles have sufficiently much excess area to deform substantially in the flow, the resulting dynamic behavior is anything but linear response (even though, remarkably, often still very regular). One obviously exciting realization of this problem is the flow of red blood cells through thin capillaries,³⁴ and therefore the problem of vesicles in flow has been rather extensively studied, using a wide variety of numerical techniques. Typically, on the large scales that matter the membrane can be captured by a triangulated surface, while numerous techniques for incorporating the hydrodynamics have been employed, among them linear stability theory (Misbah, 2006; Vlahovska and Gracia, 2007; Lebedev et al., 2007; Kaoui et al., 2009), Oseen-tensor interactions (Kraus et al., 1996), the immersed boundary method (Eggleton and Popel, 1998; Bagchi, 2007), stochastic rotation dynamics (Noguchi and Gompper, 2004, 2005a,b, 2007; McWhirter et al., 2009) dissipative particle dynamics (Pivkin and Karniadakis, 2008), Lattice Boltzmann techniques (Zhang et al., 2007, 2008), or boundary integral methods (Sukumaran and Seifert, 2001; Zhao and Shaqfeh, 2011; Zhao et al., 2011; Biben et al., 2011; Spann et al., 2014). Alternatively, both membrane and fluid can be described together using a dynamic phase field functional (Biben and Misbah, 2003; Beaucourt et al., 2004; Biben et al., 2005; Campelo and Hernández-Machado, 2006, 2007a,b, 2008). For recent reviews, see Vlahovska et al. (2009, 2013) and Li et al. (2013b).

The aim of such studies is to understand, how the dynamic response of the vesicle depends on key dimensionless parameters (Kaoui et al., 2009). The most important ones are: (i) the reduced volume $\tilde{V} = V/V_0$, where V is the vesicle volume and $V_0 = (4/3)\pi R_0^3$ is the volume of a sphere of the same area $A = 4\pi R_0^2$ as the vesicle; (ii) the viscosity contrast η_{in}/η_{out} between the inside and the outside of the vesicle; and (iii) the capillary number $Ca = \eta_{out} R_0 \dot{\gamma} / \kappa$, where $\dot{\gamma}$ is the shear rate. Depending on the values of these parameters, vesicles respond to the flow in different ways. If the viscosity contrast is small, they “tank-tread,” meaning that their *mathematical shape* in the flow is stationary but their *physical lipid constituents* periodically orbit that shape; conversely, if the viscosity contrast is large, vesicles tumble in the flow. Between these two regimes there might exist a range in which the vesicle’s main axis librates in the flow but does not fully rotate around (a motion also termed “vacillating-breathing”). Where these transitions happen in turn depends on the Capillary number.

Evidently, these problems are enormously complex. We have seen that the surface geometry of deformed vesicles is described by a theory that is purely geometric and, as a consequence, very nonlinear. Coupling it to the idiosyncrasies of hydrodynamic flow problems, even in the linear Stokes regime and for weakly deformed vesicles, is very challenging due to the highly nontrivial shape of the moving boundary—namely, the vesicle’s surface itself. But when hydrodynamic stresses deform the vesicle, they essentially have to reckon with the membrane’s stress tensor as their key counter-player, and so the concepts and techniques examined in this review will remain highly useful. However, new membrane stresses beyond those from a purely fluid-elastic Hamiltonian arise due to dynamic phenomena, such as shear and finite relaxation times, and bold strides have been made to combine these into

a general unified framework (Lomholt et al., 2005). But that is another story and shall be told another time.

Acknowledgements

My way of thinking about differential geometry has been deeply influenced by Jemal Guven, whose superb intuition, elegant mastery of the math, and infectious enthusiasm for beautiful results is a constant source of inspiration. While working with him and my first student Martin Müller, I came to understand some of the core concepts presented in this review. I am also grateful to Pablo Vázquez Montejó, Luca Deseri, Robert Haussman, Karpur Shukla, and Zach McDargh for critical reading and constructive comments on the manuscript.

References

- Agrawal, A., Steigmann, D.J., 2008. Coexistent fluid-phase equilibria in biomembranes with bending elasticity. *J. Elast.* 93 (1), 63–80.
- Arkhypov, A., Yin, Y., Schulten, K., 2008. Four-scale description of membrane sculpting by bar domains. *Biophys. J.* 95 (6), 2806–2821.
- Ayton, G., Voth, G.A., 2002. Bridging microscopic and mesoscopic simulations of lipid bilayers. *Biophys. J.* 83 (6), 3357–3370.
- Bagchi, P., 2007. Mesoscale simulation of blood flow in small vessels. *Biophys. J.* 92 (6), 1858–1877.
- Baoukina, S., Marrink, S.J., Tieleman, D.P., 2012. Molecular structure of membrane tethers. *Biophys. J.* 102, 1866–1871.
- Bartolo, D., Fournier, J.B., 2003. Elastic interaction between “hard” or “soft” pointwise inclusions on biological membranes. *Eur. Phys. J. E* 11, 141–146.
- Bassereau, P., Sorre, B., Lévy, A., 2014. Bending lipid membranes: experiments after W. Helfrich’s model. *Adv. Colloid Interface Sci.* 208, 47–57.
- Baumgart, T., Das, S., Webb, W.W., Jenkins, J.T., 2005. Membrane elasticity in giant vesicles with fluid phase coexistence. *Biophys. J.* 89 (2), 1067–1080.
- Baumgart, T., Capraro, B.R., Zhu, C., Das, S.L., 2011. Thermodynamics and mechanics of membrane curvature generation and sensing by proteins and lipids. In: Leone, S.R., Cremer, P.S., Groves, J.T., Johnson, M.A. (Eds.), *Ann. Rev. Phys. Chem.*, pp. 483–506.
- Beaucourt, J., Rioual, F., Séon, T., Biben, T., Misbah, C., 2004. Steady to unsteady dynamics of a vesicle in a flow. *Phys. Rev. E* 69, 011906.
- Ben Shaul, A., Szeleifer, I., Gelbart, W.M., 1985. Chain organization and thermodynamics in micelles and bilayers. 1. Theory. *J. Chem. Phys.* 83 (7), 3597–3611.
- Bennett, V., 1985. The membrane skeleton of human-erythrocytes and its implication for more complex cells. *Ann. Rev. Biochem.* 54, 273–304.
- Biben, T., Misbah, C., 2003. Tumbling of vesicles under shear flow within an advected-field approach. *Phys. Rev. E* 67, 031908.
- Biben, T., Kassner, K., Misbah, C., 2005. Phase-field approach to three-dimensional vesicle dynamics. *Phys. Rev. E* 72, 041921.
- Biben, T., Farutin, A., Misbah, C., 2011. Three-dimensional vesicles under shear flow: numerical study of dynamics and phase diagram. *Phys. Rev. E* 83, 031921.
- Bitbol, A.F., Constantin, D., Fournier, J.B., 2012. Bilayer elasticity at the nanoscale: the need for new terms. *PLoS ONE* 7 (11), e48306.
- Blaschke, W., 1929. *Vorlesungen über Differentialgeometrie III*. Springer, Berlin.
- Bloom, M., Evans, E., Mouritsen, O.G., 1991. Physical properties of the fluid lipid-bilayer component of cell membranes: a perspective. *Quart. Rev. Biophys.* 24 (3), 293–397.
- Brakke, K., 2012. The Surface Evolver, Version 2.50. <http://www.susqu.edu/brakke/evolver/evolver.html>
- Brandt, E.G., Braun, A.R., Sachs, J.N., Nagle, J.F., Edholm, O., 2011. Interpretation of fluctuation spectra in lipid bilayer simulations. *Biophys. J.* 100 (9), 2104–2111.
- Brannigan, G., Brown, F.L.H., 2007. Contributions of Gaussian curvature and non-constant lipid volume to protein deformation of lipid bilayers. *Biophys. J.* 92 (3), 864–876.
- Brannigan, G., Tamboli, A.C., Brown, F.L.H., 2004. The role of molecular shape in bilayer elasticity and phase behavior. *J. Chem. Phys.* 121 (7), 3259–3271.
- Brannigan, G., Philips, P.F., Brown, F.L.H., 2005. Flexible lipid bilayers in implicit solvent. *Phys. Rev. E* 72 (1), 011915.
- Brochard, F., Lennon, J.F., 1975. Frequency spectrum of flicker phenomenon in erythrocytes. *J. Phys.* 36 (11), 1035–1047.
- Brochard, F., de Gennes, P.G., Pfeuty, P., 1976. Surface-tension and deformations of membrane structures – relation to 2-dimensional phase-transitions. *J. Phys.* 37 (10), 1099–1104.
- Brown, F.L.H., 2008. Elastic modeling of biomembranes and lipid bilayers. *Ann. Rev. Phys. Chem.* 59, 685–712.
- Bukman, D.J., Yao, J.H., Wortis, M., 1996. Stability of cylindrical vesicles under axial tension. *Phys. Rev. E* 54, 5463–5468.
- Campelo, F., Hernández-Machado, A., 2006. Dynamic model and stationary shapes of fluid vesicles. *Eur. Phys. J. E* 20 (1), 37–45.
- Campelo, F., Hernández-Machado, A., 2007a. Shape instabilities in vesicles: a phase-field model. *Eur. Phys. J. Special Top.* 143 (1), 101–108.
- Campelo, F., Hernández-Machado, A., 2007b. Model for curvature-driven pearling instability in membranes. *Phys. Rev. Lett.* 99, 088101.

³⁴ Well, almost. Red blood cells have a polymerized spectrin network underneath their bilayer (Bennett, 1985), which equips them with a nonzero shear modulus that contributes to their elastic response (Li et al., 2005).

- Campelo, F., Hernández-Machado, A., 2008. Polymer-induced tubulation in lipid vesicles. *Phys. Rev. Lett.* 100, 158103.
- Canham, P.B., 1970. The minimum energy of bending as a possible explanation of the biconcave shape of the human red blood cell. *J. Theor. Biol.* 26 (1), 61–81.
- Capovilla, R., Guven, J., 2002a. Stresses in lipid membranes. *J. Phys. A: Math. Gen.* 35, 6233–6247.
- Capovilla, R., Guven, J., 2002b. Geometry of lipid vesicle adhesion. *Phys. Rev. E* 66, 041604.
- Capovilla, R., Guven, J., 2004. Stress and geometry of lipid vesicles. *J. Phys.: Condens. Matter* 16, S2187–S2191.
- Capovilla, R., Guven, J., Santiago, J.A., 2002. Lipid membranes with an edge. *Phys. Rev. E* 66, 021607.
- Capovilla, R., Guven, J., Santiago, J.A., 2003. Deformations of the geometry of lipid vesicles. *J. Phys. A: Math. Gen.* 36 (23), 6281.
- Castro-Villarreal, P., Guven, J., 2007a. Inverted catenoid as a fluid membrane with two points pulled together. *Phys. Rev. E* 76, 011922.
- Castro-Villarreal, P., Guven, J., 2007b. Axially symmetric membranes with polar tethers. *J. Phys. A: Math. Theor.* 40 (16), 4273.
- Chernomordik, L.V., Kozlov, M.M., Melikyan, G.B., Abidor, I.G., Markin, V.S., Chizmadzhev, Y.A., 1985. The shape of lipid molecules and monolayer membrane fusion. *Biochim. Biophys. Acta – Biomembranes* 812 (3), 643–655.
- Cooke, I.R., Deserno, M., 2005. Solvent-free model for self-assembling fluid bilayer membranes: stabilization of the fluid phase based on broad attractive tail potentials. *J. Chem. Phys.* 123, 224710.
- Cooke, I.R., Kremer, K., Deserno, M., 2005. Tunable generic model for fluid bilayer membranes. *Phys. Rev. E* 72, 011506.
- Cuvellier, D., Derényi, I., Bassereau, P., Nassoy, P., 2005. Coalescence of membrane tethers: experiments, theory, and applications. *Biophys. J.* 88 (4), 2714–2726.
- Döbereiner, H.G., Selchow, O., Lipowsky, R., 1999. Spontaneous curvature of fluid vesicles induced by trans-bilayer sugar asymmetry. *Eur. Biophys. J.* 28 (2), 174–178.
- Darling, R.W.R., 1994. *Differential Forms and Connections*, 1st ed. Cambridge University Press, Cambridge.
- David, F., Leibler, S., 1991. Vanishing tension of fluctuating membranes. *J. Phys. II (France)* 1 (8), 959–976.
- de Gennes, P.G., Prost, J., 1993. *The Physics of Liquid Crystals*. Oxford University Press, Oxford, UK.
- Dean, D.S., Manghi, M., 2006. Fluctuation-induced interactions between domains in membranes. *Phys. Rev. E* 74, 021916.
- den Otter, W.K., 2009. Free energies of stable and metastable pores in lipid membranes under tension. *J. Chem. Phys.* 131 (20), 205101.
- Deseri, L., Zurlo, G., 2013. The stretching elasticity of biomembranes determines their line tension and bending rigidity. *Biomech. Model. Mech.* 12 (6), 1233–1242.
- Deseri, L., Piccioni, M.D., Zurlo, G., 2008. Derivation of a new free energy for biological membranes. *Contin. Mech. Thermodyn.* 20 (5), 255–273.
- Deserno, M., Müller, M.M., Guven, J., 2007. Contact lines for fluid surface adhesion. *Phys. Rev. E* 76, 011605.
- Deserno, M., 2009. Mesoscopic membrane physics: concepts, simulations, and selected applications. *Macromol. Rapid Commun.* 30 (9–10), 752–771.
- Dimova, R., 2014. Recent developments in the field of bending rigidity measurements on membranes. *Adv. Colloid Interface Sci.* 208, 225–234.
- do Carmo, M., 1976. *Differential Geometry of Curves and Surfaces*. Prentice Hall, Englewood Cliffs, NJ.
- do Carmo, M., 1992. *Riemannian Geometry*. Birkhäuser, Boston, MA.
- Dommersnes, P.G., Fournier, J.B., 1999a. Casimir and mean-field interactions between membrane inclusions subject to external torques. *Europhys. Lett.* 46, 256–261.
- Dommersnes, P.G., Fournier, J.B., 1999b. *n*-body study of anisotropic membrane inclusions: membrane mediated interactions and ordered aggregation. *Eur. Phys. J. E* 12, 9–12.
- Dommersnes, P.G., Fournier, J.B., 2002. The many-body problem for anisotropic membrane inclusions and the self-assembly of “saddle” defects into an “egg carton”. *Biophys. J.* 83 (6), 2898–2905.
- Dommersnes, P.G., Fournier, J.B., Galatola, P., 1998. Long-range elastic forces between membrane inclusions in spherical vesicles. *Europhys. Lett.* 42 (2), 233–238.
- Eggleton, C.D., Popel, A.S., 1998. Large deformation of red blood cell ghosts in a simple shear flow. *Phys. Fluids* 10, 1834–1845.
- Evans, E.A., La Celle, P.L., 1975. Intrinsic material properties of the erythrocyte membrane indicated by mechanical analysis of deformation. *Blood* 45 (1), 29–43.
- Evans, E., Rawicz, W., 1990. Entropy-driven tension and bending elasticity in condensed-fluid membranes. *Phys. Rev. Lett.* 64, 2094–2097.
- Evans, E., Yeung, A., 1989. Apparent viscosity and cortical tension of blood granulocytes determined by micropipet aspiration. *Biophys. J.* 56 (1), 151–160.
- Evans, E., Yeung, A., 1994. Hidden dynamics in rapid changes of bilayer shape. *Chem. Phys. Lipids* 73, 39–56.
- Evans, E.A., Waugh, R., Melnik, L., 1976. Elastic area compressibility modulus of red cell membrane. *Biophys. J.* 16 (6), 585–595.
- Evans, E., Heinrich, V., Ludwig, F., Rawicz, W., 2003. Dynamic tension spectroscopy and strength of biomembranes. *Biophys. J.* 85 (4), 2342–2350.
- Evans, E.A., 1974. Bending resistance and chemically-induced moments in membrane bilayers. *Biophys. J.* 14 (12), 923–931.
- Evans, E.A., 1983. Bending elastic modulus of red blood cell membrane derived from buckling instability in micropipet aspiration tests. *Biophys. J.* 43 (1), 27–30.
- Förster, D., 1986. On the scale dependence, due to thermal fluctuations, of the elastic properties of membranes. *Phys. Lett. A* 114 (3), 115–120.
- Farago, O., 2003. “water-free” computer model for fluid bilayer membranes. *J. Chem. Phys.* 119 (1), 596–605.
- Faucon, J.F., Mitov, M.D., Méléard, P., Bivas, I., Bothorel, P., 1989. Bending elasticity and thermal fluctuations of lipid membranes – theoretical and experimental requirements. *J. Phys.* 50 (17), 2389–2414.
- Flanders, H., 1989. *Differential Forms with Applications to the Physical Sciences*. Dover, New York.
- Fournier, J.B., Barbeta, C., 2008. Direct calculation from the stress tensor of the lateral surface tension of fluctuating fluid membranes. *Phys. Rev. Lett.* 100, 078103.
- Fournier, J.B., Dommersnes, P.G., 1997. Comment on “long-range forces in heterogeneous fluid membranes”. *Europhys. Lett.* 39 (6), 681.
- Fournier, J.B., Galatola, P., 1997. Tubular vesicles and effective fourth-order membrane elastic theories. *Europhys. Lett.* 39 (2), 225.
- Fournier, J.B., Galatola, P., 2007. Critical fluctuations of tense fluid membrane tubules. *Phys. Rev. Lett.* 98, 018103.
- Fournier, J.B., Galatola, P., 2008. Corrections to the Laplace law for vesicle aspiration in micropipettes and other confined geometries. *Soft Matter* 4, 2463–2470.
- Fournier, J.B., Dommersnes, P.G., Galatola, P., 2003. Dynamin recruitment by clathrin coats: a physical step? *Comp. Ren. Biol.* 326 (5), 467–476.
- Fournier, J.B., 2007. On the stress and torque tensors in fluid membranes. *Soft Matter* 3, 883–888.
- Frankel, T., 2004. *The Geometry of Physics: An Introduction*, 3rd ed. Cambridge University Press, New York.
- Genco, I., Gliozzi, A., Relini, A., Robello, M., Scalas, E., 1993. Electroporation in symmetric and asymmetric membranes. *Biochim. Biophys. Acta – Biomembranes* 1149 (1), 10–18.
- Goetz, R., Helfrich, W., 1996. The egg carton: theory of a periodic superstructure of some lipid membranes. *J. Phys. II (France)* 6 (2), 215–223.
- Goetz, R., Gompper, G., Lipowsky, R., 1999. Mobility and elasticity of self-assembled membranes. *Phys. Rev. Lett.* 82, 221–224.
- Goldstein, H., Poole, C., Safko, J., 2002. *Classical Mechanics*, 3rd ed. Addison Wesley, San Francisco.
- Golestanian, R., Goulian, M., Kardar, M., 1996a. Fluctuation-induced interactions between rods on membranes and interfaces. *Europhys. Lett.* 33, 241.
- Golestanian, R., Goulian, M., Kardar, M., 1996b. Fluctuation-induced interactions between rods on a membrane. *Phys. Rev. E* 54, 6725.
- Gosselin, P., Mohrbach, H., Müller, M.M., 2011. Interface-mediated interactions: entropic forces of curved membranes. *Phys. Rev. E* 83, 051921.
- Goulian, M., Bruinsma, R., Pincus, P., 1993a. Long-range forces in heterogeneous fluid membranes. *Europhys. Lett.* 22, 145–150.
- Goulian, M., Bruinsma, R., Pincus, P., 1993b. Long-range forces in heterogeneous fluid membranes (erratum). *Europhys. Lett.* 23, 155.
- Granek, R., 1997. From semi-flexible polymers to membranes: anomalous diffusion and reptation. *J. Phys. II (France)* 7 (12), 1761–1788.
- Guven, J., Müller, M.M., 2008. How paper folds: bending with local constraints. *J. Phys. A: Math. Gen.* 41 (5), 055203.
- Guven, J., Vázquez Montejó, P., 2012. Confinement of semiflexible polymers. *Phys. Rev. E* 85, 026603.
- Guven, J., Vázquez Montejó, P., 2013. Force dipoles and stable local defects on fluid vesicles. *Phys. Rev. E* 87, 042710.
- Guven, J., Vázquez Montejó, P., 2013. Constrained metric variations and emergent equilibrium surfaces. *Phys. Lett. A* 377, 1507–1511.
- Guven, J., Müller, M.M., Vázquez Montejó, P., 2012. Conical instabilities on paper. *J. Phys. A: Math. Gen.* 45, 015203.
- Guven, J., Hanna, J.A., Müller, M.M., 2013. Whirling skirts and rotating cones. *New J. Phys.* 15 (11), 113055.
- Guven, J., 2004. Membrane geometry with auxiliary variables and quadratic constraints. *J. Phys. A: Math. Gen.* 37, L313–L319.
- Hague, C.V., Postle, A.D.P., Attard, G.S.A., Dymond, M.K.D., 2013. Spontaneous tubulation of membranes and vesicles reveals membrane tension generated by spontaneous curvature. *Farad. Discuss.* 161, 481–497.
- Hamm, M., Kozlov, M., 1998. Tilt model of inverted amphiphilic mesophases. *Eur. Phys. J. B* 6 (4), 519–528.
- Hamm, M., Kozlov, M., 2000. Elastic energy of tilt and bending of fluid membranes. *Eur. Phys. J. E* 3 (4), 323–335.
- Harmandaris, V.A., Deserno, M., 2006. A novel method for measuring the bending rigidity of model lipid membranes by simulating tethers. *J. Chem. Phys.* 125 (20), 204905.
- Heinrich, V., Svetina, S., Žekš, B., 1993. Nonaxisymmetric vesicle shapes in a generalized bilayer-couple model and the transition between oblate and prolate axisymmetric shapes. *Phys. Rev. E* 48, 3112–3123.
- Heinrich, M., Tian, A., Esposito, C., Baumgart, T., 2010. Dynamic sorting of lipids and proteins in membrane tubes with a moving phase boundary. *Proc. Natl. Acad. Sci. (USA)* 107 (16), 7208–7213.
- Helfrich, W., Servuss, R.M., 1984. Undulations, steric interaction and cohesion of fluid membranes. *Nuovo Cimento D* 3 (1), 137–151.
- Helfrich, W., 1973. Elastic properties of lipid bilayers—theory and possible experiments. *Z. Naturforsch. C* 28 (11), 693–703.
- Helfrich, W., 1978. Steric interaction of fluid membranes in multilayer systems. *Z. Phys. A* 33 (3), 305–315.
- Helfrich, W., 1985. Effect of thermal undulations on the rigidity of fluid membranes and interfaces. *J. Phys. (France)* 46 (7), 1263–1268.
- Helfrich, W., 1994. Lyotropic lamellar phases. *J. Phys.: Condens. Matter* 6, A79–A92.
- Henriksen, J., Rowat, A.C., Ipsen, J.H., 2004. Vesicle fluctuation analysis of the effects of sterols on membrane bending rigidity. *Eur. Biophys. J.* 33 (8), 732–741.

- Hochmuth, F.M., Shao, J.Y., Dai, J., Sheetz, M.P., 1996. Deformation and flow of membrane into tethers extracted from neuronal growth cones. *Biophys. J.* 70 (1), 358–369.
- Hochmuth, R.M., 2000. Micropipette aspiration of living cells. *J. Biomech.* 33 (1), 15–22.
- Hofsäß, C., Lindahl, E., Edholm, O., 2003. Molecular dynamics simulations of phospholipid bilayers with cholesterol. *Biophys. J.* 84 (4), 2192–2206.
- Hu, J.G., Ou-Yang, Z.C., 1993. Shape equations of the axisymmetric vesicles. *Phys. Rev. E* 47, 461–467.
- Hu, M., Briguglio, J.J., Deserno, M., 2012. Determining the Gaussian curvature modulus of lipid membranes in simulations. *Biophys. J.* 102 (6), 1403–1410.
- Hu, M., de Jong, D.H., Marrink, S.J., Deserno, M., 2013a. Gaussian curvature elasticity determined from global shape transformations and local stress distributions: a comparative study using the MARTINI model. *Farad. Discuss.* 161, 365–382.
- Hu, M., Diggins, P., Deserno, M., 2013b. Determining the mean curvature modulus of a lipid membrane by simulating buckling. *J. Chem. Phys.* 138, 214110.
- Imparato, A., Shillcock, J.C., Lipowsky, R., 2005. Shape fluctuations and elastic properties of two-component bilayer membranes. *Europhys. Lett.* 69 (4), 650–656.
- Israelachvili, J.N., Mitchell, D.N., Ninham, B.W., 1976. Theory of self-assembly of hydrocarbon amphiphiles into micelles and bilayers. *J. Chem. Soc.: Farad. Trans. II* 72, 1525–1568.
- Iwata, F., Nagami, S., Sumiya, Y., Sasaki, A., 2007. Nanometre-scale deposition of colloidal Au particles using electrophoresis in a nanopipette probe. *Nanotechnology* 18 (10), 105301.
- Jülicher, F., Lipowsky, R., 1993. Domain-induced budding of vesicles. *Phys. Rev. Lett.* 70, 2964–2967.
- Jülicher, F., Lipowsky, R., 1996. Shape transformations of vesicles with intramembrane domains. *Phys. Rev. E* 53, 2670–2683.
- Jülicher, F., Seifert, U., 1994. Shape equations for axisymmetric vesicles: a clarification. *Phys. Rev. E* 49, 4728–4731.
- Jülicher, F., Seifert, U., Lipowsky, R., 1993. Conformal degeneracy and conformal diffusion of vesicles. *Phys. Rev. Lett.* 71, 452–455.
- Jenkins, J.T., 1977a. The equations of mechanical equilibrium of a model membrane. *SIAM J. Appl. Math.* 32 (4), 755–764.
- Jenkins, J.T., 1977b. Static equilibrium configurations of a model red blood cell. *J. Math. Biol.* 4 (2), 149–169.
- Kamien, R.D., 2002. The geometry of soft materials: a primer. *Rev. Mod. Phys.* 74, 953–971.
- Kaoui, B., Farutin, A., Misbah, C., 2009. Vesicles under simple shear flow: elucidating the role of relevant control parameters. *Phys. Rev. E* 80, 061905.
- Karatekin, E., Sandre, O., Guitouni, H., Borghi, N., Puech, P.H., Brochard-Wyart, F., 2003. Cascades of transient pores in giant vesicles: line tension and transport. *Biophys. J.* 84 (3), 1734–1749.
- Kim, K.S., Neu, J., Oster, G., 1998. Curvature-mediated interactions between membrane proteins. *Biophys. J.* 75, 2274–2291.
- Kleinert, H., 1986. Thermal softening of curvature elasticity in membranes. *Phys. Lett. A* 114, 263–268.
- Komura, S., Lipowsky, R., 1992. Fluctuations and stability of polymerized vesicles. *J. Phys. II (France)* 2 (8), 1563–1575.
- Kozlov, M., Winterhalter, M., 1991. Elastic moduli for strongly curved monolayers, position of the neutral surface. *J. Phys. II France* 1 (9), 1077–1084.
- Kozlovsky, Y., Kozlov, M.M., 2002. Stalk model of membrane fusion: solution of energy crisis. *Biophys. J.* 82 (2), 882–895.
- Kralj-Iglic, V., Svetina, S., Žekš, B., 1993. The existence of non-axisymmetric bilayer vesicle shapes predicted by the bilayer couple model. *Eur. Biophys. J.* 22 (2), 97–103.
- Kraus, M., Wintz, W., Seifert, U., Lipowsky, R., 1996. Fluid vesicles in shear flow. *Phys. Rev. Lett.* 77, 3685–3688.
- Kreyszig, E., 1991. *Differential Geometry*. Dover, New York.
- Kwok, R., Evans, E., 1981. Thermoelasticity of large lecithin bilayer vesicles. *Biophys. J.* 35 (3), 637–652.
- Landau, L.D., Lifshitz, E.M., 1999. *Theory of Elasticity*. Butterworth-Heinemann, Oxford.
- Lebedev, V.V., Turitsyn, K.S., Vergeles, S.S., 2007. Dynamics of nearly spherical vesicles in an external flow. *Phys. Rev. Lett.* 99, 218101.
- Li, J., Dao, M., Lim, C.T., Suresh, S., 2005. Spectrin-level modeling of the cytoskeleton and optical tweezers stretching of the erythrocyte. *Biophys. J.* 88 (5), 3707–3719.
- Li, J., Pastor, K.A., Shi, A.C., Schmid, F., Zhou, J., 2013a. Elastic properties and line tension of self-assembled bilayer membranes. *Phys. Rev. E* 88, 012718.
- Li, X., Vlahovska, P.M., Karniadakis, G.E., 2013b. Continuum- and particle-based modeling of shapes and dynamics of red blood cells in health and disease. *Soft Matter* 9, 28–37.
- Lin, H.K., Zandi, R., Mohideen, U., Pryadko, L.P., 2011. Fluctuation-induced forces between inclusions in a fluid membrane under tension. *Phys. Rev. Lett.* 107, 228104.
- Lindahl, E., Edholm, O., 2000. Mesoscopic undulations and thickness fluctuations in lipid bilayers from molecular dynamics simulations. *Biophys. J.* 79 (1), 426–433.
- Lipowsky, R., Leibler, S., 1986. Unbinding transitions of interacting membranes. *Phys. Rev. Lett.* 56, 2541–2544.
- Lipowsky, R., 1991. The conformation of membranes. *Nature* 349, 475–481.
- Lipowsky, R., 2013. Spontaneous tubulation of membranes and vesicles reveals membrane tension generated by spontaneous curvature. *Farad. Discuss.* 161, 305–331.
- Lipowsky, R., 2014. Coupling of bending and stretching deformations in vesicle membranes. *Adv. Colloid Interface Sci.* 208, 14–24.
- Litster, J.D., 1975. Stability of lipid bilayers and red blood cell membranes. *Phys. Lett. A* 53 (3), 193–194.
- Liu, Y., Nagle, J., 2004. Diffuse scattering provides material parameters and electron density profiles of biomembranes. *Phys. Rev. E* 69, 040901.
- Lomholt, M.A., Miao, L., 2006. Descriptions of membrane mechanics from microscopic and effective two-dimensional perspectives. *J. Phys. A: Math. Gen.* 39 (33), 10323–10354.
- Lomholt, M.A., Hansen, P.L., Miao, L., 2005. A general theory of non-equilibrium dynamics of lipid-protein fluid membranes. *Eur. Phys. J. E* 16 (4), 439–461.
- Lorenzen, S., Servuss, R.M., Helfrich, W., 1986. Elastic torques about membrane edges. *Biophys. J.* 50 (4), 565–572.
- Lovelock, D., Rund, H., 1989. *Tensors, Differential Forms, and Variational Principles*. Dover, New York.
- Müller, M.M., Deserno, M., Guven, J., 2005a. Interface-mediated interactions between particles: a geometrical approach. *Phys. Rev. E* 72, 061407.
- Müller, M.M., Deserno, M., Guven, J., 2005b. Geometry of surface-mediated interactions. *Europhys. Lett.* 69, 482–488.
- Müller, M.M., Deserno, M., Guven, J., 2005c. Interface-mediated interactions between particles: a geometrical approach. *Phys. Rev. E* 72, 061407.
- Müller, M.M., Deserno, M., Guven, J., 2007. Balancing torques in membrane-mediated interactions: exact results and numerical illustrations. *Phys. Rev. E* 76, 011921.
- Müller, M.M., Ben Amar, M., Guven, J., 2008. Conical defects in growing sheets. *Phys. Rev. Lett.* 101, 156104.x
- Müller, M.M., 2007. *Theoretical Studies of Fluid Membrane Mechanics*. Ph.D. thesis. University of Mainz, Germany <http://ubm.opus.hbz-nrw.de/volltexte/2007/1475/>
- Maleki, M., Seguin, B., Fried, E., 2013. Kinematics, material symmetry, and energy densities for lipid bilayers with spontaneous curvature. *Biomech. Model. Mech.* 12 (5), 997–1017.
- Marques, F.C., Neves, A., 2012. Min-max theory and the Willmore conjecture. *Ann. Math.* (in press), Eprint: arXiv:1202.6036.
- Marrink, S.J., Mark, A.E., 2001. Effect of undulations on surface tension in simulated bilayers. *J. Phys. Chem. B* 105 (26), 6122–6127.
- Marrink, S.J., de Vries, A.H., Mark, A.E., 2004. Coarse grained model for semiquantitative lipid simulations. *J. Phys. Chem. B* 108 (2), 750–760.
- May, S., Ben-Shaul, A., 1999. Molecular theory of lipid-protein interaction and the L_{α} - H_{II} transition. *Biophys. J.* 76 (2), 751–767.
- May, E.R., Narang, A., Kopelevich, D.I., 2007a. Role of molecular tilt in thermal fluctuations of lipid membranes. *Phys. Rev. E* 76, 021913.
- May, E.R., Narang, A., Kopelevich, D.I., 2007b. Molecular modeling of key elastic properties for inhomogeneous lipid bilayers. *Mol. Simul.* 33 (9–10), 787–797.
- May, S., 2000. Protein-induced bilayer deformations: the lipid tilt degree of freedom. *Eur. Biophys. J.* 29 (1), 17–28.
- McWhirter, J.L., Noguchi, H., Gompper, G., 2009. Flow-induced clustering and alignment of vesicles and red blood cells in microcapillaries. *Proc. Natl. Acad. Sci. U.S.A.* 106 (15), 6039–6043.
- Merkel, R., Sackmann, E., Evans, E., 1989. Molecular friction and epitaxial coupling between monolayers in supported bilayers. *J. Phys. France* 50 (12), 1535–1555.
- Miao, L., Seifert, U., Wortis, M., Döbereiner, H.G., 1994. Budding transitions of fluid-bilayer vesicles: the effect of area-difference elasticity. *Phys. Rev. E* 49, 5389–5407.
- Milner, S.T., Roux, D., 1992. Flory theory of the unbinding transition. *J. Phys. I France* 2 (9), 1741–1754.
- Misbah, C., 2006. Vacillating breathing and tumbling of vesicles under shear flow. *Phys. Rev. Lett.* 96, 028104.
- Mitchison, J.M., Swann, M.M., 1954. The mechanical properties of the cell surface: I. The cell elastimeter. *J. Exp. Biol.* 31 (3), 443–460.
- Monnier, S., Rochal, S.B., Parmeggiani, A., Lorman, V.L., 2010. Long-range protein coupling mediated by critical low-energy modes of tubular lipid membranes. *Phys. Rev. Lett.* 105, 028102.
- Morris, C., Homann, U., 2001. Cell surface area regulation and membrane tension. *J. Membr. Biol.* 179 (2), 79–102.
- Nagle, J.F., Jablin, M.S., Tristram-Nagle, S., Akabori, K., 2014. What are the true values of the bending modulus of simple lipid bilayers? *Chem. Phys. Lipids*, <http://dx.doi.org/10.1016/j.chemphyslip.2014.04.003>, same issue as this contribution.
- Nagle, J.F., 2013. Basic quantities in model biomembranes. *Farad. Discuss.* 161, 11–29.
- Naito, H., Okuda, M., Ou-Yang, Z.C., 1993. Counterexample to some shape equations for axisymmetric vesicles. *Phys. Rev. E* 48, 2304–2307.
- Napoli, G., Vergori, L., 2010. Equilibrium of nematic vesicles. *J. Phys. A: Math. Theor.* 43, 445201.
- Nelson, P., Powers, T., 1993. Renormalization of chiral couplings in tilted bilayer membranes. *J. Phys. II (France)* 3 (10), 1535–1569.
- Nelson, D., Piran, T., Weinberg, S. (Eds.), 2004. *Statistical Mechanics of Membranes and Surfaces*, 2nd ed. World Scientific, Singapore.
- Nickerson, H.K., Manning, G.S., 1988. Intrinsic equations for a relaxed elastic line on an oriented surface. *Geom. Ded.* 27 (2), 127–136.
- Nicolson, M.M., 1949. The interaction between floating particles. *Math. Proc. Cambridge Philos. Soc.* 45, 288–295.
- Noguchi, H., Gompper, G., 2004. Fluid vesicles with viscous membranes in shear flow. *Phys. Rev. Lett.* 93, 258102.
- Noguchi, H., Gompper, G., 2005a. Dynamics of fluid vesicles in shear flow: effect of membrane viscosity and thermal fluctuations. *Phys. Rev. E* 72, 011901.

- Noguchi, H., Gompper, G., 2005b. Shape transitions of fluid vesicles and red blood cells in capillary flows. *Proc. Natl. Acad. Sci. U.S.A.* 102 (40), 14159–14164.
- Noguchi, H., Gompper, G., 2007. Swinging and tumbling of fluid vesicles in shear flow. *Phys. Rev. Lett.* 98, 128103.
- Noguchi, H., 2011. Anisotropic surface tension of buckled fluid membranes. *Phys. Rev. E* 83, 061919.
- Ou-Yang, Z.C., Helfrich, W., 1987. Instability and deformation of a spherical vesicle by pressure. *Phys. Rev. Lett.* 59, 2486–2488.
- Ou-Yang, Z.C., Helfrich, W., 1989. Bending energy of vesicle membranes: general expressions for the first, second, and third variation of the shape energy and applications to spheres and cylinders. *Phys. Rev. A* 39, 5280–5288.
- Pan, J., Mills, T.T., Tristram-Nagle, S., Nagle, J.F., 2008. Cholesterol perturbs lipid bilayers nonuniversally. *Phys. Rev. Lett.* 100 (19), 198103.
- Pan, J., Tristram-Nagle, S., Kučerka, S., Nagle, J.F., 2008a. Temperature dependence of structure, bending rigidity, and bilayer interactions of dioleoylphosphatidylcholine bilayers. *Biophys. J.* 94 (1), 117–124.
- Pan, J., Tristram-Nagle, S., Nagle, J.F., 2009. Effect of cholesterol on structural and mechanical properties of membranes depends on lipid chain saturation. *Phys. Rev. E* 80 (2), 021931.
- Park, J.M., Lubensky, T.C., 1996. Interactions between membrane inclusions on fluctuating membranes. *J. Phys. I (France)* 7, 1217–1235.
- Pinkall, U., Sterling, I., 1987. Willmore surfaces. *Math. Intell.* 9 (2), 38–43.
- Pivkin, I.V., Karniadakis, G.E., 2008. Accurate coarse-grained modeling of red blood cells. *Phys. Rev. Lett.* 101, 118105.
- Powers, T., Nelson, P., 1995. Fluctuating membranes with tilt order. *J. Phys. II (France)* 5 (11), 1671–1678.
- Rangamani, P., Benjamini, A., Agrawal, A., Smit, B., Steigmann, D.J., Oster, G., 2013. Small scale membrane mechanics. *Biomech. Model. Mech.* 1–15.
- Raphael, R.M., Waugh, R.E., 1996. Accelerated interleaflet transport of phosphatidylcholine molecules in membranes under deformation. *Biophys. J.* 71, 1374–1388.
- Rawicz, W., Olbrich, K., McIntosh, T., Needham, D., Evans, E., 2000. Effect of chain length and unsaturation on elasticity of lipid bilayers. *Biophys. J.* 79 (1), 328–339.
- Reynwar, B.J., Deserno, M., 2011. Membrane-mediated interactions between circular particles in the strongly curved regime. *Soft Matter* 7, 8567–8575.
- Safinya, C.R., Roux, D., Smith, G.S., Sinha, S.K., Dimon, P., Clark, N.A., et al., 1986. Steric interactions in a model multilayered membrane system: a synchrotron X-ray study. *Phys. Rev. Lett.* 57, 2718–2721.
- Safran, S.A., 1994. *Statistical Thermodynamics of Surfaces, Interfaces, and Membranes*. Perseus, Cambridge.
- Schneider, M.B., Jenkins, J.T., Webb, W.W., 1984a. Thermal fluctuations of large cylindrical phospholipid-vesicles. *Biophys. J.* 45 (5), 891–899.
- Schneider, M.B., Jenkins, J.T., Webb, W.W., 1984b. Thermal fluctuations of large quasi-spherical bimolecular phospholipid-vesicles. *Biophys. J.* 45 (9), 1457–1472.
- Schrlau, M.G., Falls, E.M., Ziober, B.L., Bau, H.H., 2008. Carbon nanopipettes for cell probes and intracellular injection. *Nanotechnology* 19 (1), 015101.
- Schutz, B., 1980. *Geometric Methods in Mathematical Physics*. Cambridge University Press, Cambridge, UK.
- Seifert, U., Langer, S.A., 1993. Viscous modes of fluid bilayer membranes. *Europhys. Lett.* 23, 71–76.
- Seifert, U., Lipowsky, R., 1990. Adhesion of vesicles. *Phys. Rev. A* 42, 4768–4771.
- Seifert, U., Lipowsky, R., 1995. Chapter 8: Morphology of vesicles. In: Lipowsky, R., Sackmann, E. (Eds.), *Structure and Dynamics of Membranes*; vol. 1 of *Handbook of Biological Physics*. North-Holland, Amsterdam, pp. 403–463.
- Seifert, U., Berndt, K., Lipowsky, R., 1991. Shape deformations of vesicles: phase diagram for spontaneous-curvature and bilayer-coupling models. *Phys. Rev. A* 44, 1182–1202.
- Seifert, U., Shillcock, J., Nelson, P., 1996. Role of bilayer tilt difference in equilibrium membrane shapes. *Phys. Rev. Lett.* 77, 5237–5240.
- Seifert, U., 1991. Vesicles of toroidal topology. *Phys. Rev. Lett.* 66, 2404–2407.
- Seifert, U., 1997. Configurations of fluid membranes and vesicles. *Adv. Phys.* 46 (1), 13–137.
- Selinger, J.V., MacKintosh, F.C., Schnur, J.M., 1996. Theory of cylindrical tubes and helical ribbons of chiral lipid membranes. *Phys. Rev. E* 53, 3804–3818.
- Semrau, S., Idema, T., Holtzer, L., Schmidt, T., Storm, C., 2008. Accurate determination of elastic parameters for multicomponent membranes. *Phys. Rev. Lett.* 100 (8), 088101.
- Shiba, H., Noguchi, H., 2011. Estimation of the bending rigidity and spontaneous curvature of fluid membranes in simulations. *Phys. Rev. E* 84, 031926.
- Siegel, D.P., Kozlov, M.M., 2004. The Gaussian curvature elastic modulus of n-monomethylated dioleoylphosphatidylethanolamine: relevance to membrane fusion and lipid phase behavior. *Biophys. J.* 87 (1), 366–374.
- Siegel, D.P., 2006. Determining the ratio of the Gaussian curvature and bending elastic moduli of phospholipids from Q_{II} phase unit cell dimensions. *Biophys. J.* 91 (2), 608–618.
- Siegel, D.P., 2008. The Gaussian curvature elastic energy of intermediates in membrane fusion. *Biophys. J.* 95 (11), 5200–5215.
- Siegel, D.P., 2010. Fourth-order curvature energy model for the stability of bicontinuous inverted cubic phases in amphiphile-water systems. *Langmuir* 26 (11), 8673–8683.
- Spann, A.P., Zhao, H., Shaqfeh, E.S.G., 2014. Loop subdivision surface boundary integral method simulations of vesicles at low reduced volume ratio in shear and extensional flow. *Phys. Fluids* 26 (3), 031902.
- Spivak, M., 1970. *A Comprehensive Introduction to Differential Geometry*, vol. 2. Publish or Perish, Boston, MA.
- Spivak, M., 1975a. *A Comprehensive Introduction to Differential Geometry*, vol. 3. Publish or Perish, Boston, MA.
- Spivak, M., 1975b. *A Comprehensive Introduction to Differential Geometry*, vol. 4. Publish or Perish, Boston, MA.
- Steigmann, D.J., 1999. Fluid films with curvature elasticity. *Arch. Rational Mech. Anal.* 150 (2), 127–152.
- Sukumar, S., Seifert, U., 2001. Influence of shear flow on vesicles near a wall: a numerical study. *Phys. Rev. E* 64, 011916.
- Svetina, S., Žekš, B., 1989. Membrane bending energy and shape determination of phospholipid vesicles and red blood cells. *Eur. Biophys. J.* 17 (2), 101–111.
- Szleifer, I., Ben Shaul, A., Gelbart, W.M., 1985. Chain organization and thermodynamics in micelles and bilayers, 2. model calculations. *J. Chem. Phys.* 83 (7), 3612–3620.
- Szleifer, I., Kramer, D., Ben-Shaul, A., Roux, D., Gelbart, W.M., 1988. Curvature elasticity of pure and mixed surfactant films. *Phys. Rev. Lett.* 60, 1966–1969.
- Szleifer, I., Kramer, D., Ben-Shaul, A., Gelbart, W.M., Safran, S.A., 1990. Molecular theory of curvature elasticity in surfactant films. *J. Chem. Phys.* 92, 6800–6817.
- Szule, J.A., Fuller, N.L., Rand, R.P., 2002. The effects of acyl chain length and saturation of diacylglycerols and phosphatidylcholines on membrane monolayer curvature. *Biophys. J.* 83 (2), 977–984.
- Templer, R.H., Khoo, B.J., Seddon, J.M., 1998. Gaussian curvature modulus of an amphiphile monolayer. *Langmuir* 14 (26), 7427–7434.
- Thomsen, G., 1924. Über konforme Geometrie I: Grundlagen der konformen Flächen-theorie. *Abh. Math. Sem. Hamburg* 3, 31–56.
- Tian, A., Baumgart, T., 2008. Sorting of lipids and proteins in membrane curvature gradients. *Biophys. J.* 96 (7), 2676–2688.
- Tian, A., Johnson, C., Wang, W., Baumgart, T., 2007. Line tension at fluid membrane domain boundaries measured by micropipette aspiration. *Phys. Rev. Lett.* 98, 208102.
- Tolpekina, T.V., den Otter, W.K., Briels, W.J., 2004. Simulations of stable pores in membranes: system size dependence and line tension. *J. Chem. Phys.* 121 (16), 014–8020.
- Tu, Z.C., Ou-Yang, Z.C., 2003. Lipid membranes with free edges. *Phys. Rev. E* 68, 061915.
- Tu, Z.C., Ou-Yang, Z.C., 2004. A geometric theory on the elasticity of bio-membranes. *J. Phys. A: Math. Gen.* 37 (47), 11407.
- Tu, Z.C., Ou-Yang, Z.C., 2008. Elastic theory of low-dimensional continua and its applications in bio- and nano-structures. *J. Comput. Theor. Nanos.* 5 (4), 422–448.
- Tu, Z.C., Seifert, U., 2007. Concise theory of chiral lipid membranes. *Phys. Rev. E* 76, 031603.
- Tu, Z.C., Ge, L.Q., Li, J.B., Ou-Yang, Z.C., 2005. Elasticity of polymer vesicles by osmotic pressure: an intermediate theory between fluid membranes and solid shells. *Phys. Rev. E* 72, 021806.
- Tu, Z.C., 2011. Geometry of membranes. *J. Geom. Symm. Phys.* 24, 45–75.
- Uline, M., Szleifer, I., 2012. Mode specific elastic constants for the gel, liquid-ordered, and liquid-disordered phases of DPPC/DOPC/cholesterol model lipid bilayers. *Farad. Discuss.* 161, 177–191.
- Vlahovska, P.M., Gracia, R.S., 2007. Dynamics of a viscous vesicle in linear flows. *Phys. Rev. E* 75, 016313.
- Vlahovska, P.M., Podgorski, T., Misbah, C., 2009. Vesicles and red blood cells in flow: from individual dynamics to rheology. *Comp. Ren. Phys.* 10 (8), 775–789.
- Vlahovska, P.M., Barthes-Biesel, D., Misbah, C., 2013. Flow dynamics of red blood cells and their biomimetic counterparts. *Comp. Ren. Phys.* 14 (6), 451–458.
- Wang, Z.J., Deserno, M., 2010a. A systematically coarse-grained solvent-free model for quantitative phospholipid bilayer simulation. *J. Phys. Chem. B* 114 (34), 11207–11220.
- Wang, Z.J., Deserno, M., 2010b. Systematic implicit solvent coarse-graining of bilayer membranes: lipid and phase transferability of the force field. *New J. Phys.* 12, 095004.
- Wang, Z.J., Frenkel, D., 2005. Modeling flexible amphiphilic bilayers: a solvent-free off-lattice Monte Carlo study. *J. Chem. Phys.* 122 (23), 154701.
- Watson, M.C., Brown, F.L., 2010. Interpreting membrane scattering experiments at the mesoscale: the contribution of dissipation within the bilayer. *Biophys. J.* 98 (6), L9–L11.
- Watson, M.C., Penev, E.S., Welch, P.M., Brown, F.L.H., 2011. Thermal fluctuations in shape, thickness, and molecular orientation in lipid bilayers. *J. Chem. Phys.* 135, 244701.
- Watson, M.C., Brandt, E.G., Welch, P.M., Brown, F.L.H., 2012. Determining biomembrane bending rigidities from simulations of modest size. *Phys. Rev. Lett.* 109 (2), 028102.
- Waugh, R.E., Song, J., Svetina, S., Žekš, B., 1992. Local and nonlocal curvature elasticity in bilayer membranes by tether formation from lecithin vesicles. *Biophys. J.* 61 (4), 974–982.
- Weikl, T.R., Kozlov, M.M., Helfrich, W., 1998. Interaction of conical membrane inclusions: effect of lateral tension. *Phys. Rev. E* 57, 6988–6995.
- Weikl, T.R., 2003. Indirect interactions of membrane-adsorbed cylinders. *Eur. Phys. J. E* 12, 265–273.
- Wennerström, H., Olsson, U., 2014. The undulation force; theoretical results versus experimental demonstrations. *Adv. Colloid Interface Sci.* 208, 10–13.
- White, J.H., 1973. A global invariant of conformal mappings in space. *Proc. Am. Math. Soc.* 38, 162–164.
- Willmore, T.J., 1965. Note on embedded surfaces. *An. Stiint. Univ. "Al. I. Cuza" Iasi (Sec. Ia) Mat.* 11, 493–496.
- Willmore, T.J., 1982. *Total Curvature in Riemannian Geometry*. Ellis Horwood, Chichester, New York.

- Willmore, T.J., 2012. *An Introduction to Differential Geometry*. Dover, New York.
- Yao, Z., Sknepnek, R., Thomas, C.K., Olvera de la Cruz, M., 2012. Shapes of pored membranes. *Soft Matter* 8, 11613–11619.
- Yolcu, C., Deserno, M., 2012. Membrane-mediated interactions between rigid inclusions: an effective field theory. *Phys. Rev. E* 86, 031906.
- Yolcu, C., Rothstein, I.Z., Deserno, M., 2011. Effective field theory approach to Casimir interactions on soft matter surfaces. *Europhys. Lett.* 96 (2), 20003.
- Yolcu, C., Haussman, R.C., Deserno, M., 2014. The effective field theory approach towards membrane-mediated interactions between particles. *Adv. Colloid Interface Sci.* 208, 89–109.
- Zhang, J., Johnson, P.C., Popel, A.S., 2007. An immersed boundary Lattice-Boltzmann approach to simulate deformable liquid capsules and its application to microscopic blood flows. *Phys. Biol.* 4 (4), 285–295.
- Zhang, J., Johnson, P.C., Popel, A.S., 2008. Red blood cell aggregation and dissociation in shear flows simulated by Lattice-Boltzmann method. *J. Biomech.* 41, 47–55.
- Zhao, H., Shaqfeh, E.S.G., 2011. The dynamics of a vesicle in simple shear flow. *J. Fluid Mech.* 674, 578–604.
- Zhao, H., Spann, A.P., Shaqfeh, E.S.G., 2011. The dynamics of a vesicle in a wall-bound shear flow. *Phys. Fluids* 23 (12), 12 pages, article number: 121901.
- Zhelev, D.V., Needham, D., 1993. Tension-stabilized pores in giant vesicles: determination of pore size and pore line tension. *Biochim. Biophys. Acta - Biomembranes* 1147 (1), 89–104.
- Zheng, W.M., Liu, J., 1993. Helfrich shape equation for axisymmetric vesicles as a first integral. *Phys. Rev. E* 48, 2856–2860.
- Zilman, A.G., Granek, R., 1996. Undulations and dynamic structure factor of membranes. *Phys. Rev. Lett.* 77, 4788–4791.
- Zilman, A.G., Granek, R., 2002. Membrane dynamics and structure factor. *Chem. Phys.* 284, 195–204.
- Zurlo, G., 2007. *Material and Geometric Phase Transitions in Biological Membranes*. Ph.D. thesis. University of Pisa, Italy <http://etd.adm.unipi.it/t/etd-11142006-173408/>